


Spring 2017

# Assessing Seasonal and Spatial Variability in the Hydrogeochemistry of Glacial Meltwater in Iceland

Anisha Tuladhar

Western Kentucky University, [anisha.tuladhar873@topper.wku.edu](mailto:anisha.tuladhar873@topper.wku.edu)

Follow this and additional works at: <http://digitalcommons.wku.edu/theses>

 Part of the [Geology Commons](#), [Geophysics and Seismology Commons](#), [Glaciology Commons](#), and the [Other Oceanography and Atmospheric Sciences and Meteorology Commons](#)

---

## Recommended Citation

Tuladhar, Anisha, "Assessing Seasonal and Spatial Variability in the Hydrogeochemistry of Glacial Meltwater in Iceland" (2017). *Masters Theses & Specialist Projects*. Paper 1960.  
<http://digitalcommons.wku.edu/theses/1960>

This Thesis is brought to you for free and open access by TopSCHOLAR®. It has been accepted for inclusion in Masters Theses & Specialist Projects by an authorized administrator of TopSCHOLAR®. For more information, please contact [topscholar@wku.edu](mailto:topscholar@wku.edu).

ASSESSING TEMPORAL AND SPATIAL VARIABILITY IN THE  
HYDROGEOCHEMISTRY OF GLACIER MELTWATER IN ICELAND

A Thesis  
Presented to the Faculty of the  
Department of Geography and Geology  
Western Kentucky University  
Bowling Green, Kentucky

In Partial Fulfillment  
Of the Requirements for the Degree  
Master of Science

By  
Anisha Tuladhar

May 2017


ASSESSING TEMPORAL AND SPATIAL VARIABILITY IN THE  
HYDROGEOCHEMISTRY OF GLACIER MELTWATER IN ICELAND

Date Recommended 21 April 2017

  
\_\_\_\_\_  
Dr. Jason Polk, Director of Thesis

 4/18/17  
\_\_\_\_\_  
Dr. Nahid Gani

  
\_\_\_\_\_  
Dr. Thorsteinn Thorsteinsson

  
\_\_\_\_\_  
Dean, Graduate School      4/24/17  
Date

## ACKNOWLEDGEMENTS

I heartily thank my advisor Dr. Jason Polk for all the time spent working with me and for his encouraging guidance throughout this research project. Thank you for consistently steering me in the right direction in research writing. I would also like to thank my committee members, Dr. Nahid Gani and Dr. Thorsteinn Thorsteinsson, for their invaluable input and suggestions. I also thank Dr. Leslie North for her overwhelming support in this project. I am eternally grateful to James Graham and Caleb Koostra for assisting me with sampling and analyzing ice-cold water in the field. I would like to extend my sincere thanks to Mr. Orn Gudmundson and Dr. Bernard Strenecky for helping with my visa processing for Iceland. Thanks are due to many grant and scholarship sponsors from Western Kentucky University (WKU) for financial support of my research, including RCAP grant, WKU Graduate School grant, Lifetime Achievement grant, Office of Scholar Development, World topper Scholarship, and the Department of Geology and Geography Grant. I am grateful to Mr. Njall Fannar Reynisson for providing me timely hydromet data. My appreciation goes to Pauline Norris of WKU Advanced Materials Institute, for valuable suggestions, and equipment use for lab analysis. My appreciation goes to Dr. Jun Yan and Dolly Na-Yemeh for assisting with the GIS work. I would like to thank Anusha Bitra and Kegan McClanahan for further suggestions with sample analysis. Finally, I must express gratitude to my family and to Binod Shilpakar for providing me continuous support and encouragement throughout my graduate studies.

## TABLE OF CONTENTS

Chapter 1	
1.0 Introduction.....	1
Chapter 2	
2.0 Literature review.....	5
2.1 Glaciers and climate change.....	5
2.2 Iceland and climate change.....	8
2.3 Hydrogeochemistry of Glacial Meltwater.....	13
2.4 Processes Controlling the Hydrochemistry of Glacial Meltwater.....	18
2.4.1 Bedrock Geology.....	18
2.4.2 Anthropogenic inputs.....	20
2.4.3 Effect of Climate Change on Glacier-Fed Water Resource Chemistry.....	21
2.5 Hydrogeochemical Studies in Iceland.....	22
Chapter 3	
3.0 Study Area.....	29
3.1 Vatnajökull.....	35
3.2 Eyjafjallajökull.....	37
3.3 Mýrdalsjökull.....	39
Chapter 4	
4.0 Methodology.....	41
4.1 Sampling Preparation.....	41
4.2 Calibration.....	41
4.3 Field Measurements.....	42
4.4 Sample collection.....	42
4.5 Secondary Data Collection.....	45
4.6 Data Analysis.....	45
Chapter 5	
5.0 Results and Discussion.....	47
5.1 Hydrogeochemical parameters.....	47
5.1.1 Data Analysis.....	49
5.2 Elevated Solute Concentrations in Samples from Eyjafjallajökull.....	53
5.3 Temporal Variation of Ions from Fjallsjökull Glacier.....	56
5.4 Geochemical variability.....	60
5.4.1 Variability of pH, Specific Conductivity, and DO.....	63
5.4.2 Variability of SO <sub>4</sub> , S, and F.....	68
5.4.3 Spatial and temporal variations of TSS.....	73
5.5 Ion variability and dominance.....	78
5.5.1 Elemental Ratios.....	84
5.5.2 Ion Dominance Comparison.....	86
5.5.3 Other elements.....	88

5.6 TDS Variability.....	90
5.7 Geochemical Composition of Jökulsárlón Lagoon.....	92
5.8 Spatial Variation with Respect to Geographic Location.....	94
Chapter 6	
6.0 Conclusions.....	97
References.....	102
Appendices.....	118

## LIST OF FIGURES

Figure 2.1. Simulated responses of icecaps to the climate-change scenario .....	11
Figure 2.2. The extent of southeast Vatnajökull glacier outlets at different times.....	12
Figure 2.3. Change in temperature in Iceland .....	13
Figure 3.1. Topography of Iceland.....	30
Figure 3.2. Principle elements of the geology in Iceland.....	31
Figure 3.3. Distribution of active volcanic systems in Iceland .....	32
Figure 3.4. Map of Iceland showing sampling sites.....	33
Figure 3.5. Sampling sites at Solheimajökull.....	34
Figure 3.6. Sampling sites at Jökulsárlón.....	35
Figure 3.7. Vatnajökull, showing sampling stations .....	37
Figure 3.8. Eyjafjallajökull, showing sampling stations .....	38
Figure 3.9. Mýrdalsjökull, showing sampling stations .....	40
Figure 5.1. Study area showing hydrometric stations V263 and V413.....	48
Figure 5.2. Hourly variation of conductivity.....	49
Figure 5.3. Daily variation of conductivity .....	50
Figure 5.4. Mean conductivity and volcanic phases .....	50
Figure 5.5. Temporal variation of ions from Fjallsjökull.....	57
Figure 5.6. Total precipitation (mm) of the station at Skaftafell.....	62
Figure 5.7. Mean 2016 monthly temperature (°C) of the station at Skaftafell .....	62
Figure 5.8. Mean temperature (°C) of the station near Steinar.....	63
Figure 5.9. Variation of pH at sampling sites.....	66
Figure 5.10. Variation of specific conductivity at sampling sites .....	66

Figure 5.11. Variation of DO at sampling sites.....	68
Figure 5.12. Variation of water temperature at sampling sites.....	68
Figure 5.13. Spatial and temporal distribution of SO <sub>4</sub> .....	69
Figure 5.14. Spatial and temporal distribution of S .....	70
Figure 5.15. Variation of SO <sub>4</sub> and sampling sites .....	71
Figure 5.16. Variation of S and sampling sites .....	71
Figure 5.17. Variation of F and sampling sites .....	72
Figure 5.18. Variation of TSS and sampling sites.....	74
Figure 5.19. Spatial and temporal distribution of TSS.....	75
Figure 5.20. Variation of Turbidity at sampling sites .....	75
Figure 5.21. Map of Mýrdalsjökull showing major Ions .....	80
Figure 5.22. Map of Vatnajökull showing major Ions .....	80
Figure 5.23. Map of Eyjafjallajökull showing major ions .....	81
Figure 5.24. Piper plot of Mýrdalsjökull.....	82
Figure 5.25. Piper plot of Vatnajökull.....	82
Figure 5.26. Piper plot of Eyjafjallajökull.....	83
Figure 5.27. C ratios and sampling sites.....	85
Figure 5.28. Na/Cl and sampling sites .....	85
Figure 5.29. Monthly K/Cl.....	86
Figure 5.30. Spatial variation of specific conductivity .....	95
Figure 5.31. Spatial variation of specific conductivity with location .....	95



## LIST OF TABLES

Table 2.1. Recent contributions to ongoing sea-level rise .....	7
Table 3.1. Sampling sites and letter codes used for sampling .....	33
Table 3.2. Characteristics of Vatnajökull outlet glaciers .....	36
Table 4.1. Field sampling.....	43
Table 4.2. Sample preservations and analytical methods .....	44
Table 5.1. Minimum and maximum concentrations .....	54
Table 5.2. Chemical composition of water during jökulhlaups .....	55
Table 5.3. Geochemical values for Fjallsjökull .....	56
Table 5.4. Sample site categorization .....	60
Table 5.5. Ranges for geochemical parameters .....	64
Table 5.6. Categorization of TDS .....	91
Table 5.7. Physical and chemical concentrations of Jökulsárlón.....	92

# ASSESSING TEMPORAL AND SPATIAL VARIABILITY IN THE HYDROGEOCHEMISTRY OF GLACIAL MELTWATER IN ICELAND

Anisha Tuladhar

May 2017

134 pages

Directed by: Jason Polk, Nahid Gani, Thorsteinn Thorsteinsson

Department of Geography and Geology

Western Kentucky University

A detailed comparative geochemical characterization of three different types of Iceland glacial systems was conducted during June, August, and October, 2016. The study was carried out at a total of 11 outlet glacier rivers flowing from the icecaps Vatnajökull, Eyjafjallajökull, and Mýrdalsjökull. A total of 75 grab samples were collected (25 for each sampling period). The hydrogeochemical variations of Icelandic glacial meltwater are influenced by volcanic activity, temporal changes, and geographical location, which differed between the sampling sites within the glaciers and icecaps. Lower pH range, and comparatively higher and variable specific conductivity,  $\text{SO}_4$ , S and F is linked to higher volcanic influences, including residuals from the 2010 eruption at Eyjafjallajökull (located above a tectonic plate boundary zone). High concentrations of Al and Fe were found at Kötlujökull and Kvíárjökull, both of which are close to active volcanic zones. Changes in hydrogeochemistry of the meltwater caused by volcanic activity may be used to forecast eruptions and jökulhlaups; however, given the variability of Icelandic meltwater chemistry, high-resolution monitoring should be done in order to determine a precursor threshold for an volcanic event, as the chemical composition of one jökulhlaup could be within normal range for a different glacier.

TSS concentrations depicted high spatial and temporal variation as the highest and lowest values of TSS drained from the same glacier. Hydrogeochemical weathering is driven by  $\text{Na-HCO}_3$  and  $\text{Ca-HCO}_3$  dissolution. Concentrations of ions varied with

respect to their geographic location, as specific conductivity increase distance downstream from glaciers, proglacial lagoons, and river reaches. Ca, Mg, K, Na, and  $\text{HCO}_3$  increased from 1984 to 2016 for Fjallsjökull, which may be from an increased weathering rate, due to temperature,  $\text{CO}_2$  increase, and increased erosion beneath glaciers under a changing climate.

This study of hydrogeochemical variation in Icelandic glaciers complements the database of physical and chemical compositions of understudied glaciers. The hydrogeochemical variations of Icelandic glacial meltwater throughout a diverse sample of glaciers and their respective icecaps are related to internal and external factors, and their diversity indicates a much more complex set of processes underway at the different icecaps and their respective glaciers.

## Chapter 1

### 1.0 Introduction

Glaciers cover about 10% of the Earth's surface and contain about 75% of its freshwater (USGS 2015). They exhibit a complex hydrology, with seasonal melting derived from different parts of a glacier's catchment, including melting from basal pressure and movement. The melting also takes place internally, through the glacial drainage system, from snowmelt and air temperature fluctuations at their surface.

Glaciers are one of the components of the hydrological cycle and they play an important role in buffering stream flow (Barry and Seimon 2000). They act as water storage bodies over a range of temporal and spatial scales (Jansson et al. 2003) and provide water to downstream users and communities during periods of low precipitation in some mountain regions of the world (Kaser et al. 2010; Viviroli et al. 2011). An estimated 1/6<sup>th</sup> of the global population relies upon glacier/snow melt for its water supply (Barnett et al. 2005), and glacial meltwater provides 33% of the total runoff to rivers in Iceland (Björnsson and Pálsson 2008). Future climate scenarios for Iceland predict a warming rate of 0.25°C per decade in mid-summer and 0.35°C per decade in mid-winter, with a sinusoidal variation through the year (Jóhannesson et al. 2007), which will severely impact glacier melting rates. Over the past century, glacier coverage declined from 11% to approximately 10% of the country, which is a substantial loss over a few decades (Björnsson et al. 2013).

The Arctic is a major focal area with regard to myriad climate, water, and global environmental indicators. This stems from a recently improved understanding of the Arctic region's connection to atmospheric, oceanic, and regional processes (Webb et al. 2016). Iceland's geographical position within the North Atlantic Ocean causes it to be

highly sensitive to regional- and global-scale influences, such as changes in atmospheric temperature and fluctuations in the Gulf Stream, which directs warm ocean currents to the southern coast of the island. In addition, Iceland is facing major shifts in tourism, shipping, fishing, and other economic and environmental challenges, like many Arctic countries, in response to a changing climate. Owing to their maritime North Atlantic setting, high-mass turnover, and steep gradients, southern Iceland's glaciers are particularly sensitive to climatic fluctuations on annual to decadal timescales (Jóhannesson and Sigurðsson 1998; Sigurðsson et al. 2007), making them an ideal natural laboratory for the study of glacier response during the currently changing climatic conditions. In recent years, a warming climate has led to drastic retreat of glaciers and icecaps in Arctic countries, including Iceland, where dramatic changes in glacial river dynamics are being observed every year (Björnsson and Palsson 2008).

Glacial meltwater contributes to irrigation, drinking water sources, and hydropower. Glacial rivers can also negatively impact landscape weathering, cause flooding, transport pollutants, and serve as a source or sink for carbon dioxide; thus, shifts in the timing, volume, source, and rates of glacial meltwater dynamics can influence multiple aspects of the natural and cultural landscape. Water plays a dominant role in many glacial processes; therefore, the erosional, depositional, and environmental significance of meltwaters and associated fluvio-glacial processes are important to understand with regard to glacier dynamics within the context of climate change. Studying the geochemical characteristics of meltwater from glaciers is extremely important to better understand the weathering reactions influenced by anthropogenic and

climate change impacts, which can contribute to improving watershed and ecosystem management, as well as calculating carbon flux.

This research investigates glacial meltwater processes in Iceland toward an understanding of the hydrogeochemistry of glacier meltwater systems in different physical and temporal settings and addresses the following research questions:

- How do the hydrogeochemical characteristics of glacial meltwater change with respect to volcanic influences, temporal change, and geographic location?
- Can hydrogeochemical data for glacial meltwater be useful in developing monitoring systems in order to mitigate threats from glacial flooding?

The objective of this study is to analyze the hydrogeochemical characteristics of glacial meltwaters from Icelandic glaciers that are variable in size, geographic location, origin, and ongoing processes, like volcanic influences. To achieve this objective, physical (pH, specific conductivity, dissolved oxygen, total suspended solids, total dissolved solids, and turbidity) and chemical (cations, anions, metals) parameters were analyzed from the glacial meltwater systems.

The hydrogeochemical analysis of meltwater is a useful tool in determining the impacts of physical settings, climate influences, and anthropogenic impacts on glaciers. A link between subglacial geothermal activity, meltwater discharge, and meltwater quality can provide a potential hydrochemical basis for forecasting geothermally or volcanically induced jökulhlaups (glacial outburst floods). Geothermal products have been observed for subglacial lakes in some parts of Iceland. Changes, such as sudden increases in a geochemical parameter, might be due to increases in volcanic influences underneath the surface following hydrochemical perturbations from increased geothermal

fluid flow. Studies can help to forecast geothermally driven flood events in glacial environments and can be used for public awareness and safety for tourists and nearby settlements (Lawler et al. 1996).

Water resources are of special importance to Iceland. Most of the largest rivers in Iceland are glacially derived and transport high amounts of sediment within their course from glaciers to the ocean (Hardardottir and Snorrason 2003). Many of the glacial basins in southern Iceland deliver very high sediment yields by global standards (on the order of 10,000 T/km<sup>2</sup>/year) (Tômasson 1991; Lawler and Brown 1992). Examination of changes in suspended sediment fluxes is important to study with respect to climatic, hydrological, and glaciological fluctuations. Average suspended sediment concentrations decreased by 33% over the period 1973-1992 (Lawler et al. 1996). Studies to monitor changes in suspended sediments in these types of glacial meltwater systems can help to design a hydropower plant in Iceland, as the erosion of hydraulic machinery depends on eroding particles in the river, such as the amount of suspended sediments.

## **Chapter 2**

### **2.0 Literature Review**

Glaciers are one of the dominant freshwater sources in the world. Changes, such as increases in temperature and climate change, have not only been affecting glaciers by decreasing their size, but also affecting water quality by increased weathering. Glaciers are very important in Iceland, due to tourism and the possibility to harness them for hydropower. Hydrogeochemical studies are important in identifying the contribution from atmospheric inputs to the observed ions of meltwaters. The hydrochemical composition in glacier melts depends upon bedrock geology, atmospheric deposition, anthropogenic activities, and climate change. Given the variability of formation times and volcanic activities, the glacial meltwater varies with respect to these influences.

### **2.1 Glaciers and Climate Change**

Glaciers are flowing rivers of ice from mountains and form when snow remains in one location long enough to transform into ice, whereas ice sheets form through the accumulation of snowfall on top of continents and generally flow outward in all directions (CSI 2015). In contrast, sea ice is simply frozen ocean water that forms, grows, and melts in the ocean. Global average temperatures are expected to warm at least twice as much over the next 100 years as they have during the last century (IPCC 2013). Glaciers contribute as much as 50% of the total discharge for at least one month per year, impacting an estimated 119 million people (Schaner et al. 2012), and are among the most reliable indicators of climate change because of their sensitivity to temperature increase (Weier 1999). The expected runoff increase from glacier melt may have practical implications for the design and operation of hydroelectric power plants and water



availability. Water resources are generally under severe pressure, due to population growth, economic development, and climate change. Global warming has a direct impact on glacier melting rates, which have increased in recent decades (NSIDC 2015). With current industrialization rates, temperatures are expected to increase at least twice as much over the next 100 years compared to the past century (IPCC 2013).

Glacial runoff is considered a potentially important source of nutrients that are useable, or bioavailable, to downstream ecosystems and, as glaciers melt, there are biogeochemical considerations beyond changing sea levels (Bhatia et al. 2013). Glaciers are quite porous, with complicated systems throughout and underneath them, including moulins (meltwater inputs) and crevasses leading to the bottom, where most of the melting occurs. The more time the water spends in contact with the bedrock and sediments beneath the glacier, the more minerals and nutrients it accumulates (Bhatia et al. 2013). Glacial retreat caused by climate change has serious impacts on water quality (Moore 2009), due to increased catchment weathering and higher rates of melting.

This decrease in glacier size is known from mass balance studies. The sum of winter accumulation and summer losses of mass from glaciers and ice sheets (net surface mass balance) varies with changing climates. Dowdeswell et al. (1997) studied the surface mass balance of Arctic glaciers and the results showed predominantly negative mass balances over the past few decades. In the Arctic, glaciers and icecaps, excluding the Greenland Ice Sheet, cover about 275,000 km<sup>2</sup> of both the widely glacierized archipelagos of the Canadian, Norwegian, and Russian High Arctic, and the area north of about 60°N in Alaska, Iceland, and Scandinavia. Glaciated regions across the globe are contributing to increased global sea level rise as well (Table 2.1). The response of

glaciers to climatic warming has been computed using degree-day, glacier mass-balance models coupled to a dynamic glacier model by Jóhannesson (1997). The rate of melting is expected to continue increasing, which will contribute to additional sea level rise (NRC 2014). Glaciers bordering bodies of water are increasingly breaking off into icebergs, which float away and gradually melt into the sea. Using satellites, scientists have found that the area of sea-ice coverage each September has declined by more than 40 percent since the late 1970s, a trend that has accelerated since 2007 (Polar Research 2015).

Table 2.1. Recent contributions to ongoing sea-level rise from different glaciated regions.

<b>Glaciated regions</b>	<b>Area (km<sup>2</sup>)</b>	<b>Volume (km<sup>3</sup>)</b>	<b>Sea level equivalent (mm)</b>	<b>Annual contribution to sea-level rise (mm/yr)</b>
<b>Antarctica</b>	14,000,000	26,500,000	58*10 <sup>3</sup>	0.21 (1992-2011) 0.31 (2005-2010)
<b>Greenland</b>	1,710,000	2,850,000	7.3*10 <sup>3</sup>	0.42 (1992-2011) 0.65 (2003-2011)
<b>All GICs</b>	735,000	170,000	410	0.71 (2003-2009)
<b>Alaska</b>	89,000	20,400	55	0.15 (2003-2009)
<b>Arctic Canada</b>	146,000	44,000	110	0.17 (2004-2009)
<b>Himalaya</b>	56,000	4,600	11	0.03 (2003-2009)
<b>Iceland</b>	11,000	3,600	9	0.03 (1995-2010)
<b>Russian Arctic</b>	51,000	17,000	41	0.006 (2002-2010)
<b>Scandinavia</b>	3,000	250	0.6	0.02 (2003-2008)
<b>Svalbard</b>	34,000	9,700	24	0.02 (2003-2008)
<b>Tibetan Plateau</b>	64,000	5,000	12	0.04 (2003-2009)

Source: Thorsteinsson et al. 2013.

In recent decades, the Greenland ice sheet has decreased in size and mass as a result of warmer summer temperatures melting ice at the surface and increasing calving of ice at the island's edges. Snow cover is also decreasing as temperatures rise and snow

melts off quickly in the spring and summer. This loss of ice from Arctic landmasses not only contributes to sea level rise, but also alters the way water moves over and through the landscape, which could affect the global circulation of the oceans and atmosphere (Polar Research 2015). The rapid melting of glaciers has also reduced the area of glacier coverage by fragmenting the glaciers, with an increase in glacier numbers in the Himalayas (Bajracharya et al. 2006). Climate change is identified as the cause of 67% of glaciers retreating at a startling rate in the Himalaya (Ageta and Kadota 1992). Climate warming seems to be particularly pronounced in the Alpine and Himalaya regions. These areas are expected to be vulnerable to climate change, because snow and glacier meltwater make a substantial contribution to their runoff (Singh 1998; Rogora et al. 2003).

Glaciers are home to many species that are found nowhere else on the Earth. As temperature changes and glaciers continue to melt, these species face mounting challenges, including the possibility of extinction (Polar Research 2015). The glaciers are also home to many people, and most of the indigenous groups have ancestors who have lived there for years. The settlements near the glaciers are vulnerable as they are exposed to the effects of climate change, such as strong storms and glacial lake outburst floods (GLOF), which could result in the relocation of communities. These changes lead to global impacts, such as sea level rise, longer droughts, heat waves, cold snaps, and impacts on local fishing industry, among others (Corell et al. 2013).

## **2.2 Iceland and Climate Change**

Classified as “warm-based,” or “temperate,” Icelandic glaciers are dynamic in nature. Not only do they respond actively to climatic fluctuations, but they also constitute long-lasting reservoirs of ice that generate meltwater to replenishes the country’s main

rivers, some of which are harnessed for hydropower (Björnsson and Palsson 2008). Runoff from the area presently covered by the glaciers is predicted to increase by approximately  $0.5 \text{ ma}^{-1}$  just 30 years from now, due to reduction in the volume of the glaciers. This predicted runoff increase could lead to a significant increase in the discharge of rivers fed by meltwater from outlet glaciers and may have important consequences for the operation and planning of hydroelectric power plants in Iceland.

Recent studies on Icelandic glaciers reveal that ice losses are accelerating, thereby subtracting 2.7% ( $84 \text{ km}^3$ ) from the total icecap volume between the years 1994-95 to 2005-06 (Björnsson and Palsson 2008). Since 1985, the warmer climate has led steadily to more widespread retreat, and every non-surging outlet glacier in Iceland has been retreating since 1995 (Sigurðsson 2005). The rate of retreat has accelerated due to high summer melting, but no long-term changes in precipitation have been observed. Since 1890, the leading Vatnajökull glacier outlets retreated back as far as two to five km, and the icecap's volume decreased by about  $300 \text{ km}^3$  (~10%), contributing one mm to the rise in global sea level. Current glacier runoff comprises at least one-third of total runoff in the country (Björnsson and Palsson 2008). Because Iceland's major rivers are glacial in origin, and are, in many cases, harnessed to generate hydropower, this recession has had a noteworthy hydrological impact.

Climatic changes are likely to have substantial effects on glaciers and lead to more runoff changes in Iceland. The expected runoff increase may have practical implications for the design and operation of hydroelectric power plants, but other implications could have negative consequences, such as increased flooding. Recent measurements show that, as the average ice thickness of the Snæfellsjökull ice cap is only

30 m, most of the ice cap is likely to disappear within a few decades if the recently warming climate of Iceland persists (Jóhannesson et al. 2011). Modeling results of the Langjökull and Hofsjökull icecaps and the southern part of the Vatnajökull icecap in Iceland reveal that these glaciers may disappear over the next 100-200 years (Aðalgeirsdóttir et al. 2006).

Model run results for Hofsjökull, Langjökull, and southern Vatnajökull are illustrated in Figure 2.1. The resulting retreat rate is similar for Hofsjökull and Vatnajökull, which are predicted to lose 25% of their present volume within half a century, meaning that ice should remain only on their highest peaks for the next 200 years. Langjökull is predicted to diminish by 35% in volume over 50 years and to disappear after 150 years. Considering how fast Icelandic glaciers are predicted to melt in the near future, it is not surprising that icecaps disappeared from the island during the Climatic Optimum of the early Holocene (Björnsson and Pálsson 2008). In a span of about 50 years, some of the biggest glaciers have retreated more than a kilometer. Glaciers like Fjallsjökull (Figure 2.2) experienced 35 % of volume loss and retreated 2.2 km from ~1890 to 2010 (Hannesdóttir et al. 2015). Runoff from these glaciers is projected to increase by about 30% compared to present runoff by 2030 (Thorsteinsson and Björnsson 2011). Some of the steep glaciers, like Falljökull, have been responding to pronounced climate warming by rapidly adjusting their active length, due to changes in mass balance (Phillips et al. 2014). From 2004-2006, the glacier crossed an important dynamic threshold and effectively reduced its active length by abandoning its lower reaches to begin passive retreat processes.

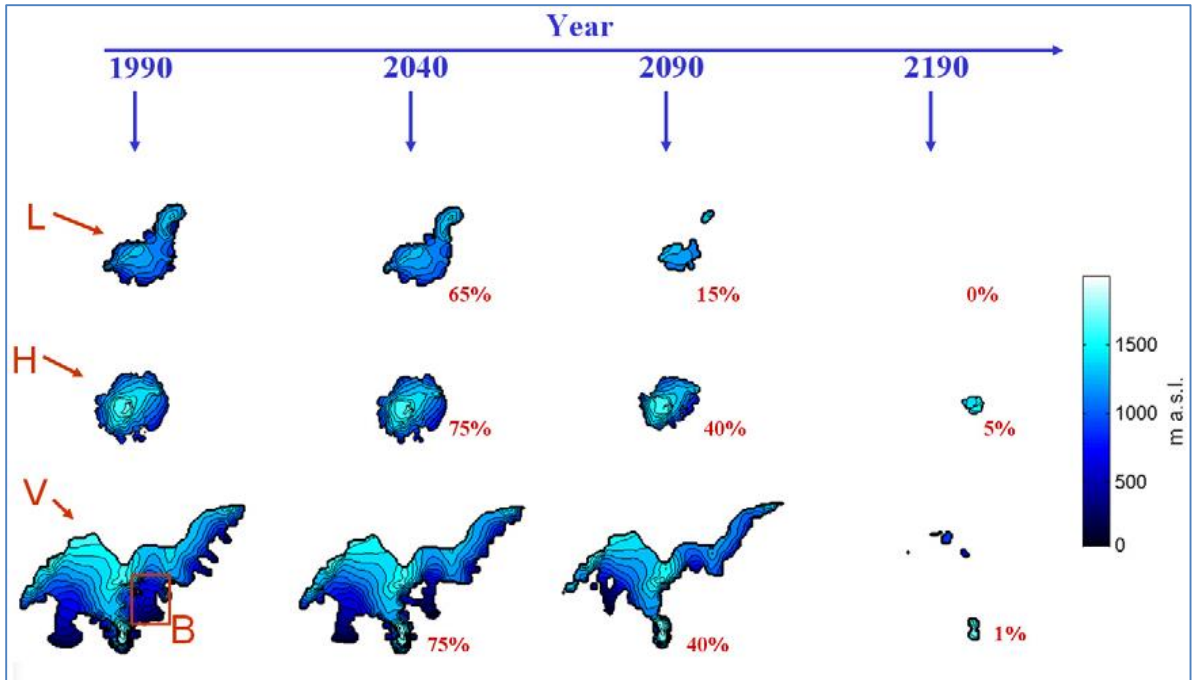


Figure 2.1. Simulated responses of icecaps to the climate-change scenario. Langjökull (L), Hofsjökull (H), and southern Vatnajökull (V) from 2000 through 2200, with the map oriented to the north.

Source: Aðalgeirsdóttir et al. (2006).

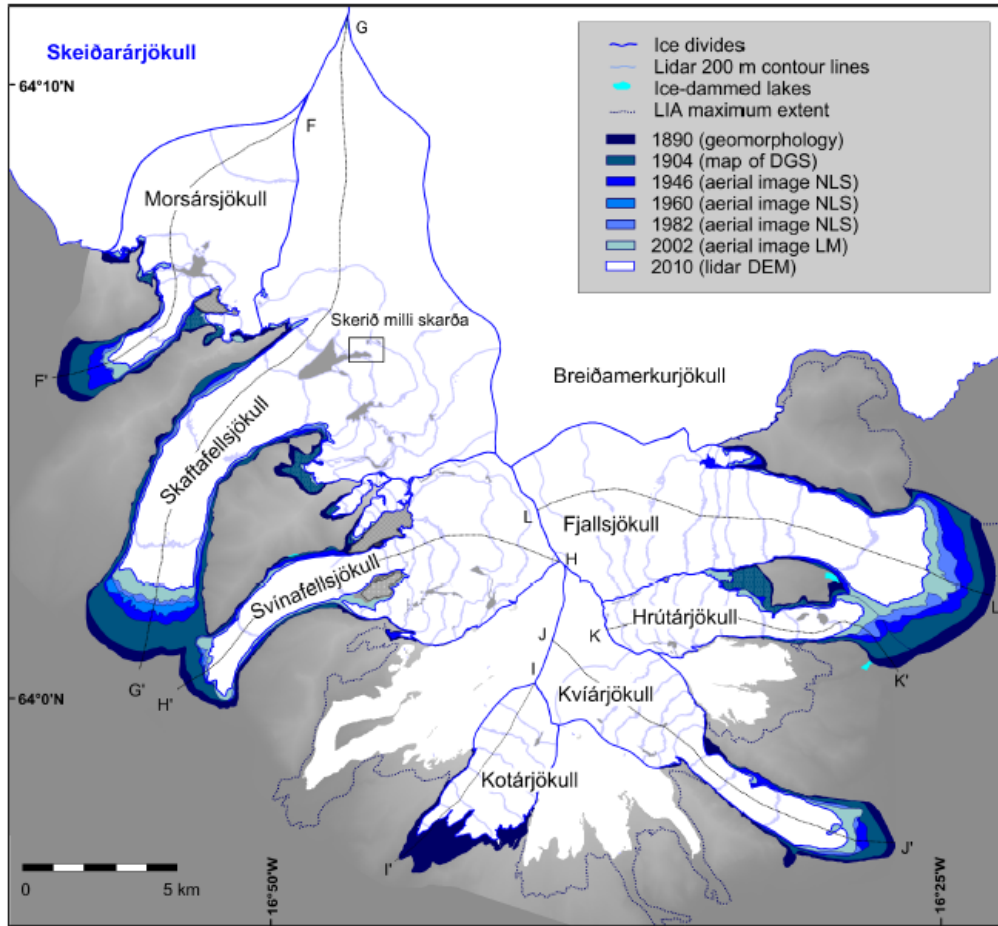


Figure 2.2. The extent of southeast Vatnajökull glacier outlets at different times. Map is oriented to the north.

Source: Hannesdóttir et al. (2015).

Plausible predictions of regional temperature and precipitation trends in Iceland were developed by the Nordic project Climate and Energy (Rummukainen 2006; Fenger 2007; Jóhannesson et al. 2007; Thorsteinsson and Bjornsson 2011), based on downscaling of global coupled atmosphere-ocean simulations. In comparison to the period 1961–1990, the project scenario predicts a warming of 2.8 °C and a 6% increase in precipitation by 2071–2100. Moreover, 2001–2010 was the warmest decade in Iceland since 1950 (Figure 2.3).

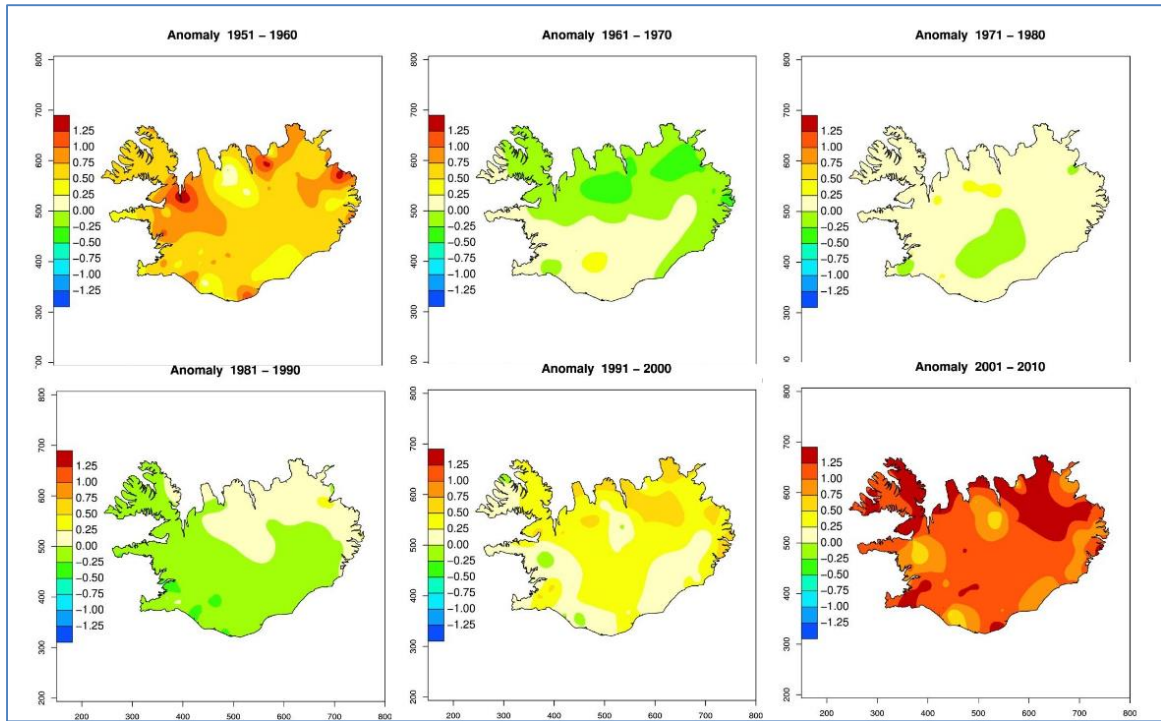


Figure 2.3. Change in temperature in Iceland. The color scale indicates departures in °C from 1951 to 2010. Map is oriented to the north.  
Source: Crochet and Jóhannesson (2011).

### 2.3 Hydrogeochemistry of Glacial Meltwater

Hydrogeochemical studies are important in identifying contributions from atmospheric inputs to the observed ions of meltwaters. Melting of snow can cause migration of soluble and insoluble impurities (Goto-Azuma et al. 1994). The solute composition of meltwater from a seasonal snowpack can significantly affect the water quality of snow-fed streams and lakes. The chemical composition of meltwater can also differ due to seasonal influences. Most of the soluble ions stored within a snowpack are removed by the first fractions of snowmelt, and ionic concentrations of snow pack and runoff water tend to decrease as the melting proceeds (Jóhannessen and Henriksen 1978; Colbeck 1981; Suzuki 1982).



Based on studies of a glacier in the Himalaya, Hasnain et al. (1989) reported that meltwaters from the glacial surface have a low solute content, whereas, after passing through the glacier, waters were found to be enriched chemically. Variations of solute concentration in meltwaters at the terminus are related to their discharge (Krishna 2011). Anderson et al. (1997) found that sediment yields were high from glaciers, which suggests that water flux, rather than physical erosion, exerted the primary control on chemical erosion by glaciers. As such, the geology of the area is the primary control on stream chemistry and some findings state that low temperatures, high dissolved oxygen, low total dissolved solids, and water rich in calcium and bicarbonate characterize clear water tributaries of snow-fed rivers. Dilution of dissolved salts takes place, due to factors like high specific runoffs and seasonal variations (Krishna 2011). Conversely, glacially fed tributaries have a slight higher dissolved load and, in order of magnitude, greater turbidity and suspended sediment loads (Maurer and Scott 1992).

Different types of weathering and ions dominate glacial meltwater systems. Analysis of surface water chemistry in the Everest region revealed aluminosilicate weathering to be the main source of dissolved cations and Si, with carbonates exerting an important control on surface water chemistry (Reynolds et al. 1995). In addition, the dominance of carbonate weathering as a major source for dissolved ions was revealed in a study of the Gangotri Glacier, India (Singh et al. 2012). A recent study of glacial streams revealed an increase in the nitrate and total phosphorous concentration in high altitude rivers in Sagarmatha (Everest) National Park (Ghimire et al. 2013). The results from the study of the geochemistry of meltwater streams from nine Alaskan glaciers showed that they are similar, as Ca is the most abundant ion and the cold waters have a

basic pH (Slatt 1972). The suspended load concentration is controlled by stream conditions during the time of sampling, including discharge.

High pH and varied electric conductivity were found in river water from a temperate glacier basin in China during the rainy season (Tao et al. 2013); Ca and Mg were dominant, accounting for about 90% of the total cations.  $\text{HCO}_3^-$ , followed by  $\text{SO}_4^{2-}$ , were the dominant anions. Precipitation and carbonate rock weathering influence river water chemistry in the rainy season and are the primary influences on ion concentrations.

Changes in climate and hydrochemical responses were studied in a high-elevation glacier in the U.S. Rocky Mountains in order to determine changes in temperature, solar radiation, and precipitation in the solute concentrations of snowpack meltwater (Williams et al. 1996). The maximum concentrations of  $\text{NH}_4^+$ ,  $\text{NO}_3^-$ , and  $\text{SO}_4^{2-}$  in snowpack meltwater were nearly four times that of bulk concentrations in a collocated snow pit. Moreover, the conductivity was four times higher in 1995 compared to 1994. Changes in climate may also influence the chemical content of stream water in high-elevation catchments by changing chemical loading from atmospheric deposition. The results indicated an increase of ~200% in  $\text{NO}_3^-$  loading from wet deposition at Niwot ridge over the last decade. Increases in precipitation in mountainous areas could directly result in an increase in the wet deposition of atmospheric pollutants, even with no increase in ambient concentration of those types of pollutants.

The major weathering process in the supraglacial streams of the Canada Glacier, Taylor Valley (Antarctica) is believed to be calcite dissolution, with little to no silicate weathering (Fortner et al. 2005). The Western Canada Glacier supraglacial streams have average  $\text{SO}_4^{2-}:\text{HCO}_3^-$  equivalent ratios of 1.0, while eastern supraglacial streams average

0.5, suggesting more sulfate salts reach and dissolve in the western supraglacial streams. Controls on glacier meltwater geochemistry switched from calcite and gypsum dissolution to both salt dissolution and silicate mineral weathering, as the glacier melt water evolved over time.

Fortner et al. (2009) determined minor and trace element concentrations of As, Cu, Cd, V, Sr, F, and major ions including Ca, Na, Mg, K, SO<sub>4</sub>, HCO<sub>3</sub>, and NO<sub>3</sub> in snow and in proglacial meltwater from Eliot Glacier, Mount Hood, Oregon. Metal:S and Metal:Cl ratios indicated negligible volcanic and marine aerosol deposition (less than 2% v/v). Crustal enrichment factors (EFs) indicated the V, Sr, and Cu in the fresh snow are derived primarily from lithogenic sources (EF<1.4). As with many other locations, including glaciers in Greenland, Italy, and Bolivia, Pb is enriched anthropogenically in Eliot Glacier snow. During the ablation season, soluble salts leach, or elute, from Eliot Glacier snow, similar to what has been observed on other temperate glaciers. Conversely, acid-leachable trace elements from particulate matter were enriched in ablation snow compared to fresh snow. This suggests that trace elements were added throughout the year via dry-deposition, including anthropogenic emissions, or are not readily dissolved during the melt season. The majority of the Eliot Glacier fresh snow SO<sub>4</sub> was non-marine, which could be introduced by anthropogenic or natural sources. The solute concentrations of all trace elements measured in the Eliot stream and glacier were well below drinking water standards and posed no immediate threats to water quality.

The study by Welch et al. (2010) detailed the importance of aeolian deposition to environmentally available elemental concentrations and distribution in Taylor Valley, Antarctica. Trace elements (As, Cd, Cu, Eu, Mo, Nd, Pr, Pt, Rb, Sm, Sr, Th, and U) were

derived almost exclusively from aeolian dust. The major ion and trace element chemistry was examined in four 60 to 105 cm deep snow pits from three Taylor Valley (TV) glaciers. All TV trace element and Ca concentrations were highly variable, both spatially and at depth, with many elements spanning three orders of magnitude, illustrating the episodic and variable nature of aeolian deposition. Proximity to valley floor sediment, wind intensity, wind direction, and glacier surface aspect explain the large degree of chemical heterogeneity between three nearby (<10 km) glacier accumulation zones.

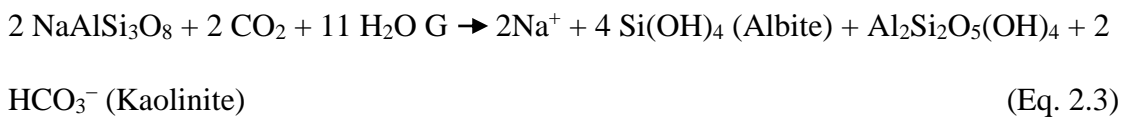
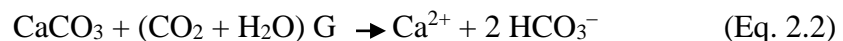
Variations in dissolved cations, total alkalinity, sulfate, and field pH values were recorded for subglacial melt and bulk meltwater at Argentière, France, in peak and recession flow conditions (Raiswell and Thomas 1984). Calcium and bicarbonate were the major cations and the bulk meltwaters acquired solutes by weathering and dissolution in a system open to atmospheric CO<sub>2</sub>. The subglacial meltwaters have closed-system characteristics and were close to saturation with calcite and quartz. Rogora et al. (2003) studied the effect of climate warming on the hydrochemistry of Alpine lakes. For lakes lying in catchments with highly soluble rocks, a comparison between the two datasets showed an increase of solute contents over the last few years. This result could be attributed to increased weathering rates, due to climate warming, but longer-term studies are needed to determine these rates. A hydrochemical study in western Greenland found Ca as the dominant cation and HCO<sub>3</sub> as the dominant anion in watersheds (Lesnek et al. 2014). Concentration of these ions increased with distance from the glacier due to the dissolution of micas, hornblende, and albite. Deglaciating watersheds had higher salinity than proglacial watersheds due to evaporative concentration of the solutes.

## 2.4 Processes Controlling the Hydrochemistry of Glacial Meltwater

The hydrogeochemical composition in glacier meltwater depends upon different factors, such as bedrock geology (Garrels and Mackenzie 1971), atmospheric deposition (Gibbs 1970; Nijampurkar et al. 1993), anthropogenic activities (Galloway 1988), and climate change (Rogora et al. 2003), interacting with each other. Collectively, these influences cause changes in the meltwater as it is released from the glacier layer by layer over time, and can also make it challenging to determine the primary influences.

### 2.4.1 Bedrock Geology

The rocks and sediments through which the water flows primarily control the natural hydrogeochemistry of streams and rivers. Weathering of rocks is the dominant mechanism controlling the hydrochemistry of drainage basins, which occurs when water flows at the ice-rock interface (Garrels and Mackenzie 1971). Chemical reactions occurring in the drainage basins are the primary source of solutes to rivers (Krishnaswami and Singh 2005). These reactions are of three types:



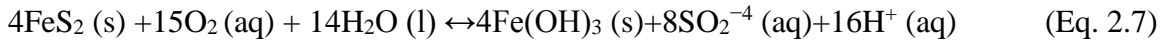
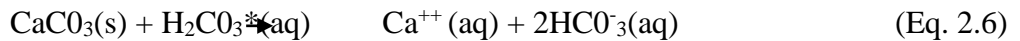
Reaction type one (Eq. 2.1) can be an important source of ions to rivers draining terrains containing evaporites and saline/alkaline soils, whereas the reaction types in Equations 2.2 and 2.3 require protons for initiation. The most common source of protons (H<sup>+</sup>) in rivers is carbonic acid generated by solution of CO<sub>2</sub> from the atmosphere in rain and from soil gas in river waters. Another source of protons for these reactions is sulfuric

acid from the oxidation of pyrites ( $\text{FeS}_2$ ). In certain regions, where there are abundant pyrites and other sulfides, there can be significant production of  $\text{H}_2\text{SO}_4$ .

The partial pressure of carbon dioxide ( $p\text{CO}_2$ ) of a solution reflects the rate at which  $\text{CO}_2$  diffuses into, or out of, solution relative to the rate of other chemical reactions. The effective  $\text{CO}_2$  pressure, or internal  $\text{CO}_2$  pressure ( $\log p\text{CO}_2$ ), can be estimated from pH values and  $\text{HCO}_3^-$  concentration. If the  $p\text{CO}_2$  of solutions is not equal to atmospheric  $p\text{CO}_2$  ( $10^{-3.5}\text{atm}$ ), it is in disequilibrium with respect to the atmosphere. When the supply of protons is more than their consumption, then high  $p\text{CO}_2$  conditions arise. Low  $p\text{CO}_2$  conditions arise when the demand of protons for chemical weathering is more than the rate of  $\text{CO}_2$  diffusion into solution (Wadham et al. 1998). The relationship between atmospheric  $\text{CO}_2$  concentrations, temperature, and the hydrologic cycle is important, as high  $\text{CO}_2$  concentrations elevate temperature, leading to a more vigorous hydrologic cycle, which, in turn, promotes extensive silicate weathering and deeper regolith development (Jacobson et al. 2015). As atmospheric  $\text{CO}_2$  levels decline, the hydrological cycle's feedback processes diminish.

The relative importance of two major proton-producing reactions, carbonation and sulfide oxidation, can be evaluated on the basis of the C-ratio ( $\text{HCO}_3^-/\text{HCO}_3 + \text{SO}_4$ ). If the carbon ratio is closer to 1, this indicates the significance of carbonation reaction involving acid hydrolysis and pure dissolution, consuming protons from atmospheric  $\text{CO}_2$  (Brown et al. 1996) (Equations 2.4, 2.5, 2.6). Conversely, if the C ratio is 0.5, this suggests a coupled reaction involving carbonate weathering and protons derived from oxidation of sulfides (Equation 2.7) (Brown et al. 1996). The chemical weathering reactions in the bulk meltwater can reflect the following reactions (Raiswell 1984;

Tranter et al. 1993; Brown et al. 1996). Weathering of  $\text{CaCO}_3$ , or calcite dissolution, is the main mechanism of solute acquisition (Brown et al. 1996), since:



where  $(g)$ ,  $(l)$ ,  $(aq)$ , and  $(s)$  denote gaseous, liquid, aqueous, and solid phases, respectively. The type, size, and debris cover of a glacier also cause profound changes in the chemical composition of glacial meltwaters. This difference may affect not only discharge amounts but also the chemical composition and fluxes of dissolved species in glacier river meltwaters.

#### 2.4.2 Anthropogenic Inputs

The chemical compositions of low-salinity waters are controlled by the amount of dissolved salts furnished by precipitation (Gibbs 1970). The emission, long-range transport, and deposition of pollutants are likely to increase with future industrialization (Galloway 1988). Major ion abundances in rivers can be modified by anthropogenic inputs, such as discharge of sewage, industrial and mining effluents, and supply from fertilizers, which can be sources for the following (Krishnaswami and Singh 2005):

- Na, Cl (NaCl in sewage, mining of sodium salts, solution of road salt, etc.),
- $\text{SO}_4$  (fertilizers, mining of pyrites, industrial wastes, atmospheric deposition from fossil fuel burning, etc.), and
- Nutrients (nitrogen and phosphorus compounds, mainly from fertilizers).

### 2.4.3 *Effect of Climate Change on Glacier-Fed Water Resource Chemistry*

Climate change impacts not only the temperature of water, but also the physiochemical properties and ecology of water. Climate warming seems to be particularly pronounced in the Alpine region, and the Himalayan rivers are expected to be very vulnerable to climate change because snow and glacier meltwater contribute substantially to their runoff (Singh et al. 1998; Rogora et al. 2003). Climate change induced reduction of snow cover over space and time, due to less precipitation and higher temperatures, means a greater exposure of rocks and soils in the watersheds, which enhances weathering processes. The enhanced weathering rate, in turn, has led to an increase solute content in European lakes (Rogora et al. 2003).

Similarly, surveys of lake water chemistry in the Khumbu Valley, Himalaya, reveal a persistent increase in the ionic content of the lake water, a trend that appears to be closely linked to increasing temperature (Lami et al. 2010). Increased temperature also results in increased rates of (bio-) chemical processes and decreased oxygen concentration in the water bodies, which, in turn, change stratification patterns (Viviroli et al. 2011). Moreover, extreme events like heavy precipitation and drought could lead to a series of changes in the water quality, like decreasing water transparency and the salinization of surface waters (Viviroli et al. 2011).

A study on spatial variations in the geochemistry of glacial meltwater streams in Taylor Valley, Antarctica, found that controls such as landscape position, channel morphology, and biotic and abiotic processes are believed to influence the stream chemistry (Welch et al. 2010). Sea-salt derived ions tend to be higher in streams that are closer to the ocean and those streams that drain the Taylor Glacier. Nutrient availability is



dependent on landscape age and varies with the distance from the coast. The streams in Taylor Valley span a wide range in composition and total dissolved solids and are surprisingly similar to the range of temperate and tropical river systems.

## 2.5 Hydrogeochemical Studies in Iceland

Several hydrogeochemical studies were conducted in the southeastern and eastern parts of Iceland. A study on solute acquisition in meltwaters of Fjallsjökull in southeast Iceland revealed variations in dissolved cations, total alkalinity, sulphate, and field pH, as recorded for samples for precipitation, supraglacial melt, and bulk meltwaters.

Supraglacial melt had a higher solute content and total alkalinity than precipitation but similar  $p\text{CO}_2$  values, indicating equilibrium with the atmosphere. The bulk meltwaters have higher solute contents, pH, and alkalinity than supraglacial melt, but have lower  $p\text{CO}_2$  values indicating chemical evolution in a closed system (Raiswell and Thomas 1984). A precipitation and snow-chemistry study on the Vatnajökull glacier revealed that the chemistry of Icelandic precipitation is dominated by marine aerosol contributions, with the exception of sulfate and calcium where some “excess concentration” is present (Gislason 1990). The increase in concentration of salts in the snow, collected in June 1988, with elevation, was attributed to chemical fractionation caused by the partial melting of snow. During partial melting the chemical constituents are preferentially leached from the snow and some ions are more readily released than others. The order of preferential release of ions from the partially melted snow is  $\text{H}^+ > \text{Mg}^{2+} > \text{Cl}^- \geq \text{Na}^+ > \text{SO}_4^{2-} > \text{K}^+ > \text{Ca}^{2+}$ . The average pH of the 1987-1988 layer was 0.28 to 0.14 units lower than the pH of the 1986-1987 layer below. The preferential release of protons from the snow caused the pH of the meltwater to be lower than the pH of residual snow.

Analysis of silicate versus carbonate weathering in Iceland discovered that 90% of the Ca in Icelandic rivers originates from the weathering of hydrothermal calcite, as opposed to Ca-bearing silicate minerals (Jacobson et al. 2015). The feedback between climate and weathering in pristine northeastern Iceland river catchments with varying glacial cover has been studied over 44 years (Gislason et al. 2009). The mean annual temperature of those catchments varied by 3.2 to 4.5 °C during the study period. For each degree of temperature increase, the runoff, mechanical weathering, and chemical weathering fluxes in these catchments were found to increase from 6 to 16%, 8 to 30%, and 4 to 14%, respectively, depending upon the catchment. Mechanical and chemical weathering increased with time in all catchments over the 44-year period. This study proved that chemical and mechanical weathering fluxes depend upon climate via changing temperature and runoff.

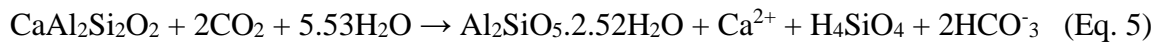
Eiriksdottir et al. (2015a) studied direct evidence of the feedback between climate and nutrient and major and trace element transport to the oceans. The study presented the climate effect on annual fluxes of 28 dissolved elements, and organic and inorganic particulate fluxes, determined over 26-42 periods in three glacial and three non-glacier river catchments located in eastern Iceland. Climate change affects the various elemental fluxes differently. In general, the more soluble the element, the more it is diluted as runoff increases. The dissolved fluxes of the more soluble elements, such as Mo, Sr, and Na, were less affected by increasing temperature and runoff than the insoluble nutrients and trace elements, including Fe, P, and Al. The dissolved fluxes of trace elements, which tend to be insoluble, were affected to a larger degree by changes in temperature and runoff than those of the soluble major elements. The study showed that

variation between the elements tends to be more pronounced for the glacial, compared to the non-glacial, rivers. The increase in particle fluxes to the oceans with increasing average air temperature and runoff is approximately twice than observed for the corresponding dissolved fluxes in the glacial rivers. It was found that the climate effect on particle transport from the glacial rivers is far higher than all other measured fluxes. This observation, together with the finding that the flux to the oceans of limiting elements such as P and Fe is dominated by particulates, suggests that particulate transport by melting glaciers has a relatively strong effect on the feedback between continental weathering, atmospheric chemistry, and climate regulation over geologic time. The results of the study demonstrated that fluxes of nutrient, trace, and major elements towards the ocean have increased substantially in the rivers of eastern Iceland over the 40-year study period in response to global warming and increased runoff.

A study on the glacial river, Jökulsá á Dal, conducted from 1998 to 2003, aimed to constrain the natural discharge regime and fluxes of suspended and dissolved material (Eiriksdottir et al. 2017). The dataset collected was used to demonstrate natural changes within the catchments and to assess the effect of climate on chemical weathering rates within the catchment. There was a positive correlation between riverine discharge and suspended load, but the correlation was negative between discharge and the concentrations of most dissolved elements (e.g., SiO<sub>2</sub>, Na, Ca, Mg, DIC, SO<sub>4</sub>, Cl, F, Sr, Mo). Eiriksdottir et al. (2014) recently studied the impact of anthropogenic alterations on river regimes and the environment in Iceland. Precipitation in southern Iceland has been monitored for decades to study long-term changes. The acid rain caused environmental damage on the continent but, after new regulations limited industrial emissions of

anthropogenic sulfur from Europe and North America, pH in the precipitation from southern Iceland increased (from 5.0 to 5.7) between 1980 and 1998. However, since 1998, the pH has once again started to decrease (from 5.7 to 5.4). The timing of this acidification of precipitation is concurrent with increased riverine sulfur fluxes in the region. The proposed causes of these changes are the development of the Nesjavellir geothermal power plant in the vicinity, which started producing electricity in 1998, and the construction and operation of the Hellisheidi geothermal power plant since 2006.

Chemical weathering of Ca-Mg silicates is a CO<sub>2</sub> sink (Eq. 5), since it consumes CO<sub>2</sub> from the atmosphere and releases divalent cations, which will react with the CO<sub>2</sub> to erode carbonate rocks (Walker et al. 1981; Berner et al. 1983).



For each 1°C of temperature change, chemical weathering changes of 2-10% have been used in models for calculating the CO<sub>2</sub> concentration of the atmosphere over the past 0.5 Ga (Wallmann 2001). In Iceland, it is expected that changes in both precipitation and chemical weathering should be higher than the global averages, due to the highly reactive basaltic bedrock easily weathering compared to other silicate rocks (White and Brantley 2003; Dupré et al. 2003; Gislason and Oelkers 2003). Icelandic rainwater is relatively rich in marine salts, due to the location of the island in the middle of the North Atlantic and to high average wind speed.

The relative role of temperature and runoff on chemical denudation rates in seven northeast Iceland river catchments was determined through the analysis of river water chemistry collected over a five-year period from 1998 to 2003 (Eiriksdottir et al. 2015b). Denudation rates were quantified from the instantaneous riverine Na fluxes. As sodium is

the major element least incorporated into secondary phases, its denudation rate is directly related to the dissolution rate of the catchments' primary rocks. Data analysis suggested that the Na chemical denudation rates of the northeast Icelandic catchment rocks increase by 13% for each degree C increase in temperature. The maximum temperature variation of the studied rivers was 15.4 °C, which would increase Na chemical denudation rates by a factor of six.

The formation of glacial lakes and installation of dams can impact the transport of riverine dissolved and particulate material to the ocean. A study on the impact of the installation of the Krahnjukar Dam in eastern Iceland revealed that the annual flux of most dissolved elements increased substantially due to the damming (Eiriksdottir et al. 2017). The fluxes of dissolved Zn, Al, Co, Ti, and Fe increased most by damming; these fluxes increased by 46 to 391%. Damming a glacial river catchment causes accumulation of large amounts of particulate matter, which otherwise would be carried to the ocean, and affects the particulate flux of non-soluble elements and essential nutrients in coastal waters (Oelkers et al. 2012; Jeandel and Oelkers 2015). Reduction of riverine particulate transport, due to damming of glacial rivers, can diminish the fertility of coastal waters. Glacial rivers are an important source of sand to the shorelines, which, if dammed, can lead to an increase in cumulative coastal erosion (Pilkey et al. 2011).

Samples of precipitation were collected and analyzed from four sampling stations in southern Iceland by Eiriksdottir et al. (2014). Sea salt ratios in the precipitation were identical to those in seawater, except Ca and SO<sub>4</sub>, which were enriched with respect to seawater. Sea salt concentrations in rainwater decreased with distance from the shore. The Eyjafjallajökull eruption in 2010 caused increased concentrations of fluoride in

precipitation in Mjóanes from May to July, 2010, but did not affect concentrations of other components measured. The annual average F concentration in the precipitation in 2010 was 2.4 times higher than during 2008-2009 and 2011-2012. From 1998 to 2004, sulfur in the river appeared in the form of  $\text{SO}_4$ , but from 2005 to 2010 sulfur was present in forms other than  $\text{SO}_4$ . At the same time, sulfur isotope ratios became lighter, indicating sulfur from volcanic/geothermal emissions.

The impacts of subglacial geothermal activity on meltwater quality in the Jokulsa, a Solheimasandi glacial meltwater river in southern Iceland, were studied by Lawler et al. (1996). Background  $\text{H}_2\text{S}$  concentrations for the Jokulsa meltwaters in summer 1989 showed that leakage of geothermal fluids into the glacial drainage network took place throughout the melt season. A major event of enhanced geothermal fluid injection was also detected. Against a background of an apparently warming geothermal reservoir, the event began on Julian day 205 (24 July) with a burst of subglacial seismic activity. Meltwater hydrochemical perturbations followed on day 209 and peaked on day 210, finally leading to a sudden and significant increase in flow on day 214. The hydrochemical excursions were characterized by strong peaks in meltwater  $\text{H}_2\text{S}$ ,  $\text{SO}_4$ , and total carbonate concentrations, transient decreases in pH, small increases in Ca and Mg, and sustained increases in electrical conductivity. The event may relate to temporary invigoration of the subglacial convective hydrothermal circulation, seismic disturbance of patterns of groundwater flow, and geothermal fluid recruitment to the subglacial drainage network, or a cyclic sweeping out of the geothermal zone by the annual wave of descending groundwater (Lawler et al. 1996). Because increases in flow follow

hydrochemical perturbations, they suggest there exists a potential to use meltwater hydrochemistry to forecast geothermally driven flood events in such environments.

The chemical composition of dissolved, degassed, and suspended fluxes of the 2002 Skaftá glacial flood, which emerged from one of the Skaftá subglacial lakes due to geothermal activity beneath the Icelandic Vatnajökull glacier, was studied by Galeczka et al. (2015). Concentrations of most dissolved elements during the flood were significantly higher than normally observed in the Skaftá River. In addition, dissolved concentrations of nutrients, such as SiO<sub>2</sub>, Fe, and V, increased more than an order of magnitude during the flood. The composition of the floodwater and the Skaftá subglacial lake, together with reaction path modeling, suggested that substantial degassing of CO<sub>2</sub> and H<sub>2</sub>S occurred at the glacial outlet during the flood. This degassing may have released as much as 262,000 and 7,980 tons of CO<sub>2</sub> and H<sub>2</sub>S, respectively, to the atmosphere, having a considerable impact on the local carbon and sulfur cycles during the flood event.

Future climate change effects have been investigated by an analysis of records, and by modeling (Jóhannesson et al. 2007). The runoff is projected to increase by 25% between 1961–2000 and 2071–2100, mainly due to increased melting of glaciers, which may disappear almost completely within the next 200 years (Thorsteinsson and Bjornsson 2011). Subglacial water courses and outlet locations of many glacial rivers are likely to change, due to the thinning of icecaps and the retreat of glacier margins. A substantial increase in the potential use of gravitational hydropower is projected and the changes in runoff, seasonality, and water flowpath require modifications in design assumptions and the operating environment of hydropower plants and other hydrological infrastructure, such as bridges and roads.

## Chapter 3

### 3.0 Study Area

An island of 103,000 km<sup>2</sup>, Iceland is located in the North Atlantic Ocean, close to the Arctic Circle. Icelandic glaciers are “warm based,” or “temperate,” and are dynamic in nature, as they respond actively to minor climate fluctuations. They constitute long-lasting reservoirs of ice that turn to meltwater and feed the country’s main rivers, some of which have been harnessed for hydropower. These icecaps conceal unexplored landforms and geological structures, including active volcanoes, geothermal sites, and subglacial lakes. Catastrophic floods (jökulhlaups) from meltwater pulses, often caused from volcanic heating and eruption below the ice, are frequent, and active volcanoes exist under 60% of the modern glaciated terrain (Björnsson and Pálsson 2008). Glaciers cover about 10% of the country and that number is declining each year (Björnsson 1978, 1979; Thorsteinsson et al. 2013). The country’s glaciers feed its largest rivers and currently provide at least one-third of the total runoff into rivers.

Iceland enjoys a relatively mild oceanic climate and small seasonal variations in temperature due to the warm Irminger current, which is a North Atlantic Ocean current settling westward off the southwest coast of Iceland. A branch of the Gulf Stream flows along the southern and western coast greatly moderating the climate. This brings mild Atlantic air in contact with colder Arctic air, resulting in a climate that is marked by frequent changes in weather leading to more rainfall in the southern and western areas than in the northern part of the island. Average winter temperatures hover around 0°C near the southern coast, where the average temperature of the warmest month is only 11 °C and the mean annual temperature is about 5 °C (Einarsson 1984). The polar East



Greenland Current along the northern coast, which occasionally brings snow ice, affects the climate. The pattern of precipitation in Iceland reflects the passage of atmospheric low-pressure cyclones across the North Atlantic Ocean from a southwesterly direction, exposing the southern coast to heavy precipitation. Precipitation is highest in Iceland on the southern side of the Vatnajökull ice cap, measured at Kvísker, measured at 1,000-4,000 mm/year (Hannesdottir et al. 2013). Figure 3.1 is a topographic map of Iceland with glacier distribution; smaller glaciers border the main icecaps. The geological map insert in Figure 3.1 shows the active volcanic zone and the central volcanoes.

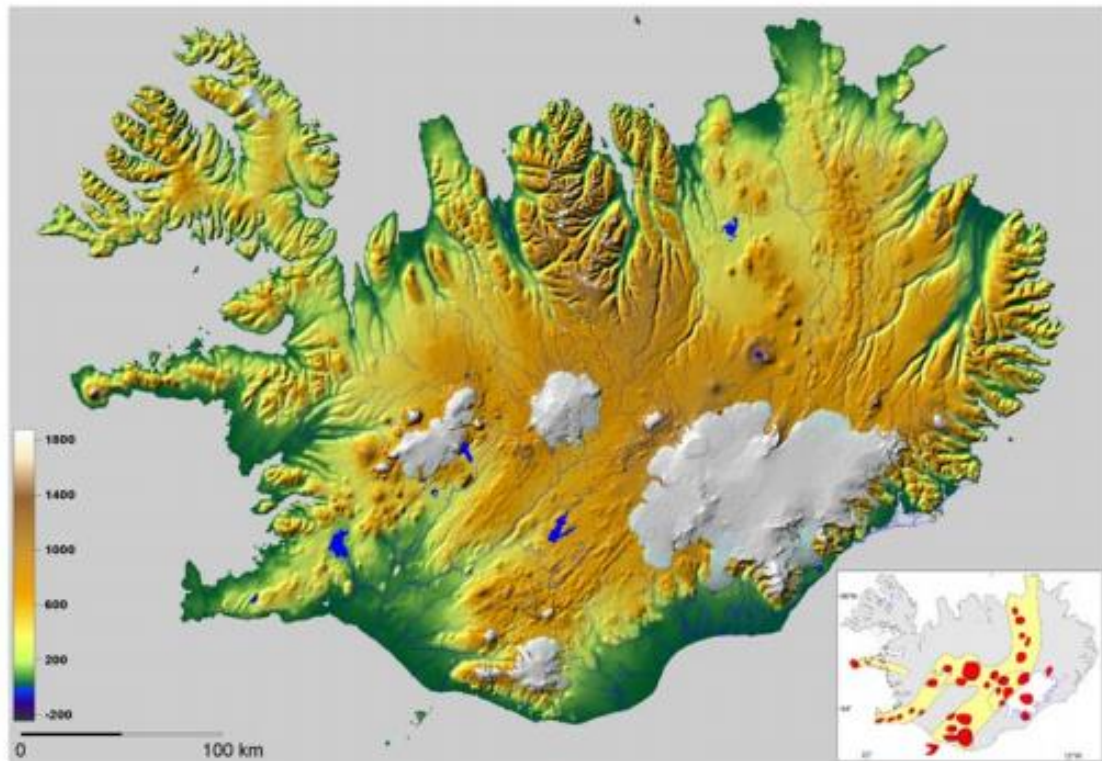


Figure 3.1. Topography of Iceland. Map is oriented to the north.  
Source: Björnsson and Pálsson (2008).

Iceland is geologically young, with all of its rocks forming over the last 16 million years. The surface of Iceland has changed radically during its brief existence by construction (i.e., volcanism and sedimentation) and degradation (i.e., erosion). Iceland

consists mainly of volcanic (igneous) rocks built up during the Miocene, Pliocene, and Quaternary. These are, from older to younger, the Tertiary Basalt Formation, the Grey Basalt Formation, the Hyaloclastite (Móberg) Formation, and the youngest formation, which consists of unconsolidated or poorly hardened beds (like till or glaciofluvial deposits) (Einarsson 1994). Iceland is entirely composed of lava flows and eruptive hyaloclastites, with widespread sedimentary areas located in between. Igneous intrusions are quite common in the roots of inactive central volcanoes in southeast Iceland. Figure 3.2 shows the principal elements of the geology in Iceland, outlining the distribution of the major geological subdivisions, including the main fault structures, volcanic zones, and belts running throughout the island.

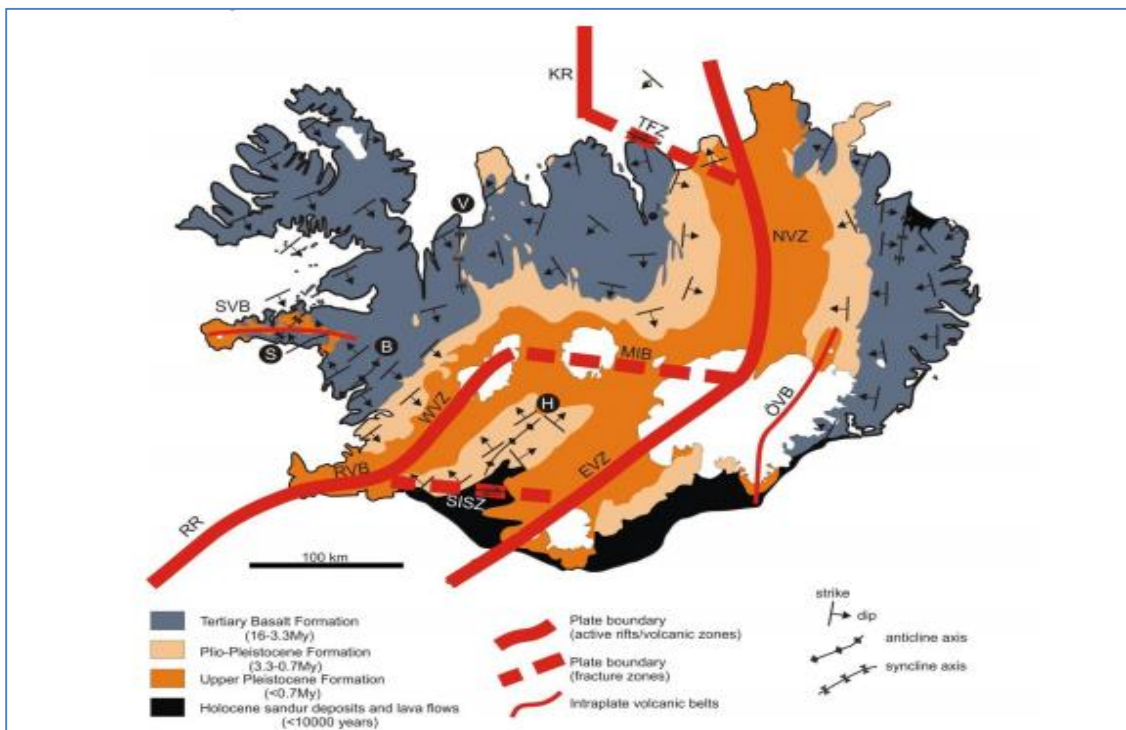


Figure 3.2. Principle elements of the geology in Iceland. Map is oriented to the North. RR, Reykjanes Ridge; RVB, Reykjanes Volcanic Belt; WVZ, West Volcanic Zone; MIB, Mid-Iceland Belt; SISZ, South Iceland Seismic Zone; EVZ, East Volcanic Zone; NVZ, North Volcanic Zone; TFZ, Tjörnes Fracture Zone; KR, Kolbeinsey Ridge; ÖVB, Örafi Volcanic Belt; and SVB, Snæfellsnes Volcanic Belt. Source: Thordarson and Hoskuldsson (2002).

Figure 3.3 shows the distribution of active volcanic systems among volcanic zones and belts in Iceland. The numbers denote the names of the fissure swarm. The large open circle indicates the approximate center of the Iceland mantle plume.

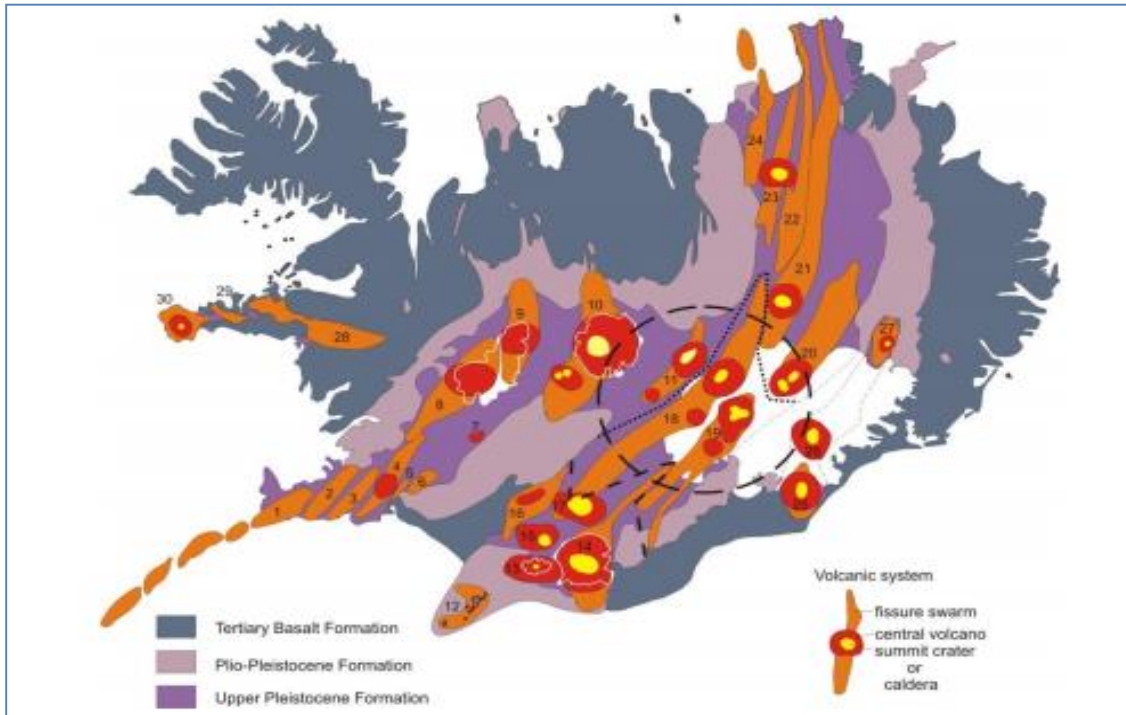


Figure 3.3. Distribution of active volcanic systems among volcanic zones and belts in Iceland. Map is oriented to the north.  
Source: Thordarson and Larsen (2007).

Figure 3.4 shows a map of Iceland with sampling sites. Table 3.1 shows the sampling sites with various outlet glaciers and icecaps. The sample codes denote the location of the sampling sites, with the first letter an initial for an icecap and the second and third letters as the outlet glacier. The numbers are assigned with respect to proximity to the glacier. For example, one denotes meltwater from the glacier, two denotes lagoon, and three denotes the river/outlet, most of which are close to a bridge (Figure 3.5). In codes containing only a one or a two, one denotes a lagoon and two denotes the outlet (Figure 3.6).

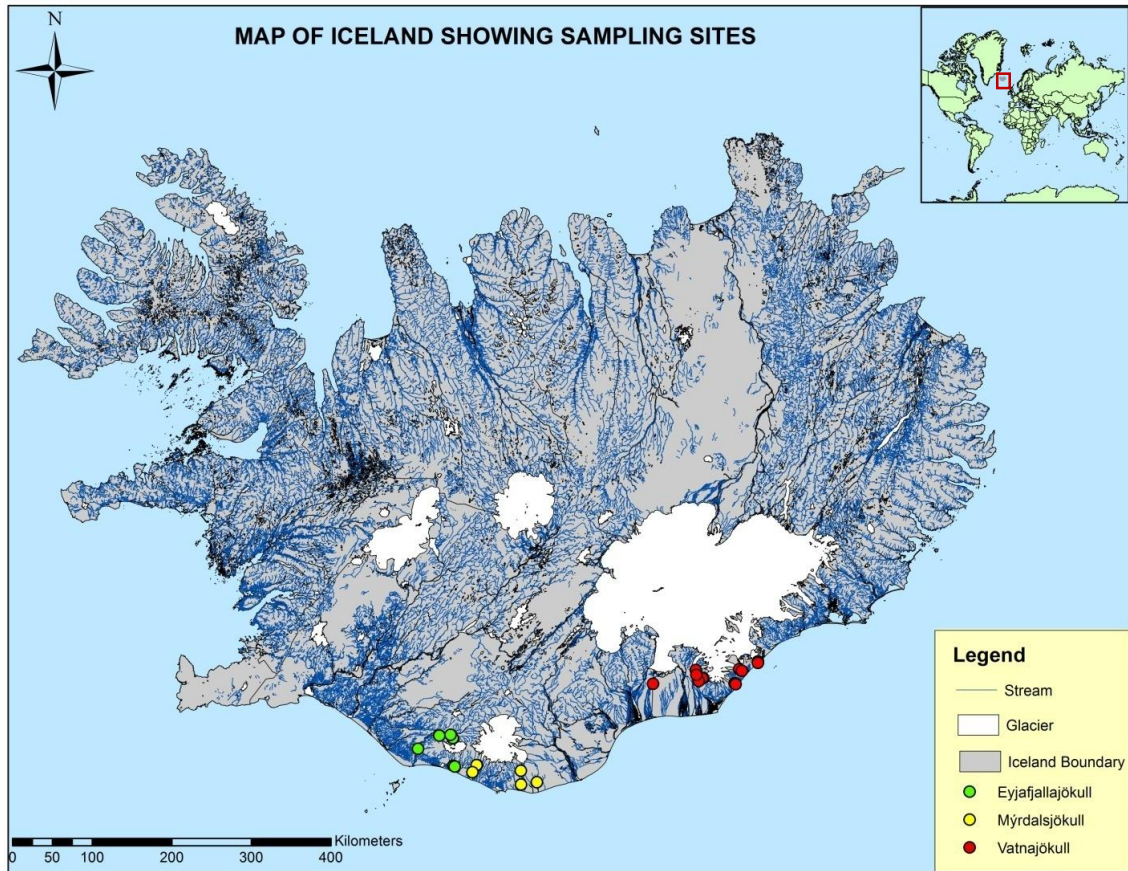


Figure 3.4. Map of Iceland showing sampling sites. The red box in the inserted world map shows the location of Iceland.

Source: Created by the author from an NLSI (2014) base map.

Table 3.1. Sampling sites and letter codes used for sampling.

Ice cap	Outlet glacier	Sample codes
Mýrdalsjökull	Solheimajökull	MSO1, MSO2, MSO3
Mýrdalsjökull	Kötlujökull	MKO1, MKO2, MKO3
Vatnajökull	Fjallsjökull	VFJ1, VFJ2
Vatnajökull	Jökulsárlón	VJS1, VJS2
Vatnajökull	Kvíárjökull	VKV1, VKV2
Vatnajökull	Falljökull	VFA1, VFA2, VFA3
Vatnajökull	Svínafellsjökull	VSV1, VSV2
Vatnajökull	Skeiðarárjökull	VSK1
Eyjafjallajökull	Gígjökull	EGI1, EGI2, EGI3
Eyjafjallajökull	Rivers	EYJ1, EJY2
Eyjafjallajökull	Seljavallajökull	ESE1
Eyjafjallajökull	Kaldaklifsjökull	EKA1

Source: Created by the author.

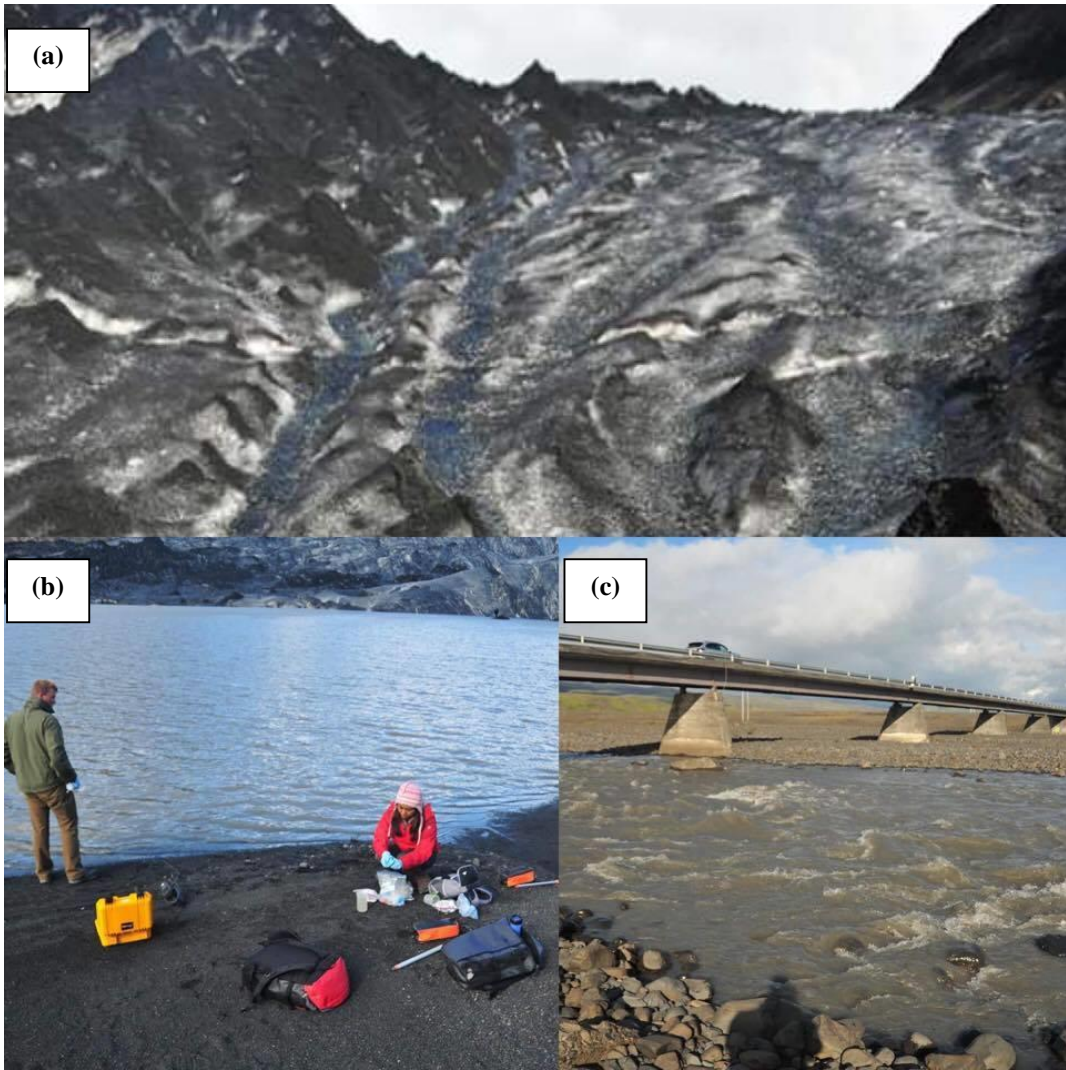


Figure 3.5. Sampling sites at Solheimajökull: (a) MSO1, (b) MSO2, and (c) MSO3  
Source: Photos courtesy of Dr. Jason Polk.

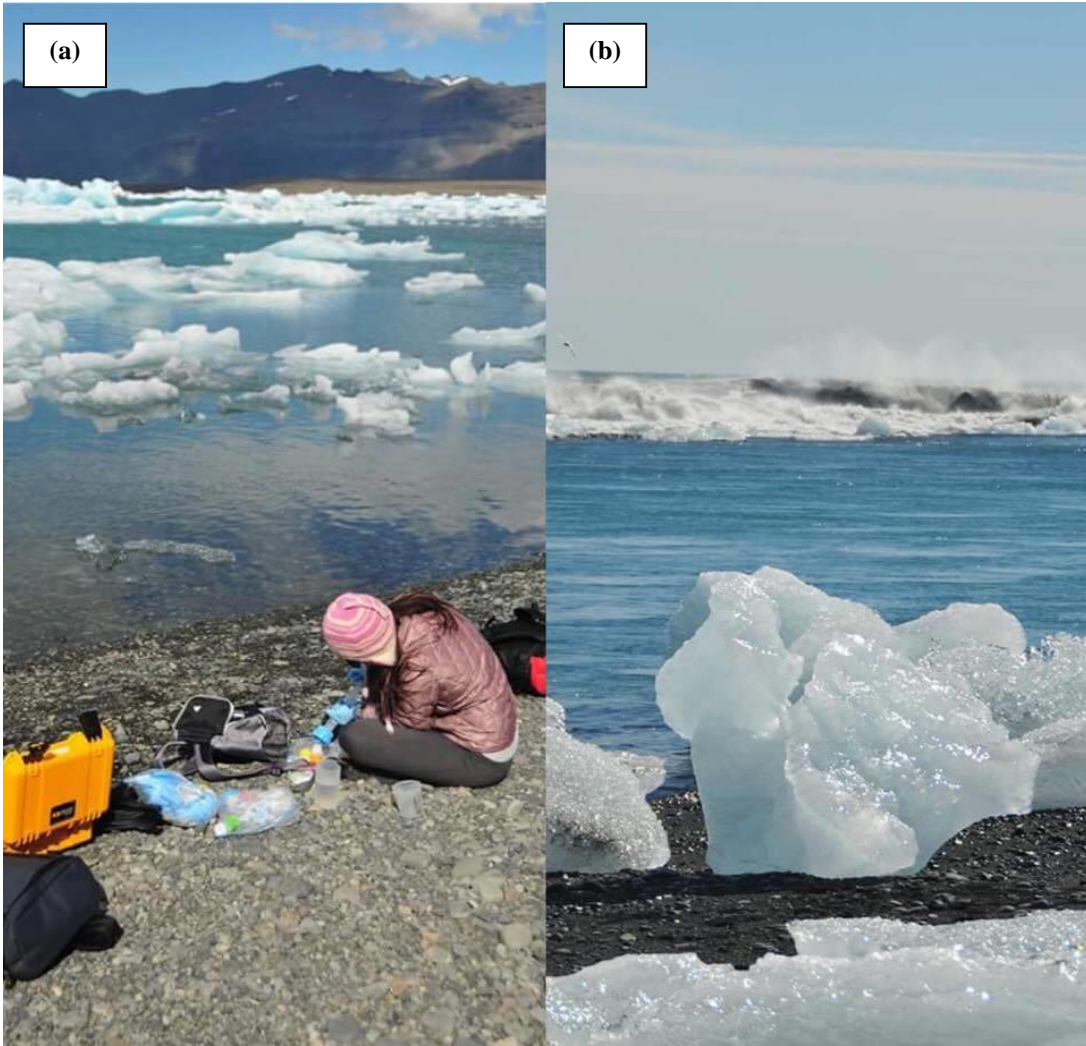


Figure 3.6. Sampling sites at Jökulsárlón: (a) VJS1 and (b) VJS2.  
Source: Photos courtesy of Dr. Jason Polk.

### 3.1 Vatnajökull

Vatnajökull is the largest ice cap in Iceland with the highest total volume. It is also one of the largest by area in Europe, with an area of 7,800 km<sup>2</sup> and an elevation of 2,110 m.a.s.l., covering more than eight percent of the country of Iceland (Bjornsson and Palsson 2008). The glaciers Fjallsjökull, Kvíárjökull, Falljökull, Svínafellsjökull, and Skeiðarárjökull, and the Jökulsárlón lagoon are outputs from the ice cap Vatnajökull (Figure 3.7). Falljökull is a tributary outlet glacier that merges with another glacier,

Virkisjökull, under debris cover on the western margin. In the period since 1932, Falljökull has undergone over 1,200 m of retreat, punctuated by one major advance of approximately 180 m, which took place between 1970 and 1990 (Sigurðsson 1998; Bradwell et al. 2013). Skeiðarárjökull is a surge-type glacier on the southern margin of Vatnajökull. To the south, the glacier terminates in the glacial lake of Fjallsjökull (Fjallsárlón). Samples were collected from Kvíárjökull, Falljökull, and Svínafellsjökull. Extrusive volcanic rocks, mainly basaltic lavas with some rhyolite, are dominant in the area and likely form the glacial bedrock (Raiswell and Thomas 1984).

Each glacier at Vatnajökull has lost between 15 and 50 % of its volume since ~1890, with the difference attributed to variable hypsometry, basal topography, and the presence of proglacial lakes that enhance melting at the termini (Hannesdóttir et al. 2015). Figure 3.7 shows the sampling stations for Vatnajökull.

Table 3.2. Characteristics of Vatnajökull outlet glaciers

<b>Glacier</b>	<b>Area (km<sup>2</sup>)</b>	<b>Length (km)</b>	<b>Slope (°)</b>	<b>Retreat (km) over 1890 to 2010</b>
Fjallsjökull	44.6	12.9	7.9	2.2
Kvíárjökull	23.2	14.1	6.0	1.5
Svínafellsjökull	33.2	12.0	9.0	0.8

Source: Hannesdóttir et al. (2015).

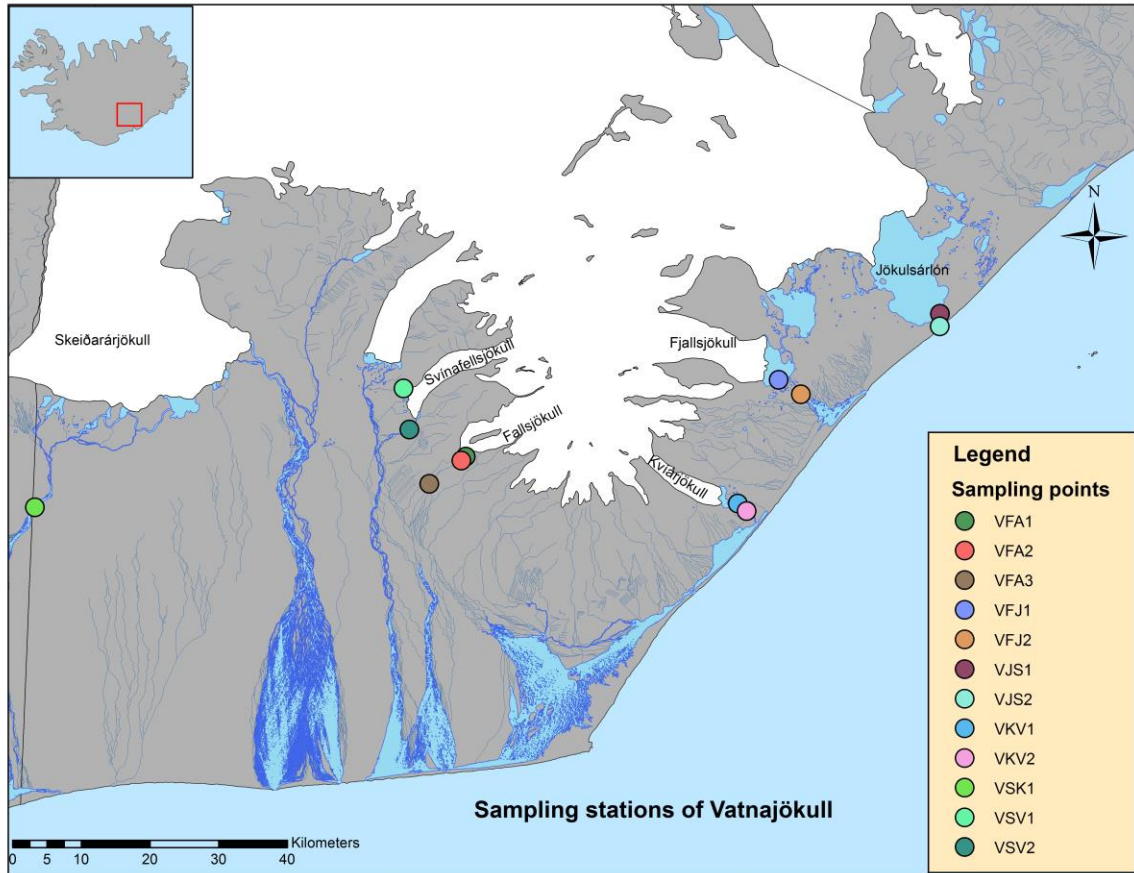


Figure 3.7. Vatnajökull, showing sampling stations.  
 Source: Created by the author from an NLSI (2014) base map.

### 3.2 Eyjafjallajökull

Eyjafjallajökull is one of the smaller icecaps in Iceland and covers the caldera of a volcano with a summit elevation of 1,600 m.a.s.l. and an area of 80 km<sup>2</sup> (Björnsson and Pálsson 2008). The volcano has erupted relatively frequently since the last glacial period, most recently in 2010. Although smaller, this ice cap is one of the most dynamic and important in the country given its location and impact on the population center of Reykjavik (Thordarson and Larsen 2007). Gígjökull is a 7.5 km-long glacier that drains north from the Eyjafjallajökull ice cap and delivers meltwater into the river Markarfljót that flows south (Figure 3.5). The glacier retreated in the first half of the 20<sup>th</sup> century, but



began an advance that lasted until 1997. From 1997-2005, the glacier retreated 700 m, leading to the expansion of the proglacial lake. The current rate of retreat is 100 m per year (Pelto 2010). Gígjökull is Eyjafjallajökull's largest outlet glacier. During the eruption of Eyjafjallajökull in 2010, the lake in front of the glacier filled with eruption material when the glacial outburst flood flowed at tremendous speed down the steep slopes of the mountain draining the lagoon. As a result, the appearance of Gígjökull glacier changed radically. Kaldaklofsjökull is a small mountain outlet glacier of Eyjafjallajökull. Seljavallajökull is an outlet glacier on the southern margin of Eyjafjallajökull. Figure 3.8 shows the sampling stations of Eyjafjallajökull.

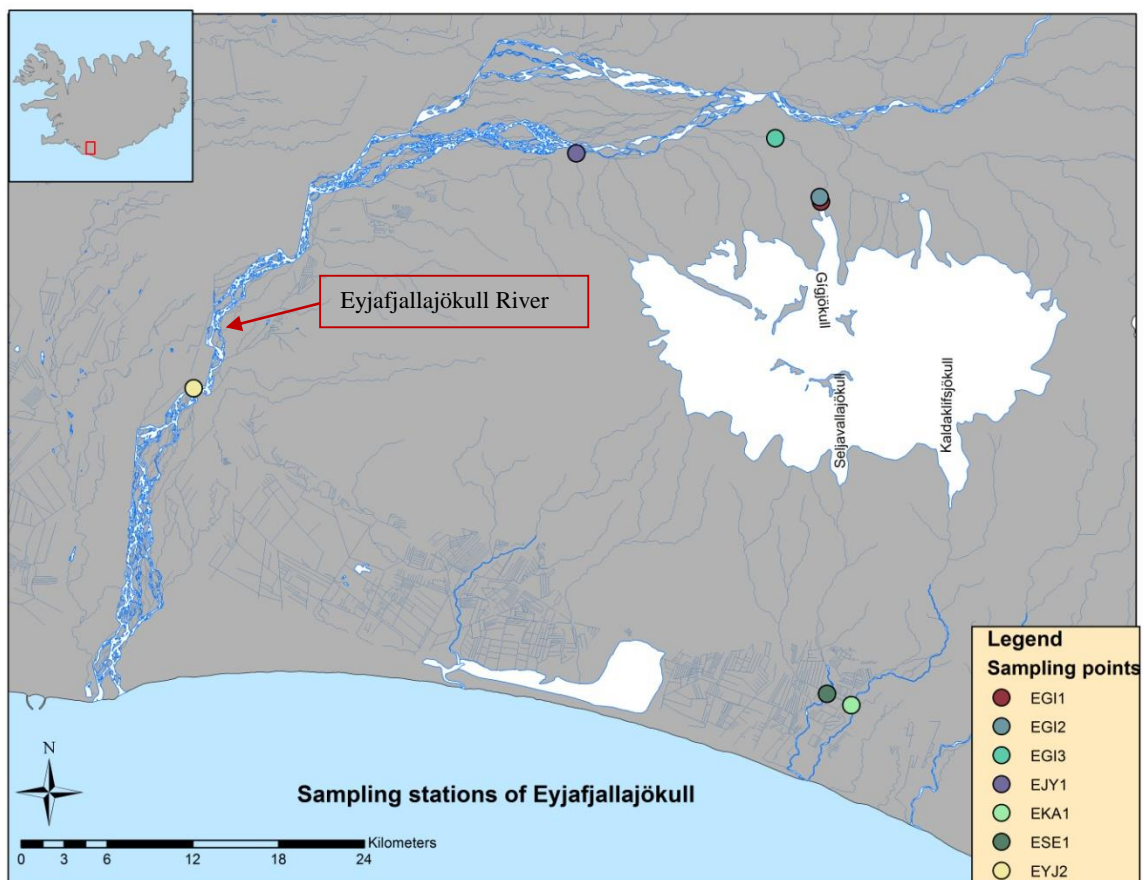


Figure 3.8. Eyjafjallajökull, showing sampling stations.  
 Source: Created by the author from an NLSI (2014) base map.

### **3.3 Mýrdalsjökull**

Mýrdalsjökull, the fourth largest icecap in Iceland, has an area of about 590 km<sup>2</sup> and is located on the south coast of the island at the southeastern end of the neovolcanic zone. The ice cap covers the active volcano Katla, which last erupted in 1918 (Larsen 2000). On average, two eruptions have occurred within the Katla system every century during the last 1,100 years (Larsen 2000); therefore, an eruption is expected in the near future. The Katla volcanic system is one of the most active volcanoes in Iceland. In addition, unloading from glacier mass loss induced by climate warming is also considered as a possible triggering mechanism for a future eruption (Sigvaldason 1981). Solheimajökull, in the southwest, shows typical characteristics of the tongue of a valley glacier. The Jokulsa basin consists of two main parts, namely the Mýrdalsjökull parent ice cap and the Solheimajökull glacier. Hyaloclastic and acid volcanic rocks dominate the geology of the basin (Carswell 1983). Kötlujökull is an outlet glacier on the southeastern margin of Mýrdalsjökull. Figure 3.9 is a map of the sampling stations for Mýrdalsjökull.

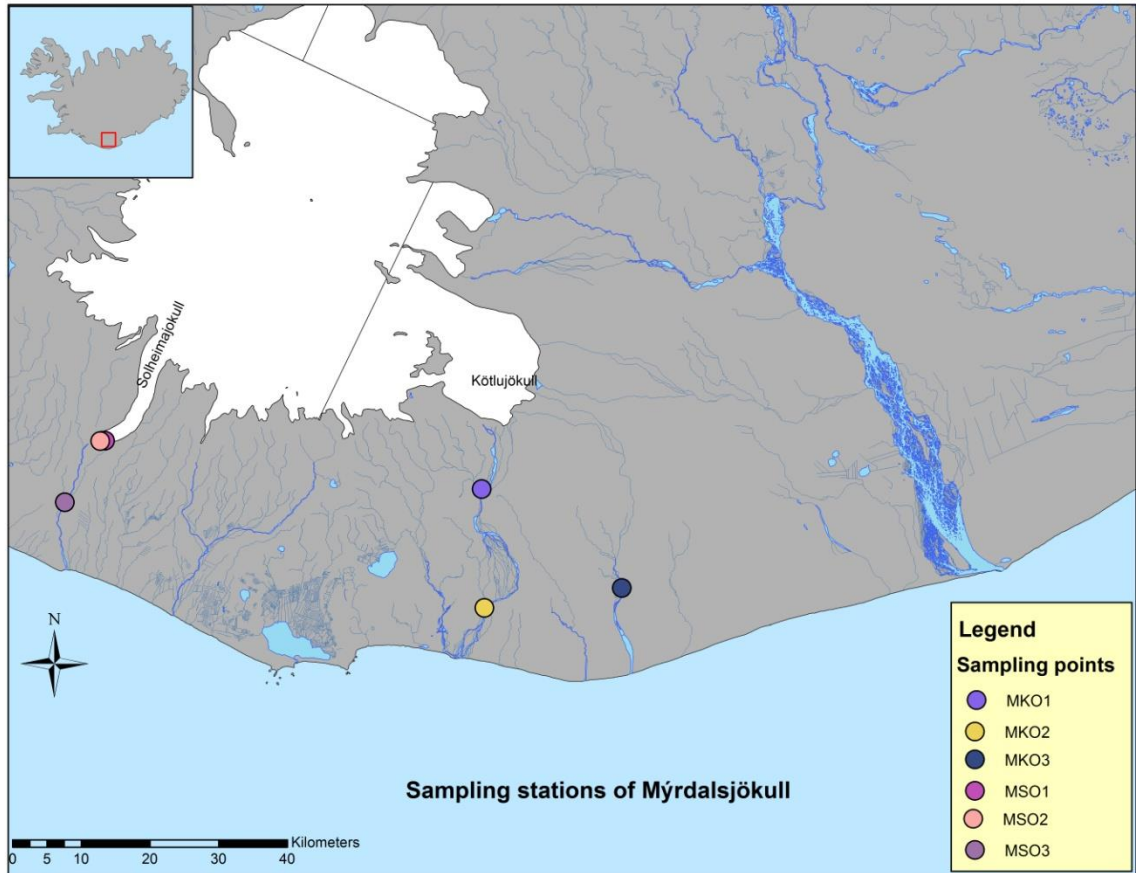


Figure 3.9. Mýrdalsjökull, showing sampling stations.  
 Source: Created by the author from an NLSI (2014) base map.

## Chapter 4

### 4.0 Methodology

A detailed hydrogeochemical assessment of Icelandic glacier meltwater variability was conducted based on different types of glaciers. The methods were undertaken in a number of steps (Figure 4.1), which included sampling preparation, calibration, field measurements, sample collection, and data analysis.

#### 4.1 Sampling Preparation

Three different sample bottles were used to collect water samples at each location with and without preservative, according to Table 4.1. A 0.0259 N sulfuric acid reagent was prepared by diluting concentrated sulfuric acid with the help of laboratory materials including a pipette, pipette filler, and volumetric flask. Crampons, snow axes, a fieldbook, a GPS, topography maps, filter papers, a filtering unit, Kimwipes, a YSI ProDSS handheld sonde, and a HACH DR900 colorimeter were brought to the field to carry out sampling, and field analysis.

#### 4.2 Calibration

A YSI (2014) ProDSS handheld sonde was calibrated for pH, dissolved oxygen (DO), specific conductivity (SpC), and nitrate, according to the user manual document #626973-01REF. Buffer solutions of four, seven, and 10 were used to calibrate pH, tap water was used for DO, a 1,413  $\mu\text{S}/\text{cm}$  standard was used for SpC, and one and 10 ppm standards were used for nitrate. The HACH DR900 colorimeter was calibrated in using deionized (DI) water for total suspended solids (TSS) and turbidity.

### 4.3 Field Measurements

Parameters with extremely low stability, such as temperature, pH, specific conductivity, dissolved oxygen, total dissolved solids, nitrate, and barometric pressure were determined in-situ using a YSI ProDSS handheld sonde. The HACH DR900 colorimeter was used to measure turbidity and total suspended solids by calibrating the instrument with DI water first and then analyzing the sample using the correct method, according to user manual document DOC022.98.80344 (Hach 2013). Surface temperature was determined at each site using a Kestrel combination anemometer. Coordinates and elevation were recorded for each site using a GPS device. Gram acid titration was conducted daily to determine alkalinity (method SM2320B) by measuring the initial pH and temperature of the sample, then adding the sulfuric reagent drop-wise until the pH stabilized to ~4.5. Titrant volume was used to calculate the alkalinity using Equation 4.1.

$$\text{Alkalinity (mg/L)} = \frac{\text{Volume of titrant} * \text{Normality (0.0259 N)} * 100000}{\text{Volume of sample}} \quad (\text{Eq. 4.1})$$

### 4.4 Sample Collection

Sampling was carried out in 2016 during three field campaigns from June 7 to 9, August 6 to 8, and October 11 to 13 at 11 outlet glaciers draining from three different icecaps. A total of 25 grab samples were collected (Figure 3.4) during each sampling period for a total of 75 samples. Samples were taken in different locations along the glacier tongues, proglacial lagoons, and glacial streams, depending upon accessibility to the area, and samples were collected from the same locations during each field campaign.

Non-acidified sample bottles were rinsed three times before collecting. The sample containers were filled with glacial water by submerging the bottle completely,

making sure there was no headspace or air bubbles. Nitric acid was used as a preservative for metals. The acidified bottles were filled making sure that the water did not overflow. Samples were filtered for metals, cations, and anions, using a syringe and 0.45  $\mu\text{m}$  filters. The labels for the sample bottles were color coded with respect to parameters and were given a code according to the ice cap and glacier from which the sample was collected, as well as the date of sampling. The samples were stored in coolers to maintain the temperature at 4°C and shipped overnight for analysis, which was carried out at the Advanced Materials Institute (AMI) at Western Kentucky University (WKU). The samples were analyzed for metals and cations using ICP-AES 200.7 Revision 4.4 and IC-SM 4110B (APHA 2014).

Table 4.1. Field sampling.

<b>Parameter</b>	<b>Volume (mL)</b>	<b>Filtered</b>	<b>Acidified</b>
Metals and Cations	60	√	√
Anions	60	√	
Alkalinity	100		

Source: Created by the author.

Table 4.2. Sample preservations and analytical methods

Test	Preservation	Minimum Sample size (mL)	Hold Time	Analytical Method
Alkalinity (HCO <sub>3</sub> )	Refrigerate	50	48 hr	Gram acid titration
Anions: Sulfate(SO <sub>4</sub> ) Nitrate (NO <sub>3</sub> -N) Chlorine(Cl) Fluoride (F)	Refrigerate	50	28 days	Ion chromatography
	Refrigerate	50	48 hr	YSI ProDSS handheld sonde
	Refrigerate	50	28 days	Ion chromatography
Cations (Ca, Mg, Na, K)	HNO <sub>3</sub> pH < 2	25-50	28 days	Inductively coupled plasma mass spectrometry (ICP-AES)
Metals Aluminum (Al), Barium (Ba), Chromium (Cr), Copper (Cu), Iron (Fe), Manganese (Mn), Nickel (Ni), Phosphorous (P), Sulphur (S), Selenium (Se), Silica (Si), Strontium (Sr), Vanadium (V), and Zinc (Zn)	HNO <sub>3</sub> pH < 2	100-250	6 months	Inductively coupled plasma mass spectrometry (ICP-AES)
pH	None(immediate analysis)	100	0.25 hr	YSI ProDSS handheld sonde
Conductivity	Refrigerate	100	28	YSI ProDSS handheld sonde
Total Suspended Solids	Refrigerate	500	7 days	HACH DR900 colorimeter
Turbidity	Refrigerate	100	48 hr	HACH DR900 colorimeter

Source: Created by the author with data from APHA (2014).

#### **4.5 Secondary Data Collection**

Temperature and precipitation data from stations Skaftafell and Steinar were obtained from the Icelandic Meteorological Office's (IMO 2016) hydromet stations for 2016. Base maps were downloaded from the National Land Survey of Iceland (NLSI 2014). Chemical compositions of water during jökulhlaups in Skeidara River were used from Palsson et al. (1999). Concentrations of ions from Fjallsjökull were obtained from Raiswell and Thomas (1984). Electrical conductivity data from April 1 to May 30, 2010, for stations near Eyjafjallajökull were obtained from the Iceland Meteorological Office.

#### **4.6 Data Analysis**

SigmaPlot 11.0 was used for creating graphs to analyze the temporal and spatial variation in physical and chemical parameters. ArcGIS 10.2 was used to create study area maps, spatial and temporal distributions, and ion dominance maps of different icecaps. The raw data were analyzed using SPSS to find the minimum and maximum of each parameter. SPSS was also used to group values according to geographical location to make bar graphs with standard deviations. A Pearson's correlation matrix was created in order to find statistical relationships between parameters. Relationships between water composition and rock type were evaluated by plotting the concentration of major cations and anions in the Tri-linear diagram using SigmaPlot 11.0. The piper diagram determines the geochemical balance and identifies the various weathering and transport mechanisms associated with each glacier. The cations and anions are shown in separate ternary plots (Figure 4.1). The apexes of the cation plot are calcium, magnesium, and sodium plus potassium cations. The apexes of the anion are sulfate, chloride, and carbonate plus hydrogen carbonate anions (Piper 1944). The diamond is a matrix transformation of a



graph of the anions (sulfate + chloride/total anions) and cations (sodium + potassium/total cations) (Srinivasa 1998).

## Chapter 5

### 5.0 Results and Discussion

Changes in hydrogeochemistry with respect to volcanic influences, temporal variation, and geographic location were analyzed. The influence of direct and indirect volcanic activities and presence of active volcanic systems is evident in the meltwater geochemistry, which can be used in order to forecast geothermal activity. Temporal variability is obvious in a range of physical and chemical parameters, which are highly variable between the sampling sites within the glaciers and icecaps. The hydrogeochemical parameters varied with geographical location, which differs with glaciers, proglacial lagoons, glacier river reaches, and mouths of glacier rivers where the river meets the ocean.

#### **5.1 Hydrogeochemical parameters to forecast geothermal activity using 2010 Hydromet Data from Iceland Rivers to Predict Jökulhlaups (Glacial floods) at Eyjafjallajökull**

The influence of volcanic activities on the hydrogeochemistry of glacial meltwater can be used to forecast geothermal activity. In Iceland, volcanic events at Eyjafjallajökull caused enormous disruption to air travel across western and northern Europe over an initial period of six days in April, 2010 (Mark 2010). Additional localized disruption continued into May, 2010. A change of wind direction sent the ash cloud south and southeast towards Europe, rather than northward. Analysis of conductivity data between two stations located south and west of the eruption was done to compare their values before, during, and after the eruption. In spatio-temporal analyses of geographic processes, temporal granularity can introduce critical issues (Meentemeyer 1989), including strong bias, to the interpretation of data. The Modifiable Temporal Unit

Problem (MTUP) is a consequence of adjustments in the temporal dimension. This case study aims to show how different time analyses can result in various outcomes in research related to high-resolution glacial flood sampling and the context in which the sampling and data must be considered in using them to forecast possible volcanically induced jökulhlaup events.

Eyjafjallajökull is one of the smaller icecaps in Iceland and covers the caldera of a volcano with a summit elevation of 1,600 m.a.s.l. and an area of 80 km<sup>2</sup> (Björnsson and Pálsson 2008). The location of the glacier is shown in Figure 5.1. The two hydrometric stations monitoring rivers nearby are V263, Jökulsá á Sólheimasandi, Sólheimasandur, and V413, Markarfljót, Einhyrningsflatir. V263 is in the south nearest the eruption.

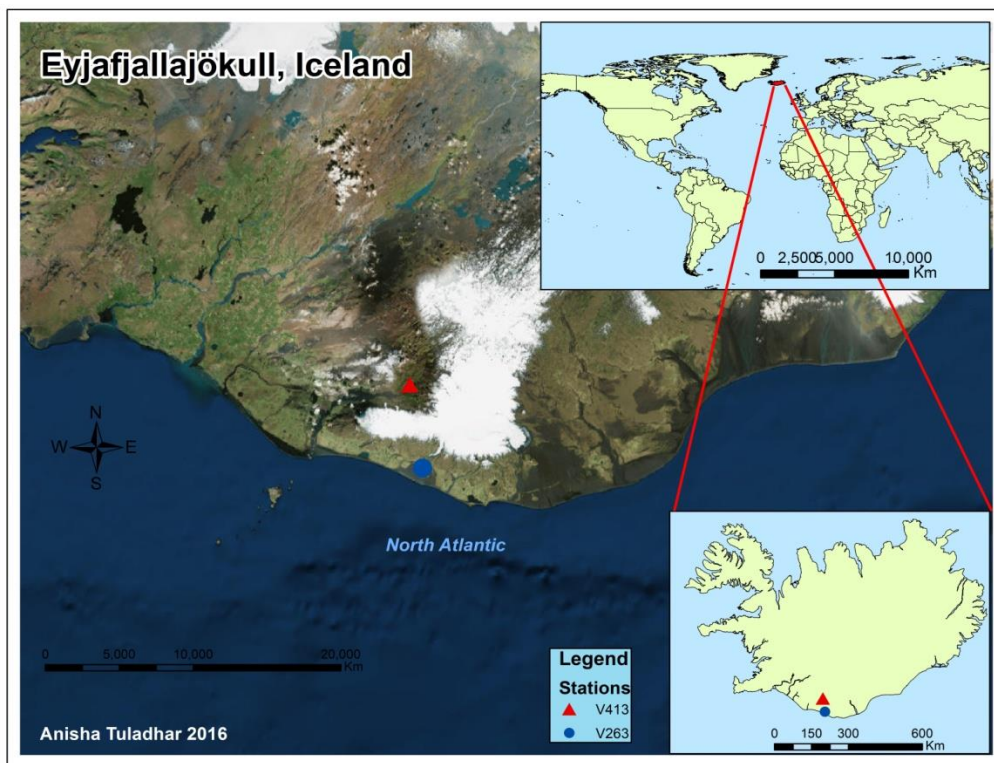


Figure 5.1. Study area showing hydrometric stations V263 and V413.  
Source: Created by the author from an ESRI (2016) base map.

### 5.1.1 Data Analysis

The conductivity data were averaged into hourly and daily data by using the summarize tool in ArcGIS 10.2. Time series and bar graphs of different eruption periods were plotted using an Excel spreadsheet. The volcano began to erupt on March 20, 2010, with nearby lava flows, and the main eruption occurred on 19 April, 2010. The eruption periods were categorized into following phases:

- Phase 1 (Apr 1-13): Before eruption.
- Phase 2 (Apr 14-18): 1<sup>st</sup> explosive phase.
- Phase 3 (May 5-17): 2<sup>nd</sup> explosive phase.
- Phase 4 (May 18-22): Eruption declined.
- Phase 5 (May-30): After eruption.

Figure 5.2 presents hourly variation of conductivity data from April 1, 2010, to May 30, 2010, and Figure 5.3 presents daily variation of conductivity from April 1, 2010, to May 30, 2010, which covers before, during, and after the eruption event occurred.

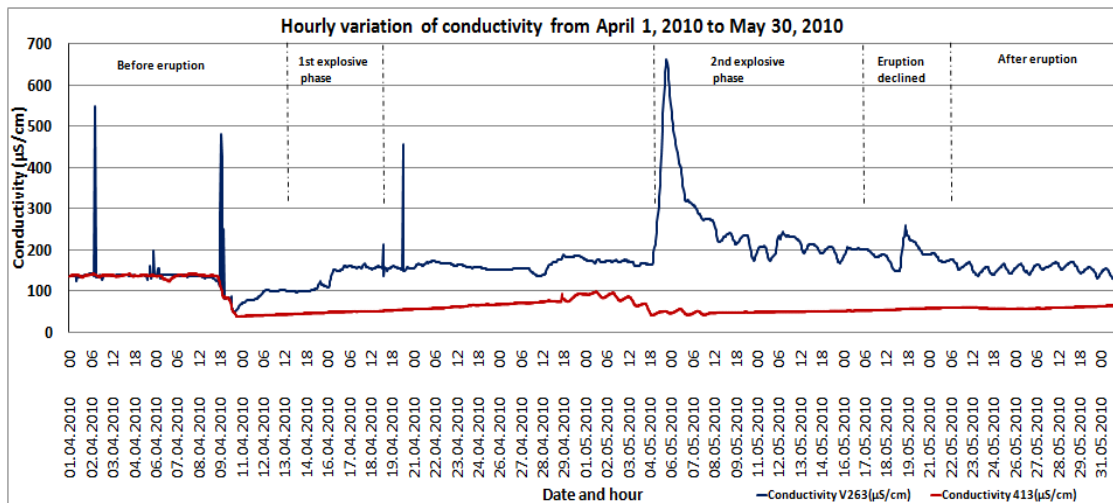


Figure 5.2. Hourly variation of conductivity from April 1, 2010, to May 30, 2010. Hours range from 00, 06, 12, and 18.

Source: Created by the author with data from the IMO (2016).

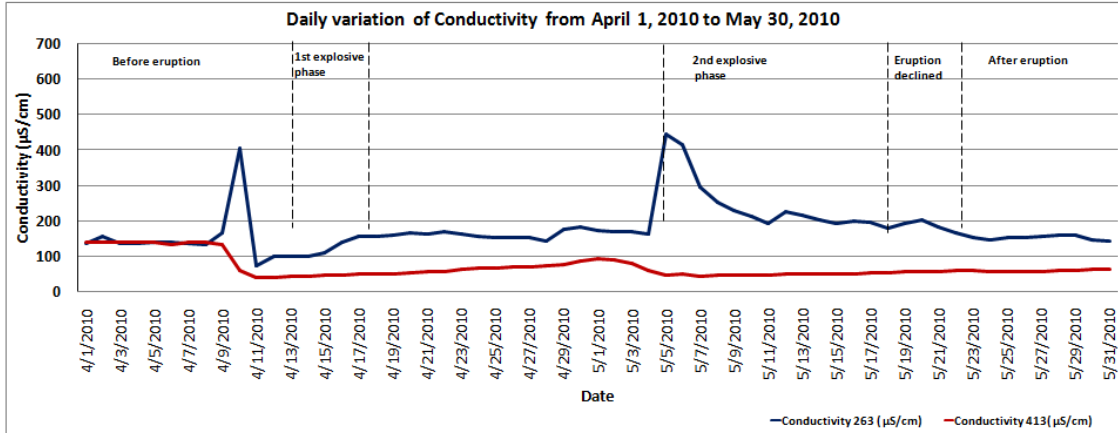


Figure 5.3. Daily variation of conductivity from April 1, 2010 to May 30, 2010.  
Source: Created by the author.

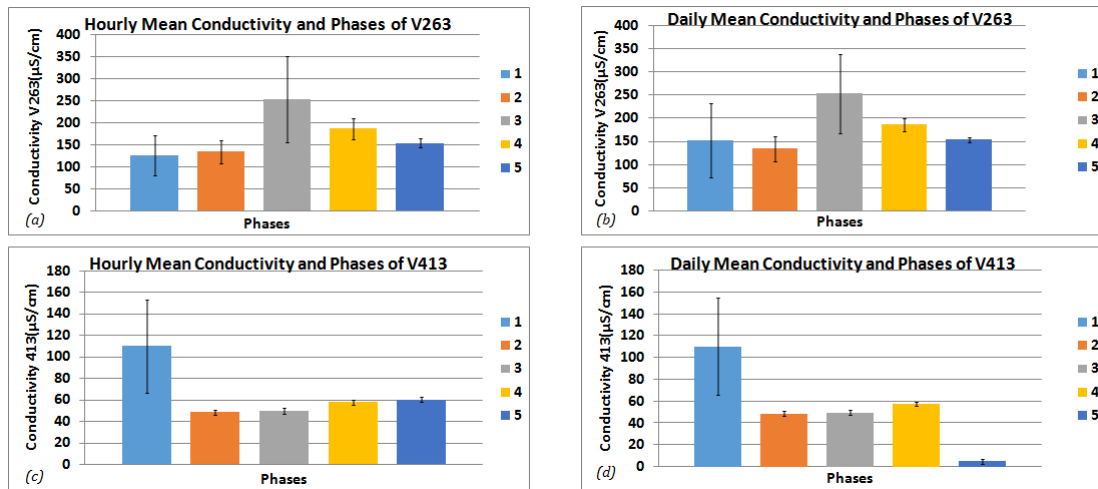


Figure 5.4. Mean conductivity and volcanic phases with standard deviation (April 1, 2010, to May 30, 2010). Hourly (a) and daily variation (b) of V263, and hourly (c) and daily (d) variation of V413.  
Source: Created by the author.

Figure 5.4 illustrates the mean conductivity and standard deviation from the two stations in hourly and daily variation. The summary statistics show difference in means and standard deviations with respect to temporal variation. This further verifies different outcomes from time-series analysis, while still demonstrating the eruption precursor data. An increase in conductivity at station V263 is presented in Figures 5.2 and 5.3, even

before the eruption, while almost no change is seen at V413. V263 shows overall increased conductivity values, due to its location at the influence of volcanic plume (south), while the conductivity actually dropped at V413. Increases in conductivity occur after the first explosive phase in Figure 5.2. The values are higher for the hourly variation than the daily variations and this is the result of different time analyses, which yield various outcomes based on smoothing of the data at daily resolution.

High conductivity before the first eruption might be due to the increase in geothermal fluids underneath the surface, following hydrogeochemical perturbations from increased flow from the activities starting March 20, even though an eruption did not occur. These effects were found at the river draining from Mýrdalsjökull, as it was near the influence of the volcanic plume. The increases in conductivity can likely be related to geothermal fluids and ash from the volcanic plume. Potential exists to use meltwater hydrochemistry to forecast geothermally-driven glacial flood events (jökulhlaups in Icelandic) in such environments (Lawler et al. 1996). Other researchers also found this potential; a sulfurous smell was noted locally before a jökulhlaup was observed in the Skafta meltwater river (northwest Vatnajökull) (Björnsson 1977). A strong increase in meltwater temperature and electrical conductivity, accompanied by a strong sulfurous smell, was also recorded in the Kverkjökull stream in northern Vatnajökull (Fenn and Ashwell 1985). Also, an increase in conductivity in the Skeiðará glacier river that forms from the Vatnajökull glacier was related to geothermal water leaking from Grímsfjall volcano (Jónsson 2014.).

The influence of temporal granularity was analyzed for conductivity values before, during, and after the volcanic activity in Eyjafjallajökull in 2010. There was an

increase in conductivity before the eruption from the station under the influence of volcanic activity. No change in conductivity value occurred at the station without the influence of volcanic activity. This further proves the potential use of meltwater hydro-chemistry to forecast geothermally-driven flood events in such environments, which can include variations in pH, Ca, Mg, SO<sub>4</sub>, S, and HCO<sub>3</sub>. There exists a change in these parameters with respect to subglacial seismic and geothermal activity, and this study shows how different temporal analysis can lead to different results, as the graphs from hourly data better indicate high ranges of electrical conductivity prior to the eruption.

Higher specific conductivity at Eyjafjallajökull is noted during August, 2016, particularly at rivers draining from Gigjökull (381.4  $\mu\text{S}/\text{cm}$ ) and Seljavallajökull (418  $\mu\text{S}/\text{cm}$ ) in the present study. These values are closer to the highest values during the 2010 eruption's daily variation (Figure 5.3), but lower than the highest at an hourly resolution (Figure 5.2); thus, it is important to account for different threshold values according to temporal variation, as some of the higher values might be normal during a certain time or under the influence of minor volcanic activity. Hourly specific conductivity or a higher-resolution study is recommended for this type of analysis, since the values were much higher ( $\sim 500$   $\mu\text{S}/\text{cm}$ ) for hourly variations. Overall, it is clear from the 2016 study that the high variability in the different parameters, likely to be a precursor in the water geochemistry prior to a flood event, makes it difficult to standardize thresholds, but with high-resolution monitoring it is possible to capture them.

## 5.2 Elevated Solute Concentrations in Samples from Eyjafjallajökull

Almost all of the 2016 samples with the highest concentrations come from rivers flowing from Eyjafjallajökull icecap glaciers (Table 5.1). The enrichment of meltwaters after passing through a glacier depends on bedrock composition and susceptibility to weathering, but a major influencing factor for meltwater is volcanic activity under Icelandic glaciers, mainly Eyjafjallajökull in the case of this study. The rivers from Eyjafjallajökull not only drain close to active volcanic zones (Figure 3.3), but are located above a tectonic plate boundary zone (Figure 3.2). Higher concentrations from this icecap may be due to increase volcanic influences that are both modern and residual ash and lavas from the recent 2010 eruption. Weathering of rocks is the dominant mechanism controlling the hydrochemistry of most drainage basins, which occurs when water flows at the ice-rock interface (Garrels and Mackenzie 1971). The icecaps Eyjafjallajökull and Mýrdalsjökull have similar rock compositions and ages, but have variability in solute composition in their meltwaters (Figure 5.10); therefore, volcanic influences, along with bedrock composition, seem to be the dominant influences controlling the hydro-geochemistry of water samples throughout the melting season.

Hydrogeochemical parameters can be used to forecast geothermal activity in the water. The increase in parameters before a volcanic eruption that triggers a jökulhlaup could be used to design automatic warning systems (Lawler et al. 1996; Snorrason et al. 1996). The spatial and temporal variability in water chemistry could pose a challenge to installing forecasting systems, especially in identifying thresholds for event alarms. Geothermal fields will emit geothermal steam melting the ice and, subsequently, dissolving into the meltwater (Kristmannsdóttir et al. 1999). The meltwater may become



acidic, due to mixing of gases from the geothermal steam, like CO<sub>2</sub>, H<sub>2</sub>S, CH<sub>4</sub>, and H<sub>2</sub>, and sediments carried in the subglacial rivers being mostly from hyaloclastites.

Table 5.1. Minimum and maximum concentrations of geochemical parameters for Iceland glacier sample sites in 2016.

Geochemical parameters	Minimum			Maximum		
	Value	Sample code	Month	Value	Sample code	Month
Ca (mg/L)	0.22	EGI1	Aug	36.08	ESE1	Aug
Na (mg/L)	0.042	MSO1	Aug	36.58	EGI3	Aug
K (mg/L)	0.026	MSO1	Aug	5.74	EGI3	Aug
Mg (mg/L)	0.057	MSO1	Aug	19.10	ESE1	Aug
HCO <sub>3</sub> (mg/L)	6.11	EGI1	Aug	479.23	ESE1	Aug
SO <sub>4</sub> (mg/L)	0 – 0.025	EGI1 MSO1 VFA1	Jun Aug Oct	19.54	EGI3	Aug
Cl (mg/L)	0.095	VFA1	Aug	50.90	EGI3	Aug
F (mg/L)	0.00 – 0.08	EGI1 MSO1	Jun Oct	0.83	EGI3	Oct
NO <sub>3</sub> (mg/L)	0	MSO1	Aug	9.62	VFA3	Jun

Source: Created by the author.

In a subglacial volcanic eruption, the meltwater will come into direct contact with the magma at the bottom of the glacier and, therefore, the geochemical changes will be significant. The water obtained from jökulhlaups draining Lake Grimsvotn and the Skafta River kettles can contain high concentrations of the total dissolved solids, and the main components are total carbonate, sulfate, silica, alkali, and alkali Earth metals, as well as some heavy metals (Table 5.2) (Palsson et al. 1999). The pH and concentration of fluoride may be greatly increased and heavy metal concentrations may increase. Table 5.2 illustrates chemical composition of water during jökulhlaups in the Skeidara River. Table 5.2 indicates higher values for the chemical parameters and lower values of pH for historic data.

Table 5.2. Chemical composition of water during jökulhlaups in the Skeidara River. Concentrations in mg/L.

Time	1954	1965	1972	1976	1982	1983	1986	1991	1996
pH/°C	-	7.0/-	7.5/-	-	6.02/22	6.45/21	6.26/24	6.20/24	6.15/18
Hydrogen sulphide (H <sub>2</sub> S)	0.0	-	-	-	0.3	0.0	<0.03	<0.03	0.04
Tot. carbonate (CO <sub>2</sub> )	-	680	480	-	595	343	384	559	535
TDS	388	416	-	-	369	359	336	386	-
Silica (SiO <sub>2</sub> )	57	56	44	50.5	60.0	56.5	62.4	67.0	65.4
Sodium (Na)	-	63.5	89.0	43.0	53.1	50.3	52.7	57.1	59.5
Potassium (K)	-	19.0	3.0	3.8	4.2	4.8	4.4	3.9	4.2
Calcium (Ca)	60.9	59.5	28.0	45.6	50.4	38.9	43.2	51.0	60.8
Magnesium (Mg)	15.6	10.4	10.0	9.9	10.8	11.8	10.7	12.6	14.4
Sulphate (SO <sub>4</sub> )	18.1	38.7	13.0	23.5	19.2	48.8	38.4	22.0	18.0
Chloride (Cl)	8.7	42.7	11.0	13.5	13.2	7.6	13.7	14.8	12.0
Fluoride (F)	0.3	0.5	-	-	0.17	0.31	0.26	0.16	0.18
Iron (Fe)	9.5	-	-	-	-	4.4	2.3	2.3	2.9

- not measured.

Source: Pálsson et al. (1999).

However, the current study found lower pH (around 6.5) during June for meltwaters draining from Solheimajökull (Table 5.5). Also, the rivers draining from Eyjafjallajökull have higher values, like those presented in most of the above parameters (Table 5.2). The rivers draining from Gígjökull (EGI3, Eyjafjallajökull ice cap) have TDS values ranging from 170 to 247 mg/L. Potassium is 5.74 mg/L, sulfate is 19.54 mg/L, and fluoride is 0.83 mg/L during August. Also, the river from Seljavallajökull (ESE1, Eyjafjallajökull ice cap) has a higher value for magnesium at 19.96 mg/L during August. Values from the Eyjafjallajökull ice cap show similar values to the jökulhlaups studied by Pálsson et al. (1999). Therefore, the results characteristic of one jökulhlaup cannot be used in order to design and plan appropriate automatic warning systems by setting a threshold, as similar values might be common with meltwater from a different glacier or ice cap, like the higher values found at Eyjafjallajökull in the sampling from June to October, as previously discussed.

Early warnings may save lives, property, and infrastructure, such as road networks, power systems, and communication systems. To be effective, the warning

system must be based on simultaneous and continuous measurements and real-time transmission of the data, as well as inbuilt warning if the measurement exceeds an alarm threshold. Seasonal changes in water chemistry should be well understood in order to put in a threshold for the alarm system. This is one of the reasons background and seasonal variations should be determined prior to determining the alarm threshold levels. As discussed previously, there is much variability between glaciers and sampling dates in the hydrogeochemical signatures measured in this study; therefore, more research is needed in order to better understand the controls on these over longer periods of time in order to determine patterns and baselines. Variations in hydrogeochemical parameters not only exist due to volcanic influences but also with time due to changes in temperature, climate changes, and/or increases in erosion within the glacier and bed rock.

### 5.3 Temporal Variation of Ions from Fjallsjökull Glacier

The concentrations of present ions were compared with a previous study conducted on solute acquisition in glacial meltwaters of Fjallsjökull by Raiswell and Thomas (1984). Table 5.3 lists the geochemical values between the year 1984 and 2016. The temporal variation of ions from Fjallsjökull is given in Figure 5.5, which indicates higher concentrations in 2016 compared to 1984.

Table 5.3. Geochemical values for Fjallsjökull for 1984 and 2016

<b>Parameter (mmol/L)</b>	<b>1984*</b>	<b>2016 (Present Study)</b>
<b>Ca<sup>2+</sup></b>	0.118±0.017	0.2937 ± 0.1681
<b>Mg<sup>2+</sup></b>	0.023±0.008	0.0762 ± 0.0228
<b>K<sup>+</sup></b>	0.005±0.002	0.0112 ± 0.0022
<b>Na<sup>+</sup></b>	0.076±0.034	0.1773± 0.0412
<b>HCO<sub>3</sub><sup>-</sup></b>	0.257±0.038	0.6356 ± 0.3304
<b>SO<sub>4</sub><sup>2-</sup></b>	0.021±0.007	0.0650 ± 0.0471

Source: Created by the author with data from Raiswell and Thomas (1984).

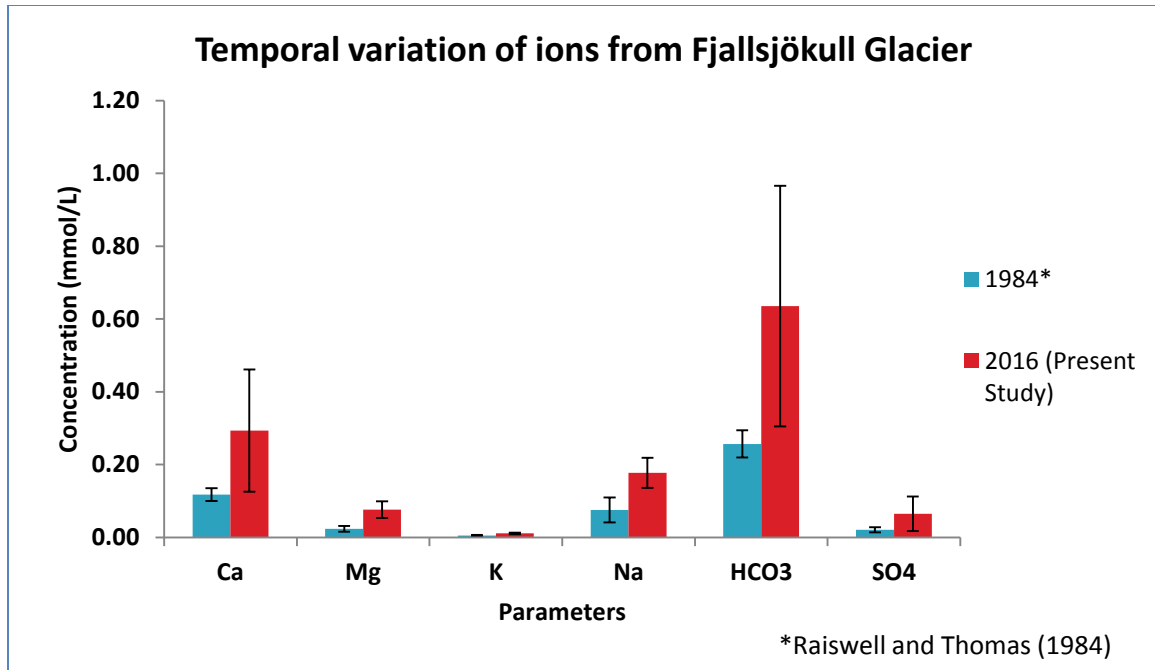


**Figure 5.5.** Temporal variation of ions from Fjallsjökull.  
Source: Created by the author with additional data from Raiswell and Thomas (1984).

The concentration of most solutes (Ca, Mg, K, Na, HCO<sub>3</sub>, and SO<sub>4</sub>) is higher in 2016 than 1984 (Figure 5.5); however, SO<sub>4</sub> at the river reach of Fjallsjökull is lower (0.002 mmol/L) during October than the mean for 1984 (0.023 mmol/L), which might be due to dilution from precipitation. Also, the SO<sub>4</sub> value during June is lower (0.0206 mmol/L) for the same site at Fjallsjökull than 11 of 20 samples taken during 1984. Based on lower SO<sub>4</sub> values than previous study, the impact of volcanic influences might be less now. Likewise, the increase in HCO<sub>3</sub> could be due to increased weathering of carbonate minerals present in the local basalts (Tranter et al. 1993); however, HCO<sub>3</sub> concentrations are the same for samples taken at river reaches during October (0.30 mmol/L) as two of twenty samples taken during 1984, which might be due to dilution during rain. The rest of the concentrations are higher for 2016. The global increase in temperature since 1984 also could lead to glacier retreat and more melting, resulting in more erosion. Glaciers

like Fjallsjökull experienced a 35% volume loss and retreated 2.2 km from ~1890 to 2010 (Hannesdóttir et al. 2015). Increases in solute concentration have also been reported in European alpine water systems (Rogora et al. 2003). A reduction of snow cover over space and time, due to less precipitation and higher temperatures, results into greater exposure of rocks and soils in the watersheds, thereby enhancing the weathering processes (Rogora et al. 2003). Therefore, the increase in solute concentrations may be due to an increase in chemical weathering from temperature increases and changes in discharge for the glacier system.

The increasing trend in the concentration of solutes could also be attributed to an increased weathering rate, due to temperature and CO<sub>2</sub> increases. During glacial retreat, the recently exposed forefield is the most chemically active part of the watershed, making high rates of weathering possible (Nowak and Hodson 2014). Also, re-routing of meltwaters can increase crustal ion yields and influence chemical weathering. More erosion beneath the glacier could also result in increased solutes. Glacial erosion processes, like plucking, transport large chunks of rocks and abrasion scrapes particles against each other (Gillaspy 2017). These processes, together with increases in meltwater, may explain the increase in solutes since 1984. Changes in climate may also influence the conductivity values; a study done to link changes in climate and hydrochemical responses in the Rocky Mountains found an increase in conductivity in 1995 to be four times that of 1994. Similarly, lake water chemistry in the Khumbu Valley, Himalaya, reveal a persistent increase in the ionic content of the lake water, a trend that appears to be closely linked to increasing temperature (Lami et al. 2010). Increased temperature also results in

increased rates of biogeochemical processes and decreased oxygen concentration in the water bodies, which, in turn, change stratification patterns (Viviroli et al. 2011).

Chemical and mechanical weathering fluxes depend upon climate via changing temperature and runoff (Gislason et al. 2009). In comparison with 1961–1990, the project scenario based on downscaling of global coupled atmospheric-ocean simulations predicts a warming of 2.8 °C and a 6% increase in precipitation by 2071–2100 in Iceland (Rummukainen 2006; Fenger 2007; Jóhannesson et al. 2007). Research found that the runoff, mechanical weathering, and chemical fluxes of northeastern Iceland river catchments increased from six to 16%, eight to 30%, and four to 14%, respectively, for each degree of temperature increase during study period of 44 years (Gislason et al. 2009). The mean annual temperature of the catchments varied from 3.2 to 4.5 °C. In Iceland, it is expected that changes in both precipitation and chemical weathering should be higher than the global averages, due to the highly reactive basaltic bedrock easily weathering compared to other silicate rocks (White and Brantley 2003; Dupré et al. 2003; Gislason and Oelkers 2003).

Increased weathering can also be related to CO<sub>2</sub> increases over the past few centuries (Plass 1959). The atmosphere and oceans continuously exchange carbon dioxide with rocks and with living organisms. They gain carbon dioxide from volcanic activity that releases gases from the Earth's interior and from the respiration and decay of organisms, and they lose carbon dioxide from the weathering of rock and decay of photosynthesis of plants. Therefore, both temperature and carbon dioxide increases from volcanic activity might also result in increased weathering, thereby releasing more solutes into the glacial meltwater system. Since the influence on hydrogeochemistry is interrelated with respect

to volcanic influences, temporal variation, and geographic location, the remaining results are discussed together with respect to hydrogeochemical variability.

## 5.4 Geochemical Variability

The sampling sites vary with geographic location both within Iceland and each icecap. Categorizations of the sampling sites are given in Table 5.4. The samples are from various outlet glaciers draining from different icecaps at different geographical locations, including glaciers, proglacial lagoons, glacier river reaches, and mouths of glacier rivers (where the rivers meet the ocean).

Table 5.4. Sample site categorization.

Ice cap	Outlet glacier	Sample codes			
		Glacier	Proglacial Lagoon	River reaches	Mouth of glacier rivers (where the river meets the ocean)
Mýrdalsjökull	Solheimajokull	MSO1	MSO2	MSO3	
Mýrdalsjökull	Kötlujökull			MKO1 MKO2 MKO3	
Vatnajökull	Fjallsjökull		VFJ1	VFJ2	
Vatnajökull	Jökulsárlón		VJS1		VJS2
Vatnajökull	Kvíárjökull		VKV1	VKV2	
Vatnajökull	Falljökull	VFA1	VFA2	VFA3	
Vatnajökull	Svínafellsjökull		VSV1	VSV2	
Vatnajökull	Skeiðarárjökull			VSK1	
Eyjafjallajökull	Gígjökull	EGI1		EGI2 EGI3	
Eyjafjallajökull	Rivers			EYJ1 EJY2	
Eyjafjallajökull	Seljavallajökull			ESE1	
Eyjafjallajökull	Kaldaklifsjökull			EKA1	

Source: Created by the author.

The geochemical parameters varied with sampling periods as the temperature and precipitation were different. Hydromet data for 2016 are presented in Figures 5.6, 5.7, and 5.8. Figure 5.6 is the total monthly precipitation of station Skaftafell, which is located close to Vatnajökull, and low values are observed during June with high values during October. Figure 5.7 illustrates mean monthly temperature data for Skaftafell, with higher values during June and August, and low values during October. The Steinar station lies close to the southern part of Eyjafjallajökull, which has a low mean temperature during June, higher during August, and is lowest during October (Figure 5.8). There could be a possible lag in meltwater during June and August as preceding months had lower discharges, even though warmer conditions prevailed. Precipitation and temperature can affect the rate by which rocks weather. Higher temperatures and greater rainfall increase the rate of chemical weathering (UH 2017); however, herein, there is high precipitation but low temperatures in October, and the lower values could be due to some dilution. Geochemical parameters like specific conductivity and concentrations of ions may be lower during October because of dilution; the increase in discharge may have led to increases in TSS , which generally increase with higher discharges (Walling 1977).



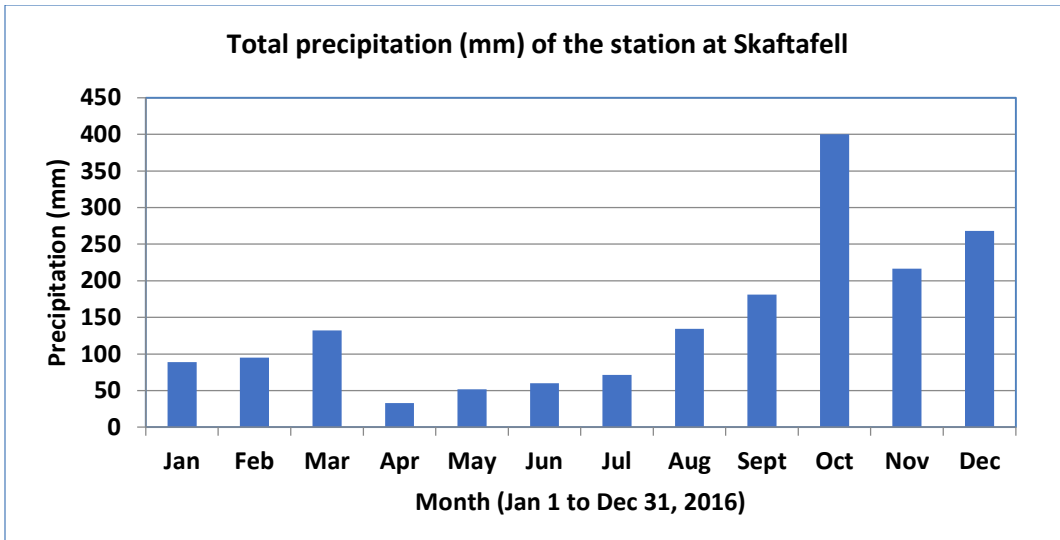


Figure 5.6. Total precipitation (mm) of the station at Skaftafell (Close to Vatnajökull). Source: Created by the author with data from the IMO (2016).

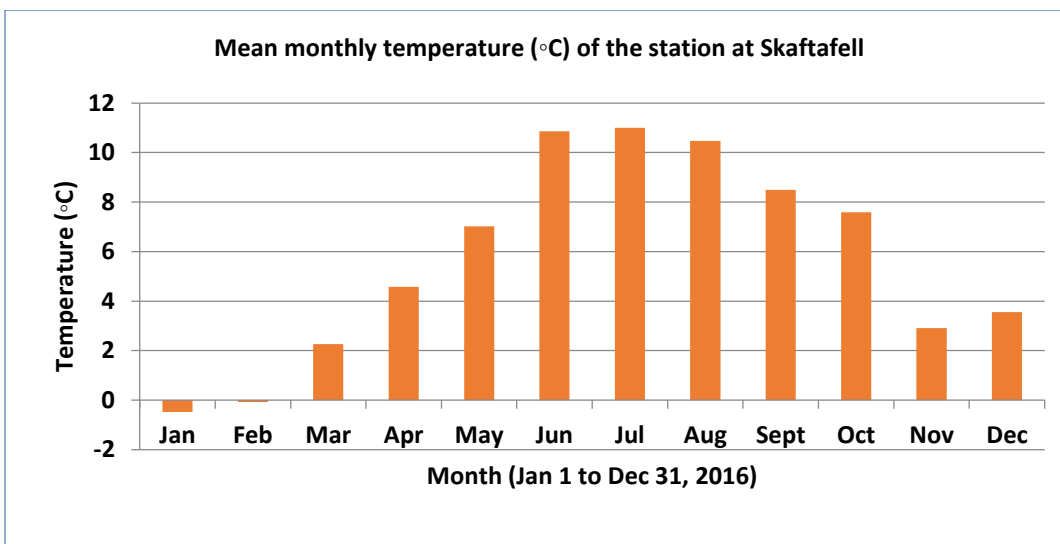


Figure 5.7. Mean 2016 monthly temperature (°C) of the station at Skaftafell (Close to Vatnajökull). Source: Created by the author with data from the IMO (2016).

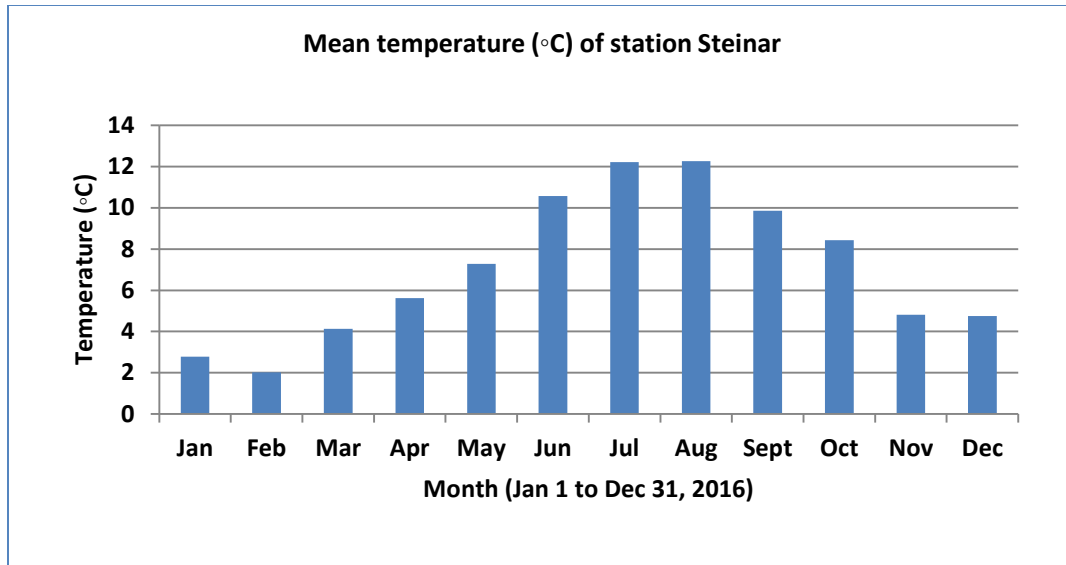


Figure 5.8. Mean temperature (°C) of the station near Steinar (Close to the southern part of Eyjafjallajökull).

Source: Created by the author with data from the IMO (2016).

#### 5.4.1 Variability of pH, Specific Conductivity, and DO

The ranges for geochemical parameters of the glacial meltwater samples are shown in Table 5.5. The parameters are highly variable between the sampling sites within the glaciers and icecaps. Temperatures of Icelandic meltwaters range between 0.3 °C and 10.9 °C during the sampling period. Their pH values range from 6.62 to 9.79, with the highest pH values (pH > 8) being for VFJ1, which is the lagoon at the terminus of Fjallsjökull glacier, an outlet of Vatnajökull icecap (Figure 5.9). The lagoon at Solheimajökull glacier, an outlet of Mýrdalsjökull (MSO2), had the lowest pH of 6.62 recorded during the June sampling event. Lower pH can be the result of limited rock-water interaction (Louvat et al. 2008), the influence of volcanic activity, presence of volcanic ash (USGS 2011), and anthropogenic pollution (Xiao 2011). Some volcanic gases, such as sulfur dioxide, dissolve in groundwater and could make the water acidic as it mixes with the meltwater (USGS 2011). Studies show that water systems under the

influence of volcanic activity are typically acidic (Palsson et al. 1999). Based on field observation, Solheimajökull exposed more volcanic ash within the ice during June, which was less in October, likely due to being washed away by rain. This could possibly be the reason for lower pH values in samples taken from Solheimajökull during June and higher values during October (Figure 5.9). Higher dust loadings of glacier ice often correspond to lower acidity, due to additions of certain cations, which could be derived from increased weathering during the melt season at the sites (Xiao 2011). The pH concentrations are higher (pH>9) during August and October at samples taken from Vatnajökull. A significant contribution from CO<sub>3</sub>, and other anions, emerges only at pH levels greater than approximately 9.0 (Anders et al. 2006).

Table 5.5. Ranges geochemical parameters: pH, specific conductivity, DO, TSS, turbidity, and water temperature.

Parameters	Minimum			Maximum		
	Value	Sample code	Month	Value	Sample code	Month
pH	6.62	MSO2	Aug	9.79	VFJ1	Oct
Specific Conductivity (µS/cm)	1.3	MSO1	Aug	418	ESE1	Aug
DO (mg/L)	11.19	EJY2	Jun	18.5	VKV1	Oct
TSS (mg/L)	0	MKO3	Jun	2440	MKO1	Oct
		ESE1		2070	MKO2	
Turbidity (NTU)	0	MKO3	Jun	906	MKO1	Oct
		ESE1		753	MKO2	
Water Temperature (°C)	0.3	VSV1	Oct	10.9	EYJ2	Aug

Source: Created by the author.

Specific conductivity ranges between 1.3 to 417 µS/cm among the sampling sites. It is highly variable in samples from Eyjafjallajökull (Figure 5.10), with the highest concentration at its outlet river, Seljavallajökull (ESE1), in August. It is lowest at Solheimajökull (MSO1) during the August sampling event. The variability is less for

samples from Mýrdalsjökull and the lowest values are for Vatnajökull sites. The latter may be due to the large size of the icecap, which homogenizes the ice forming glaciers, despite of the differences in climatic variability in the east and west parts of the icecap. Specific conductivity in streams and rivers is affected primarily by the bedrock geology of the area through which the water flows (Palacky 1981), suspended impurities, the presence of minerals and ions (EPA 2012) and, in this case, volcanic activity.

An increase in volcanic activity can lead to changes in conductivity (Gislason et al. 2002). A greater influence of volcanic activities, like the presence of 2010 eruption residuals on the Eyjafjallajökull and Mýrdalsjökull sites, might be the reason for the lower pH range and comparatively higher, and more variable, specific conductivity values for the meltwater samples. Specific conductivity from samples taken directly from the glaciers Gigjökull and Solheimajökull are lower, because they are from modern meltwater in the system. An increase in volcanic activity is typically related to increased discharge (Wilson and Head 2002), SpC, and a decrease in pH of the meltwater. Some of these changes are within the data ranges for the specified parameters during the sampling period at sites indirectly influenced by underlying volcanoes, though no direct activity was observed at any of the sites.

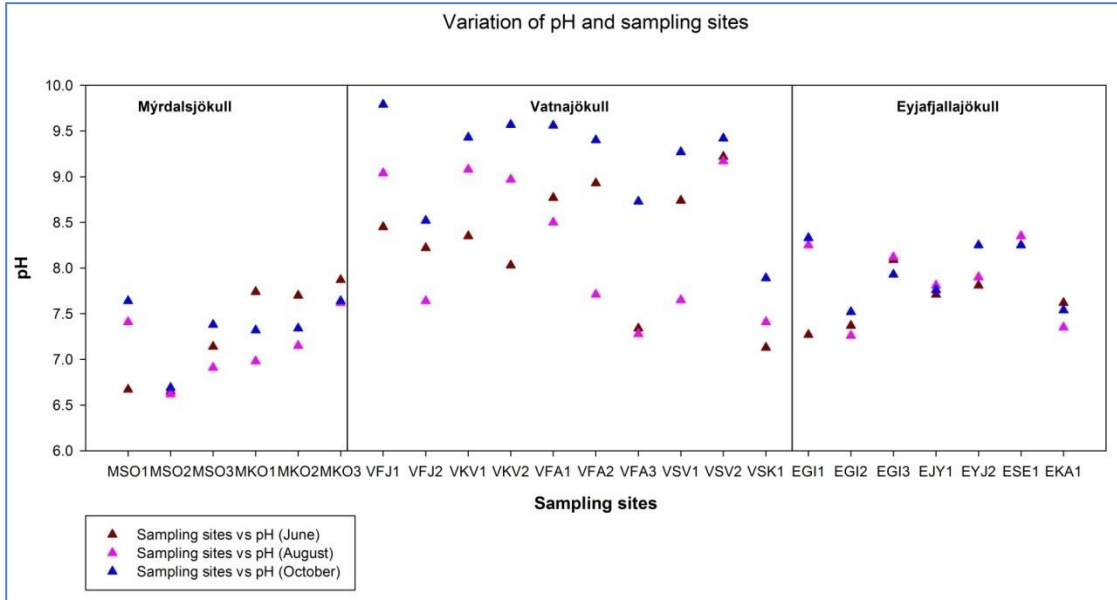


Figure 5.9. Variation of pH at sampling sites.  
Source: Created by the author.

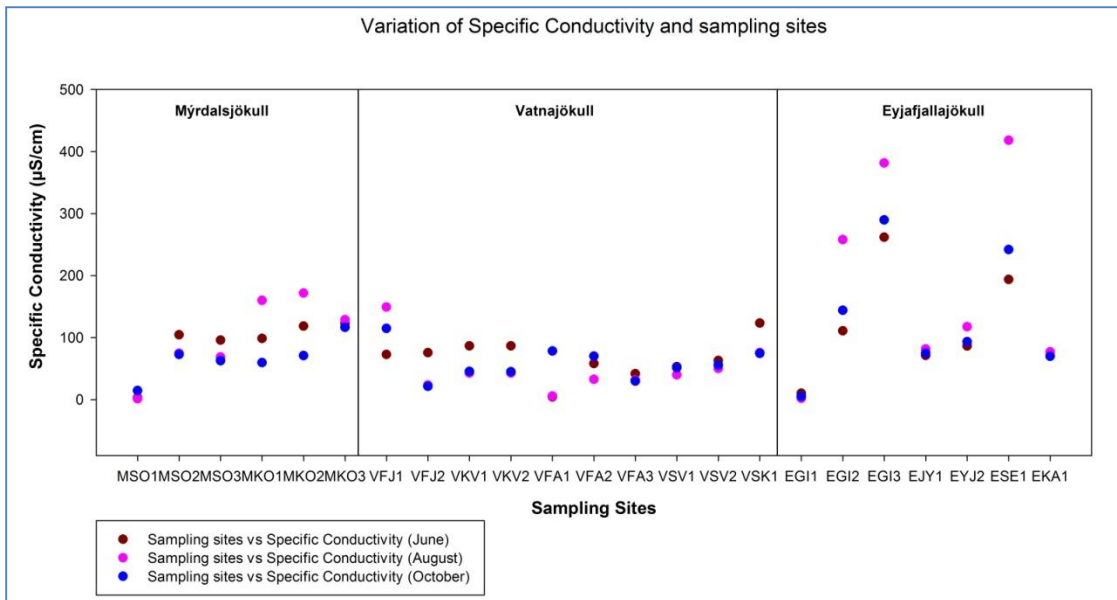


Figure 5.10. Variation of specific conductivity at sampling sites.  
Source: Created by the author.

Dissolved oxygen values are variable at most of the sites, with the highest variability at the lagoon of Kvíárjökull (VKV1) (Figure 5.11), which has the highest DO of 18.5 mg/L during October. The river Eyjafjallajökull at EYJ2 has the lowest DO of

11.19 mg/L during June. DO values vary seasonally, as they are higher during October and August, but lower during June. Oxygen concentrations tend to be higher during rainy periods, because the rain interacts with oxygen in the air as it falls (Murphy 2007). This could be the reason for higher DO during the precipitation events that occurred in October around the sampling dates for some sites (Figure 5.11).

The graphs (Figures 5.11 and 5.12) illustrate an inverse relationship between DO and water temperature, which is common (USGS 2015). The red dots in the graphs demonstrate that DO is lower during June, but water temperature is higher during the same month. Similar variability of DO and water temperature was found in a study in Antarctica by Bagshaw et al. (2011). The low temperature increases the DO content of water and subsequent internal re-melting may drive down the DO. Eyjafjallajökull has an overall high temperature range compared to the samples taken from the rest of the icecaps. Water temperatures are known to increase during volcanic activity and jökulhlaups (Palsson et al. 1999). The high ranges of water temperature could be due to volcanic influences on the samples taken from Eyjafjallajökull.

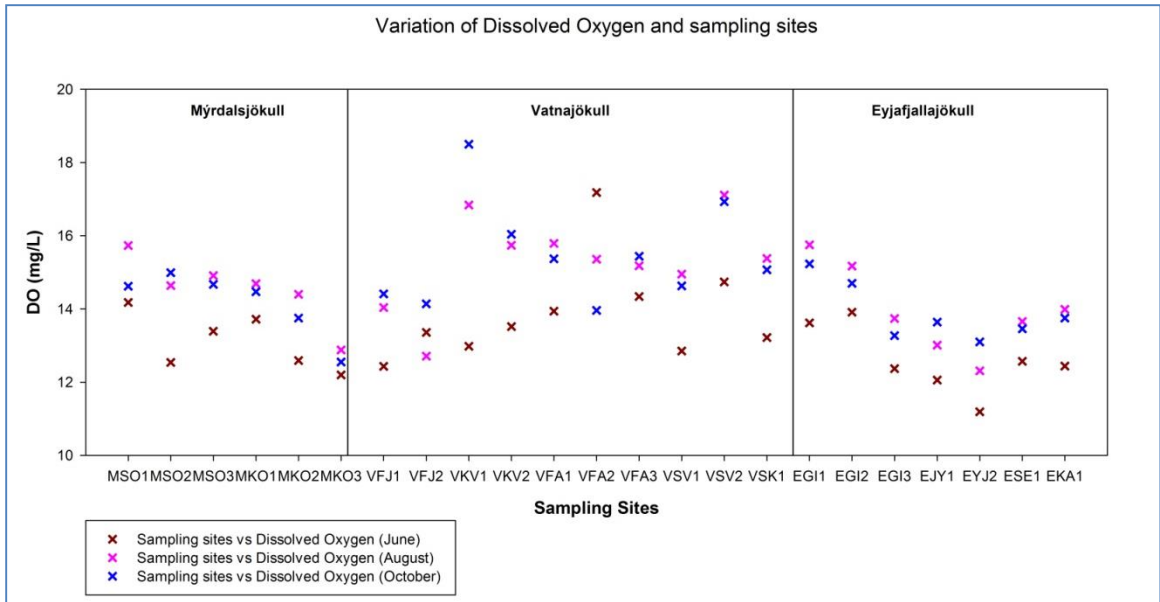


Figure 5.11. Variation of DO at sampling sites.  
Source: Created by the author.

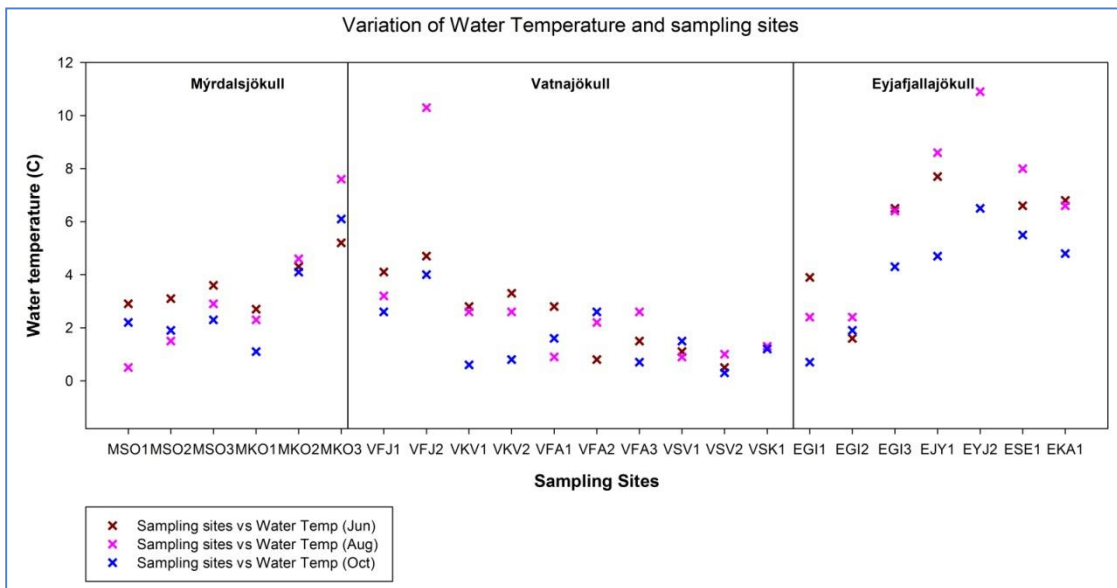


Figure 5.12. Variation of water temperature at sampling sites.  
Source: Created by the author.

#### 5.4.2 Variability of $SO_4$ , S, and F

The influence of volcanic activity is not only on pH and conductivity, but also on  $SO_4$ , S, and F. These variables are taken under consideration, because they are known to change with volcanic influence. The variations in  $SO_4$ , S, F, pH, and specific conductivity

are taken under consideration in order to investigate influences of volcanic activity on the glaciers. The spatial and temporal variation of  $\text{SO}_4$  and S are shown in Figures 5.13 and 5.14, respectively. In the rivers influenced by geothermal water, increased concentrations of sulfate are noted, and pH may either drop or increase, depending on the length of the flowpath (Kristmannsdóttir et al. 1999).

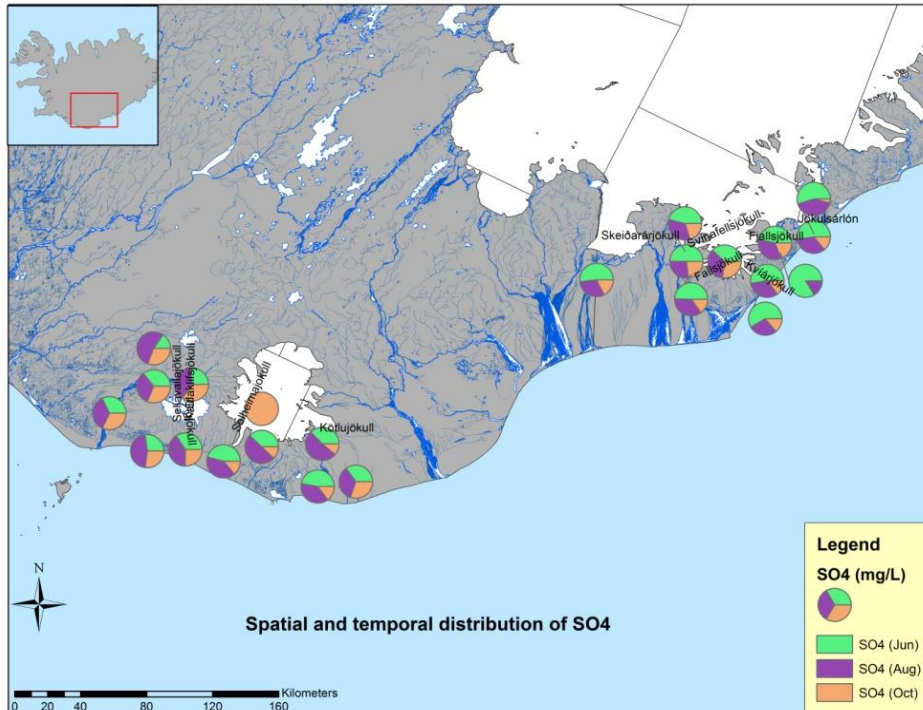


Figure 5.13. Spatial and temporal distribution of  $\text{SO}_4$ .  
Source: Created by the author from an NLSI (2014) base map.



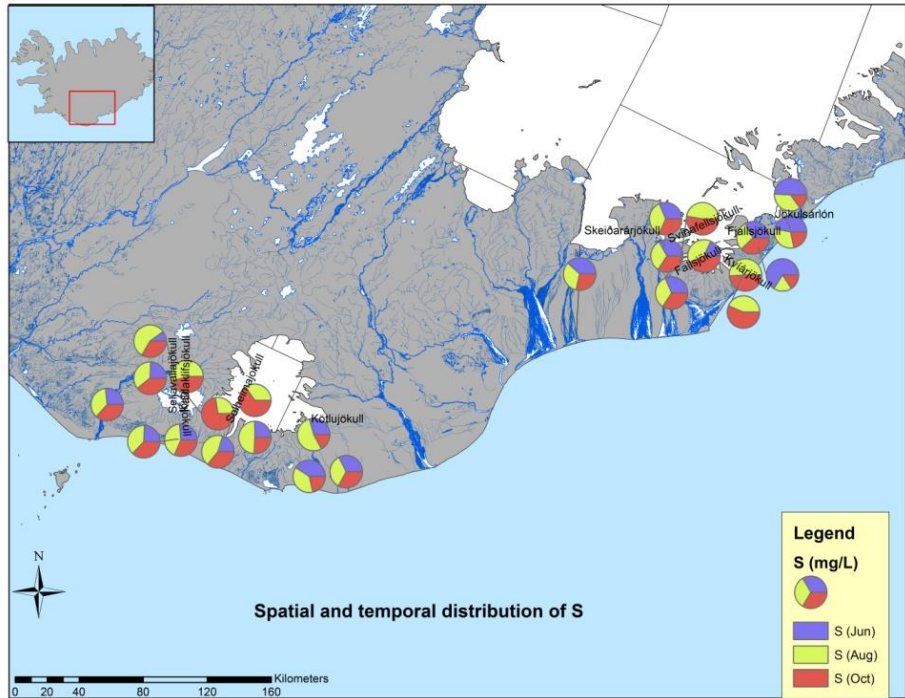


Figure 5.14. Spatial and temporal distribution of S.  
 Source: Created by the author from an NLSI (2014) base map.

High values of  $\text{SO}_4$ , S, and F were found for meltwater draining from Gígjökull (EGI2, EGI3) from the ice cap Eyjafjallajökull (Figures 5.15, 5.16, and 5.17). Meltwaters draining from Kötlujökull (Mýrdalsjökull ice cap) also have high concentrations of  $\text{SO}_4$ , S, and F. The pH values are also variable for Mýrdalsjökull samples (Figure 5.9). Samples from Vatnajökull showed the least variability amongst all icecaps for these parameters, except for Kvíárjökull, which has higher values for F (Figure 5.17).

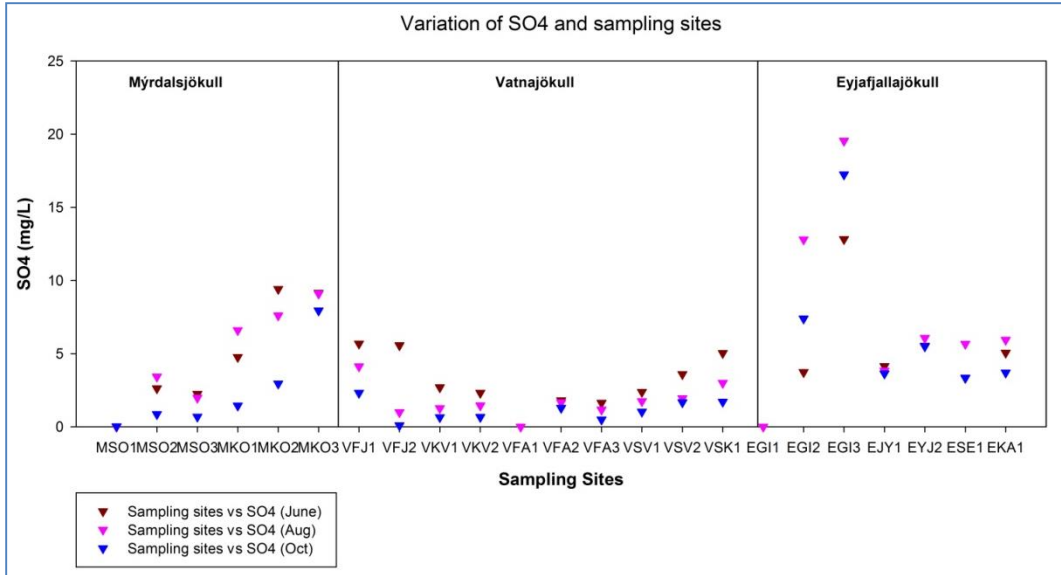


Figure 5.15. Variation of SO<sub>4</sub> and sampling sites.  
Source: Created by the author.

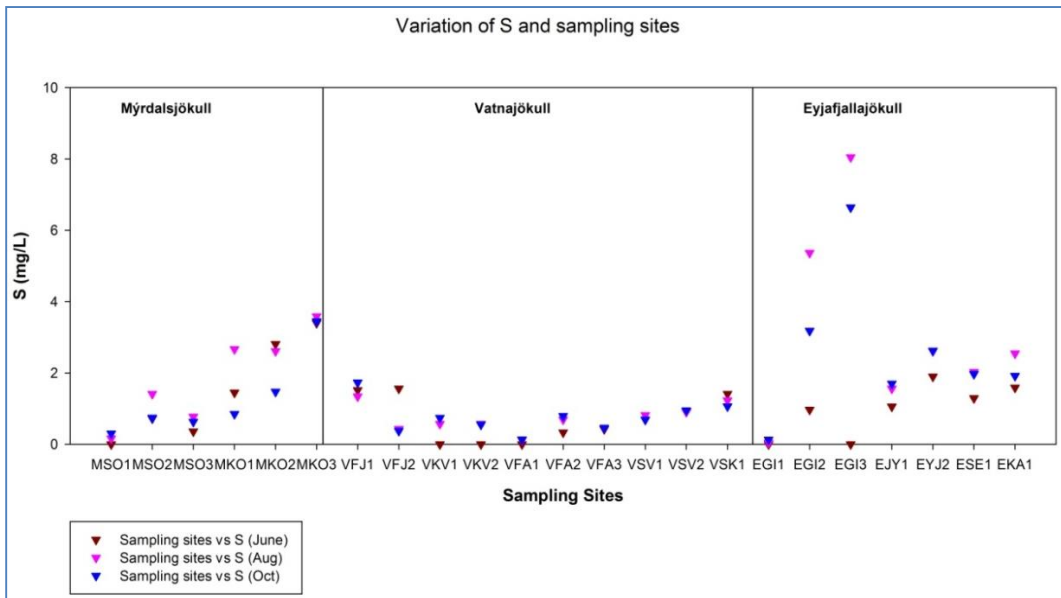


Figure 5.16. Variation of S and sampling sites.  
Source: Created by the author.

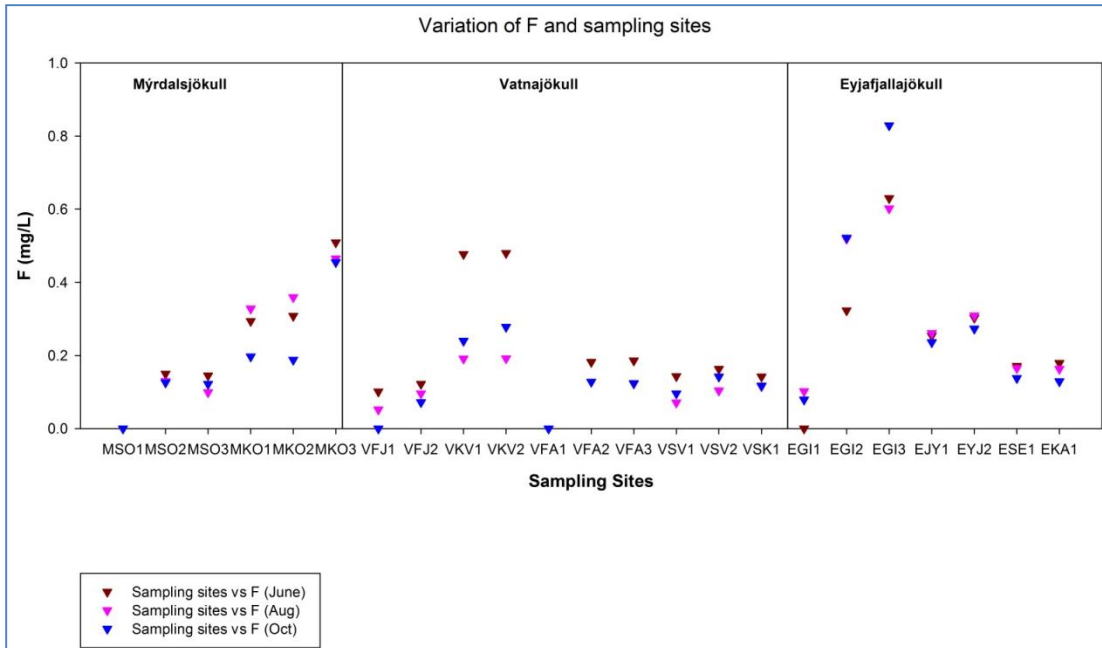


Figure 5.17. Variation of F and sampling sites.  
Source: Created by the author.

The variations in  $\text{SO}_4$ , S, and F are similar to specific conductivity value variations (Figure 5.10), as higher values are found for meltwater draining from Gígjökull (EGI2, EGI3), from the icecap Eyjafjallajökull (Figures 5.15, 5.16, and 5.17), and from Kötlujökull (Mýrdalsjökull icecap). Specific conductivity is high in variation with these ions, as they make up a large part of the dissolved ion content in the water, due to the influence from volcanic gases and weathered basalts. A greater influence of volcanic activity and influences from 2010 eruption residuals on Eyjafjallajökull and Mýrdalsjökull could be the reason for the higher values for these parameters. Samples from Vatnajökull have the least variability among all icecaps for these parameters, except for Kvíárjökull, which has higher values for fluoride (Figure 5.17). High values of specific conductivity may reveal past volcanic events that are characterized by high  $\text{SO}_4$  concentrations in ice layers (Xiao 2011). Active volcanic systems are located under these icecaps and could be the source of this, as Eyjafjallajökull is located above a tectonic

plate boundary zone (active volcanic zone). There have been recent eruptions in the icecaps Eyjafjallajökull (2010) and Mýrdalsjökull (minor activity on August 29, 2016). Active volcanic systems are also located between Fjallsjökull and Kvíárjökull at Vatnajökull. Interpolate volcanic belts cross between glaciers Fjallsjökull and Kvíárjökull in Vatnajökull. Skeiðarárjökull and Jökulsárlón, belonging to the same ice cap, do not have volcanic systems nearby. There were recent eruptions in Vatnajökull from the Grímsvötn volcano during 2011, but the sampling sites in this study are not close to it. The variations in the parameters are also because of changes in precipitation and discharge like TSS.

#### *5.4.3 Spatial and Temporal Variations of TSS*

TSS concentrations are highly variable in the Mýrdalsjökull and Vatnajökull sites and least variable in Eyjafjallajökull outputs (Figure 5.18); they range from 0 mg/L to 2,440 mg/L. The river samples taken from Kötlujökull (outlet glacier of Mýrdalsjökull), MKO3, and the river draining from Seljavallajökull (outlet glacier of Eyjafjallajökull), ESE1, have the lowest concentrations. The highest concentrations of 2,440 mg/L and 2,070 mg/L were at MKO1 and MKO2, respectively (Figure 5.18), which are also rivers draining from Kötlujökull. Physical weathering, like glacial erosion and transport, is responsible for sediment yields (Knudsen et al. 2007). Total suspended sediment concentrations are generally higher for higher discharges (Walling 1977) and most dissolved solutes (specific conductivity) cause lower values for higher discharges (due to dilution). In this case, discharge can be related to TSS, since no discharge data were available during this study at the sampling sites; hence, specific conductivity shows an inverse relationship with TSS (Figure 5.10 and Figure 5.18). The higher values of TSS

likely correspond to the higher discharge of rivers (MKO1 and MKO2) during October when discharge was visually highest due to precipitation. MKO3, however, is a smaller stream (Figure 5.19); hence, low discharge there could lead to lower TSS values than the rest of the sites at Kötlujökull.

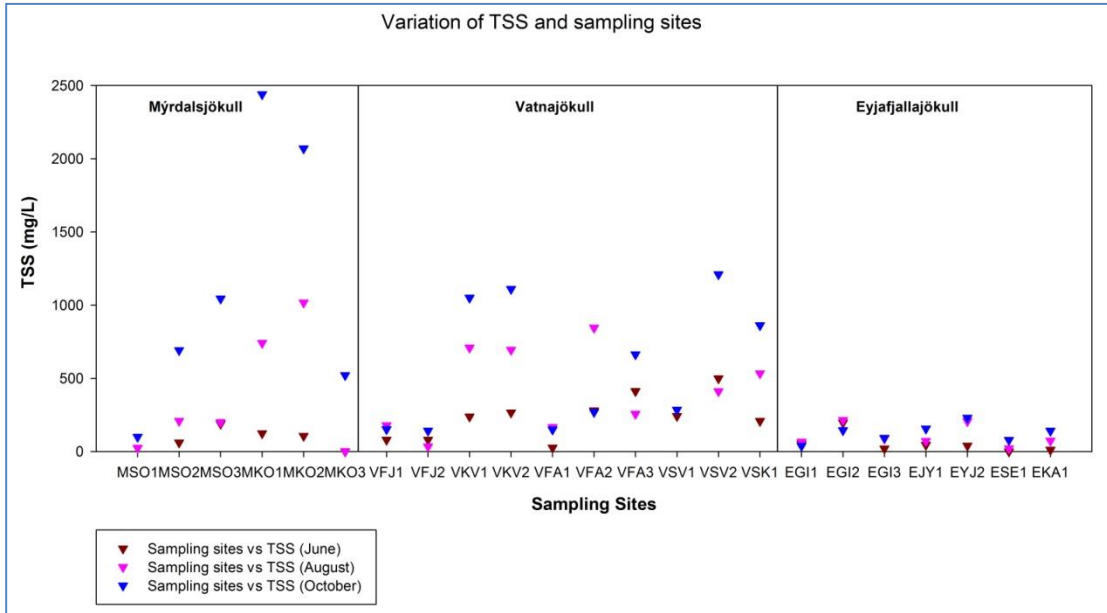


Figure 5.18. Variation of TSS and sampling sites.  
Source: Created by the author.

Turbidity values are least variable for Eyjafjallajökull and more variable for the rest of the icecaps (Figure 5.20). Turbidity was high during the month of October for Mýrdalsjökull, but high during June for Vatnajökull. The ranges are similar to TSS, with the lowest value of 0 mg/L at MKO3 and ESE1 and highest values of 906 mg/L (MKO1) and 753 (MKO2) occurring in October. The correlation of mean TSS and turbidity has a positive relationship ( $R^2 = 0.739$ ,  $p < 0.05$ ) (Appendix 13).

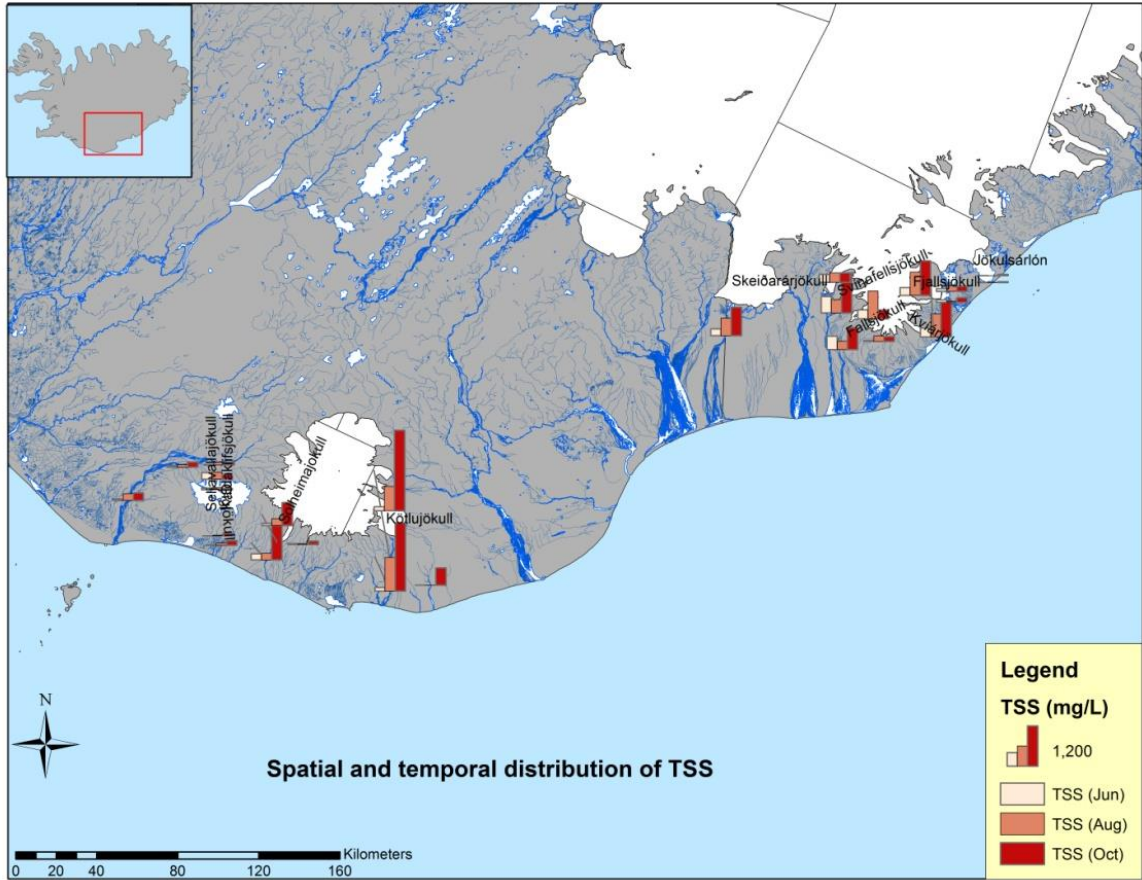


Figure 5.19. Spatial and temporal distribution of TSS.  
 Source: Created by the author from an NLSI (2014) base map.

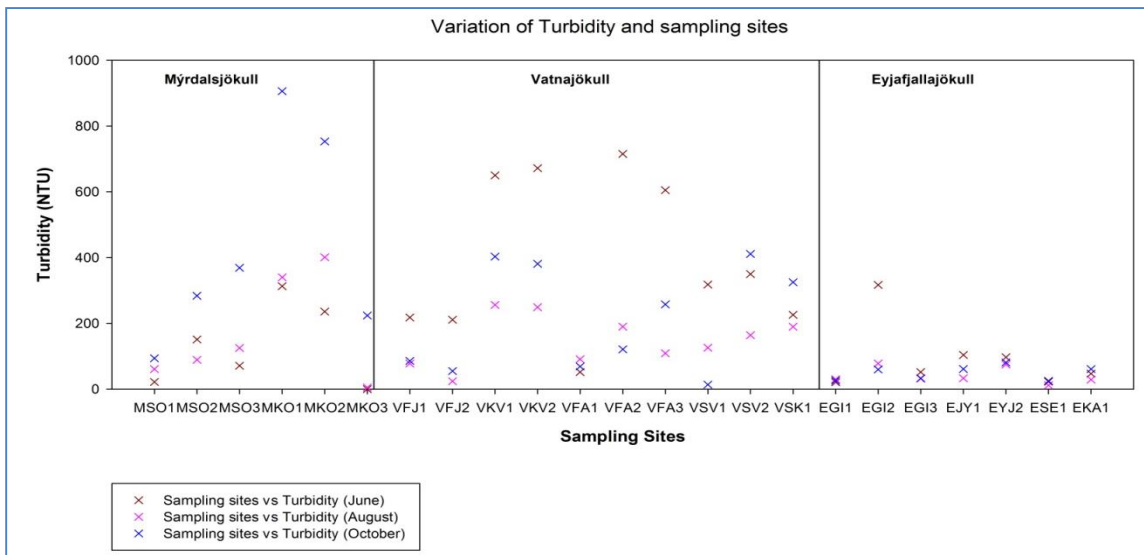


Figure 5.20. Variation of Turbidity at sampling sites.  
 Source: Created by the author.

The results for hydrogeochemical parameters indicate high variability in terms of both space and time. The total suspended solids ranged from its highest to lowest concentrations (Table 5.5) in different sampling sites of river draining from the same glacier, Kötlujökull. Also, there is a high seasonal variation in different sites of the same glacier, MKO1, 124 to 2,440 mg/L, MKO2, 106 to 2,070 mg/L, and MKO3, 0 to 521 mg/L from June to October, respectively. This indicates the importance of taking multiple samples for hydrogeochemical studies, as the lowest and highest concentrations can appear from the same glacier at different locations along its base or downstream reaches of the river formed by its meltwater.

Sediment transported to the river channels in volcanic mountainous terrain is likely influenced by climate conditions, particularly when heavy precipitation and warmer climates trigger mudflows in association with melting snow (Mouri et al. 2014). Volcanic activity has resulted in a 1.5- to 8-fold increase in total suspended solids in lakes located in Patagonia (Modenutti et al. 2013). Earthquake and seismic activity, which occurred at the end of August 2016, could possibly be the reason for higher TSS values at MKO1 and MKO2. Gurnell et al. (1996) found no significant relationship between suspended sediments in rivers and basin or glacier area; basins containing predominantly warm-based glaciers produce higher suspended sediment yields than those containing cold-based glaciers. Within their study of 90 glacier basins, Icelandic basins produce some of the highest suspended sediment yields per unit basin area, due to volcanic activity (Gurnell et al. 1996). The mean suspended sediment yield per unit area and catchment area is lower for cold-based glaciers, Alaskan basins, and other warm-based glaciers compared to Iceland. This supports finding high values of TSS (2,400

mg/L) in the present study, due to the presence of volcanic sediment, and also the high variability, since the lowest value is 0 mg/L.

Suspended sediment loads are often studied for planning of possible hydropower stations, since less sediment means higher turbine operation efficiency (Bishwakarma 2007). It should be taken under consideration that a single sampling period will not be enough for such planning, because of seasonal variation. Bigger rivers, like those formed from meltwaters draining from Kötlujökull, could be possibly considered for a hydropower plant, but the increase in TSS during October might negatively impact the turbine. The variability in total suspended solids is also important for hydrologic and geomorphic processes over long-term studies. The transport of suspended sediment is a product of erosion, and erosion and deposition processes within a basin depend heavily on factors such as climate and relief (Filizola et al. 2010), leading to higher seasonal variation. Iceland's variable precipitation, combined with extensive highlands, has an enormous energy potential up to 220 TWh/yr (Orkustofnun 2016). Of the primary energy use in Iceland, 20% was generated from hydropower in 2014. The total electricity production was 12.9 TWh from hydropower in 2014, meaning that appropriate attention should be given to developing hydropower projects on rivers carrying high sediment loads and how sampling is conducted to determine the feasibility of such installations (Bishwakarma 2007). Designing hydropower plants based only on the availability of water is not realistic, as the sediments in water limit the production most during periods of higher precipitation, which requires specific sampling in order to capture hydropower potential accurately.



## 5.5 Ion Variability and Dominance

The minimum and maximum concentrations of chemical parameters are presented in Table 5.2.1. Ca varies from 0.22 to 36.08 mg/L and Na varies from 0.042 to 36.58 mg/L. Other cations of importance are Mg (0.057 to 19.959 mg/L) and K (0.026 to 5.74 mg/L). Ca is almost always more abundant than Mg and concentrations of K are very low in comparison to the other major ions. Similar dominance patterns in ions were found by Louvat et al. (2008) in Icelandic rivers. The dominance in pattern is similar not only with glacial rivers but also with samples taken directly from glacier and proglacial lagoon sites in this study, as ~90% of Iceland is made from basaltic rocks that are rich in divalent cations, like Ca (Snæbjörnsdóttir et al. 2014).  $\text{HCO}_3^-$  varies between 6.11 and 479.23 mg/L, with the highest value found at one of the rivers draining from Eyjafjallajökull, ESE1, during August. Surprisingly, the lowest concentration belongs to the same icecap, but at a different location, which is the sample taken directly from the glacier Gígjökull (EG11). After  $\text{HCO}_3^-$ , the most concentrated anions are chloride and sulfate. The concentrations of both these anions show temporal variation similar to the ions discussed above. Cl varies from 0.095 to 50.90 mg/L and  $\text{SO}_4$  from 0.025 to 19.542 mg/L.  $\text{NO}_3^-$  ranges from 0 to 9.62 mg/L. The Cl distribution in Icelandic rivers is dominated by salts likely derived from oceanic inputs, like marine aerosols (Vasil'schik 2009) and, thus, are impacted by the sampling site location's proximity to a glacier river and its distance to the ocean.

There is a variation in ions with respect to geographic location. Most of the minimum concentrations of these ions are from samples directly taken from glacier meltwater on the glacier and the highest are for river samples from Eyjafjallajökull taken

directly from the meltwater rivers emanating from the glacier's base. Samples taken directly from the glacier Gígjökull have the lowest concentrations of calcium, bicarbonate, sulfate, fluoride, and nitrate. Meltwaters from the glacial surface on Himalayan glaciers also generally have low solute content; whereas, after passing through the glacier, waters were found to be chemically enriched (Hasnain et al. 1989). The same pattern is observed in samples taken directly from Icelandic glaciers, where the solutes are low, thereby suggesting that the majority of ion loading and weathering is taking place during basal melting and subglacial weathering processes. Higher concentrations of ions downstream might be due to increase in weathering rates (Bhatt and McDowell 2007), high erosion, and due to differences in contact time between rock and water (Louvrat et al. 2008). Lower concentrations of ions in the sample taken directly from Gígjökull might also be due to its location away from coastline, as the concentration of marine aerosols decreases sharply away from the ocean (Vasil'schik 2009). The lowest concentrations of the ions also belong to glacier meltwaters directly taken from the Solheimajökull and Falljökull glaciers from surface melt flowing off the glacier tongues despite the variability of the icecaps and glaciers. Almost all of the samples with the highest concentrations come from rivers flowing from Eyjafjallajökull icecap glaciers.

The variation of cation (Ca, Mg, Na, K) and anion ( $\text{HCO}_3$ ,  $\text{SO}_4$ , and Cl) values are plotted for each site and Figures 5.21, 5.22, and 5.23 show the distribution of spatial variation of major ions in the icecaps for June. The ion variation maps for August and October are in the Appendix (Figures A1-A6).  $\text{HCO}_3$  is the dominant anion in the icecaps and Ca and Na are the dominant cations.

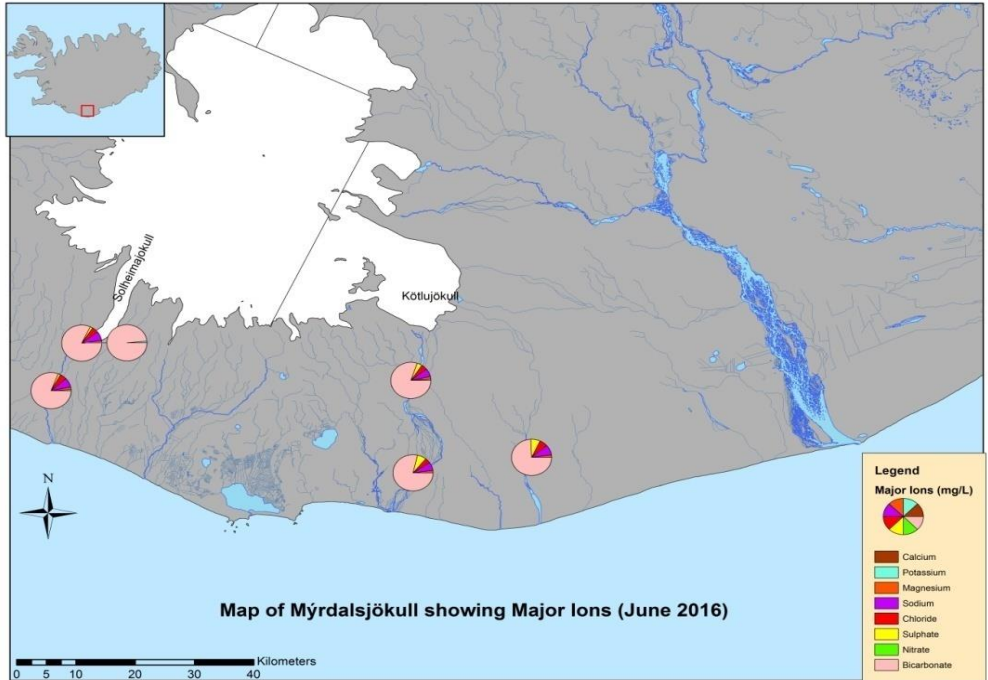


Figure 5.21. Map of Mýrdalsjökull showing major Ions (June 2016).  
Source: Created by the author from an NLSI (2014) base map.

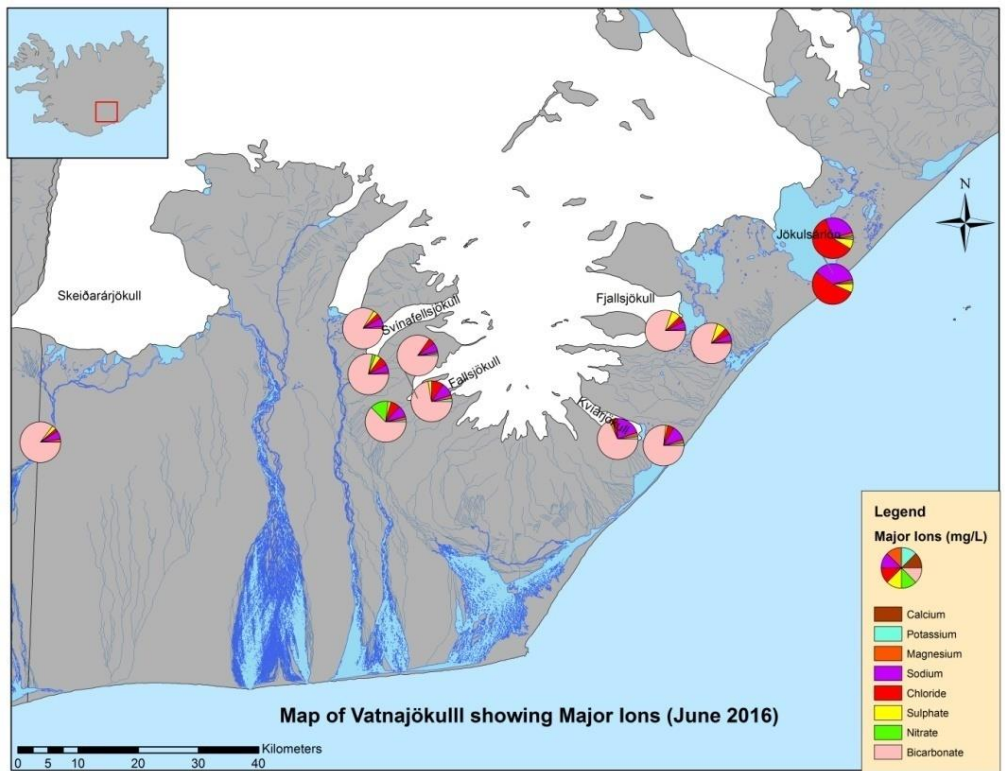


Figure 5.22. Map of Vatnajökull showing major ions (June 2016).  
Source: Created by the author from an NLSI (2014) base map.

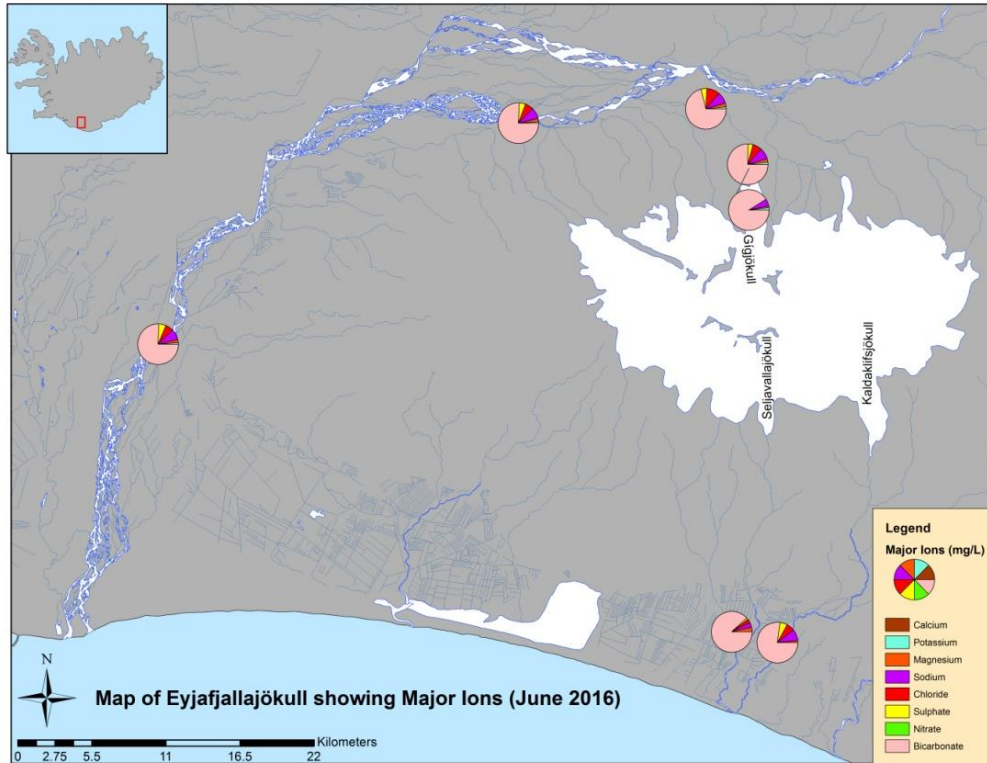


Figure 5.23. Map of Eyjafjallajökull showing major ions (June 2016).  
 Source: Created by the author from an NLSI (2014) base map.

Relationships between water composition and rock type can be evaluated by plotting the concentration of major cations and anions in a Piperplot diagram (Figures 5.24, 5.25, and 5.26). The Piper plots show that the majority of samples fall into the category of Ca-HCO<sub>3</sub> and Na-HCO<sub>3</sub> dominance. The majority of samples fall into the Na-HCO<sub>3</sub> category for Vatnajökull (Figures 5.25; Appendices A9 and 10), except for the lagoon, Jökulsárlón, which is dominated by Na-Cl (Figures 5.22 and 5.25). Eyjafjallajökull also is in the category of Na-HCO<sub>3</sub>-dominated water (Figure 5.26; Appendices A11 and A12), except for the river from Seljavallajökull, which is dominated by both Ca-HCO<sub>3</sub> and Na-HCO<sub>3</sub>.

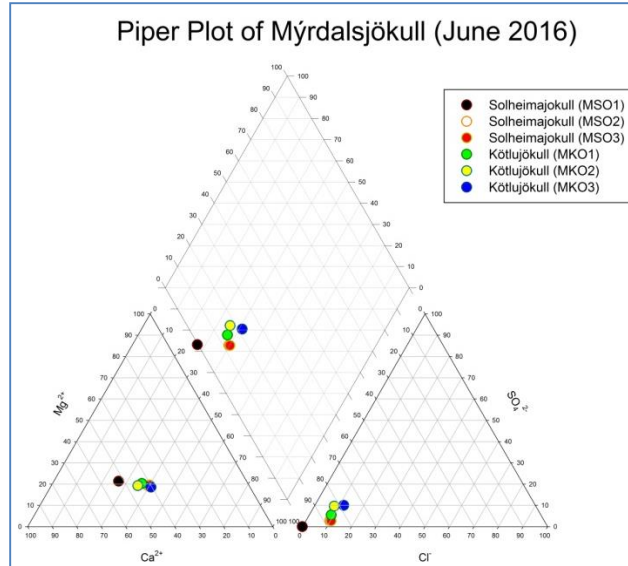


Figure 5.24. Piper plot of Mýrdalsjökull (June 2016).  
Source: Created by the author.

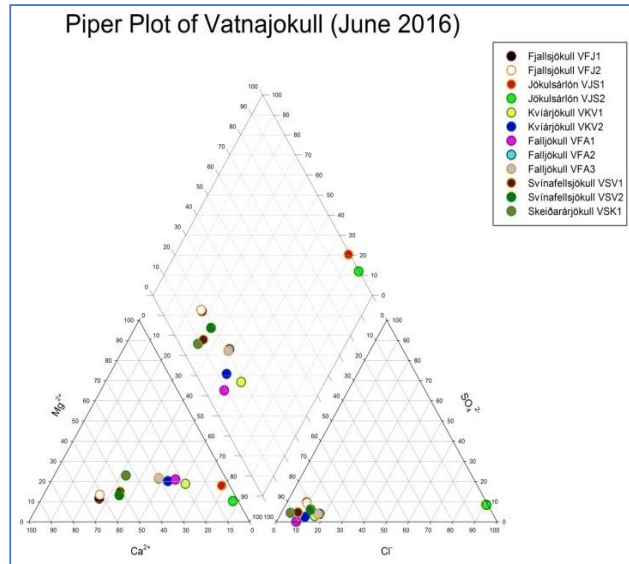


Figure 5.25. Piper plot of Vatnajökull (June 2016).  
Source: Created by the author.

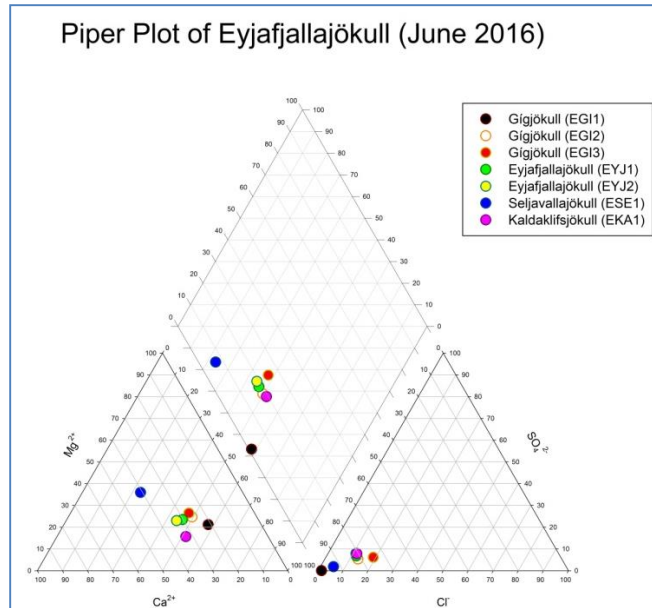


Figure 5.26. Piper plot of Eyjafjallajökull (June 2016).  
Source: Created by the author.

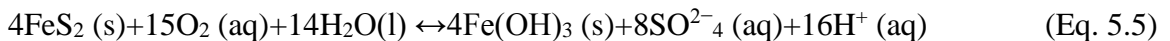
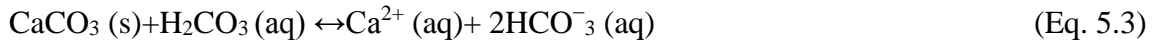
There is a positive correlation between Ca and  $\text{HCO}_3$  and Na and  $\text{HCO}_3$  with  $R^2$  values of 0.761 and 0.808, respectively ( $p < 0.05$ ) (Appendix 14). The dominance of Na and Ca, and  $\text{HCO}_3$ , and the strong relationship between Na and Ca with  $\text{HCO}_3$ , suggest that the hydrogeochemical variability is driven by Na- $\text{HCO}_3$  and Ca- $\text{HCO}_3$  weathering. It is important to know the main weathering process, because it is the source of ions in the system. Geochemical characteristics of meltwaters from the glaciers are extremely important to understand major ion chemistry and to gain insight into the geochemical weathering processes controlling glacier hydrochemistry (Singh et al. 2012).  $\text{HCO}_3$  may be derived from several sources, including from the dissociation of atmospheric  $\text{CO}_2$ , the dissolution of carbonate minerals, such as calcite (Tranter et al. 1993), and primarily from silicate rock weathering in Iceland. Marine aerosols are usually the main sources of Na (Vasil'chuk 2009). Sodium is also a major element in all igneous rock types (Stueber and Goles 1967). Ca may also be derived from basaltic rocks, which are rich in this divalent

cation and ~90% of Iceland is made from basaltic rocks (Snæbjörnsdóttir et al. 2014).

The dominant processes responsible for production of these ions can be found out with the help of determining the C ratios, as discussed below.

### 5.5.1 Elemental Ratios

The relative importance of two major proton-producing reactions, carbonation and sulfide oxidation, can be evaluated on the basis of the C-ratio. Brown et al. (1996) proposed estimation of the C ratio ( $\text{HCO}_3^-/\text{HCO}_3^-+\text{SO}_4^{2-}$ ). If the C ratio is 1.0, it indicates the significance of carbonation reaction involving acid hydrolysis and pure dissolution, consuming protons from atmospheric  $\text{CO}_2$  (Equations 5.1, 5.2 and 5.3). Conversely, if the C ratio is 0.5, this suggests a coupled reaction involving carbonate weathering and protons derived from oxidation of sulfide (Equation 5.5).



The C ratio is close to one for almost all of the samples (Figure 5.27); hence, this indicates the significance of carbonation reaction involving acid hydrolysis and pure dissolution, consuming protons from atmospheric  $\text{CO}_2$  (Brown et al. 1996) (Equations 5.1, 5.2, 5.3). The meltwaters are dominated by Na- $\text{HCO}_3^-$  and Ca- $\text{HCO}_3^-$  type weathering with carbonation as the main proton supplying geochemical reaction controlling rock weathering in the study area.

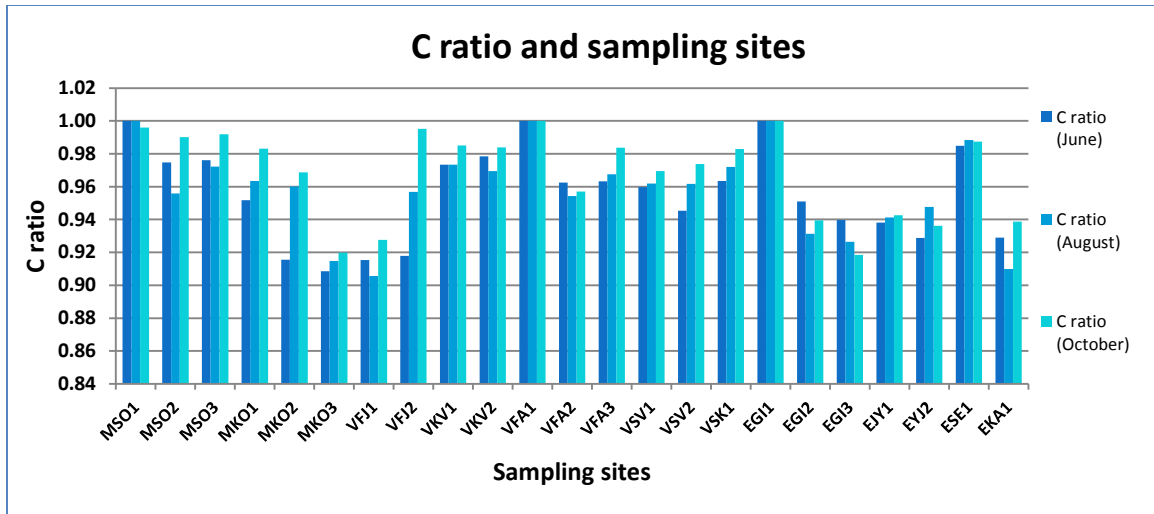


Figure 5.27. C ratios and sampling sites.  
Source: Created by the author.

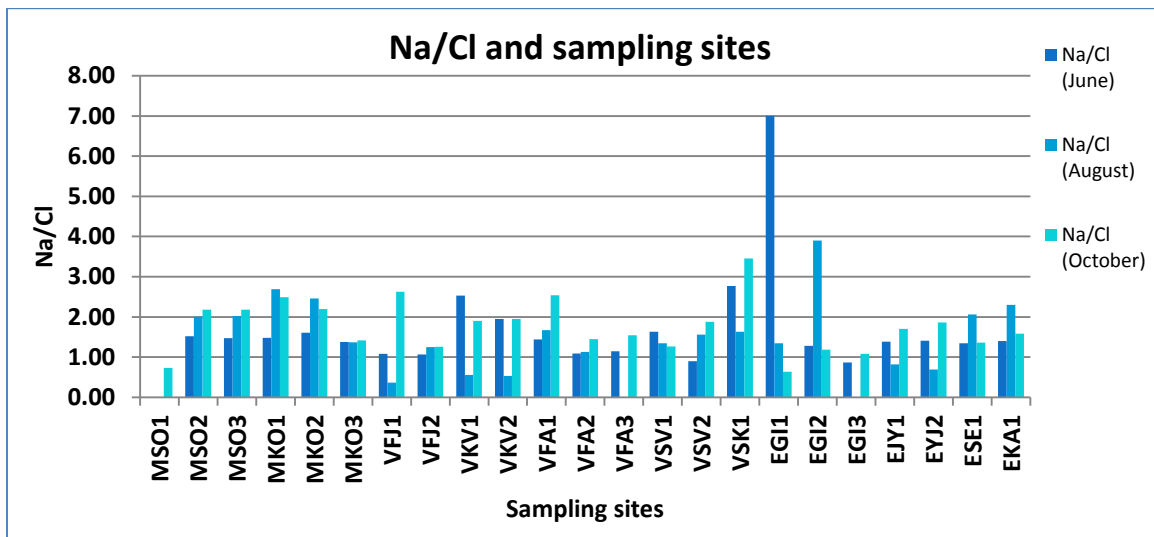


Figure 5.28. Na/Cl and sampling sites.  
Source: Created by the author.

The importance of atmospheric inputs for river water composition can also be determined by the ratio of ions to chloride. The average Na/Cl and K/Cl ratios were close to those of seawater (i.e. Na/Cl = 1.0 and K/Cl = 0.2, respectively) (Figures 5.28 and 5.29). Most of the samples have an Na/Cl ratio close to 1 and a K/Cl ratio close to 0.2, except for the sample taken directly from Gígjökull (EGI1). These ratios indicate a contribution from atmospheric precipitation to the observed dissolved ion concentrations



in the meltwater samples. The ratio at EGI3 indicates a relatively minor contribution from atmospheric precipitation to observed dissolved ions.

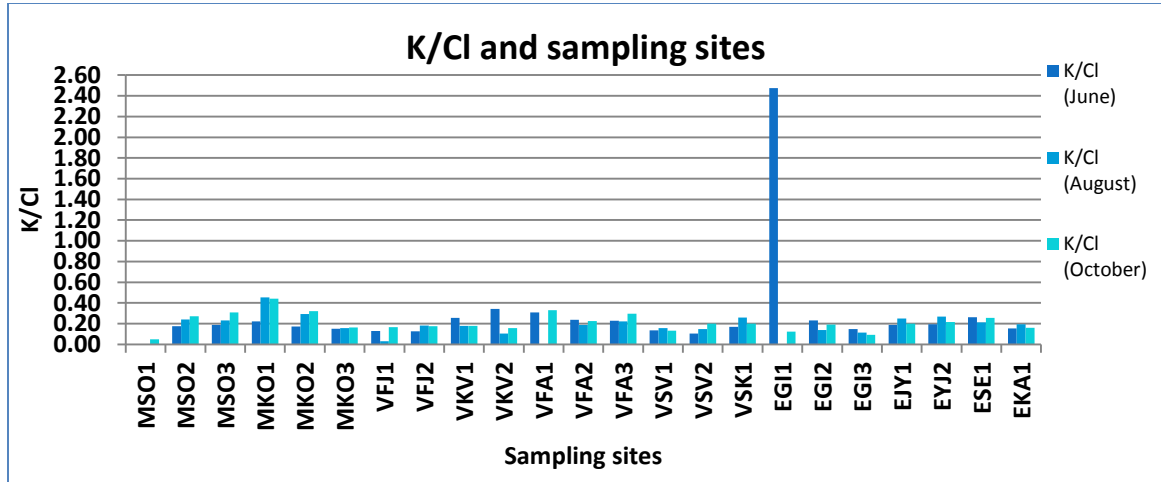


Figure 5.29. Monthly K/Cl.  
Source: Created by the author.

### 5.5.2 Ion Dominance Comparison

Global mean runoff has a dominance pattern of  $Ca > Mg > Na > K$  for cations and  $HCO_3 > Cl > SO_4$  for anion dominance (Livingstone 1963). The Himalaya (Hasnain et al. 1989; Ahmad and Hasnain 2001; Tuladhar et al. 2015), along with the European Alps (Brown et al. 1993; Collins 1979; Thomas and Raiswell 1984), have the same dominance patterns. Greenland (Rasch et al. 2000) and Iceland (Raiswell and Thomas 1984; Steinþórsson and Oskarsson 1983), however, have a different dominance pattern, where Ca and Na are the dominant ions, instead of Ca and Mg, which is also in agreement with the results of this study for Iceland (Figures 5.21, 5.22, and 5.23; Table 5.1).

The location of the sampled Icelandic glaciers close to the ocean might be the reason Na is higher, since marine aerosols are usually the main source for Na (Vasil'chuk 2009). Weathering of Na-bearing igneous rocks might also contribute to higher Na;

however,  $\text{HCO}_3^-$  is the dominant anion in the aforementioned glacial runoff systems, regardless of the location, and this holds true for the sites in this study as well. The range in this study is highly variable (6.11 to 479.23 mg/L, Table 5.2.1) compared to the Himalaya (12.93 to 78.10 mg/L) (Tuladhar et al. 2015). Several factors might be the reason for higher  $\text{HCO}_3^-$  in Iceland, including dissolution from atmospheric  $\text{CO}_2$  (Figure 5.27) and higher  $\text{CO}_2$  from volcanic activity (Dessert et al. 2002). Moreover, the presence of Ca-rich basalt rocks and their capacity for sequestering  $\text{CO}_2$  in carbonate minerals (Rosenbauer et al. 2012) could also be the reason for high  $\text{HCO}_3^-$  in Icelandic glaciers in this study. Compared to a global average, the chemical weathering rates of basalt in southwest Iceland are also high and rather variable (Gislason et al. 1996). Studies suggest that the contribution of Si-weathering to global atmospheric  $\text{CO}_2$  sequestration may be only 6%, while up to 94% may be from carbonate weathering (Liu et al. 2011). Mass balance calculations of mineral-weathering contributions to the dissolved ions from the High Himalayan Crystalline Series watershed indicate that 82% of the  $\text{HCO}_3^-$  flux is derived from the weathering of carbonate minerals and only 18% is derived from silica weathering (Blum et al. 1998). Transient consumption of atmospheric  $\text{CO}_2$  by chemical weathering in Iceland is greater than  $\text{CO}_2$  degassing from the Icelandic mantle plume (Gislason et al. 1996); however, long-term consumption by weathering of Ca-Mg silicates and precipitation of Ca-Mg carbonates in the ocean is less than the  $\text{CO}_2$  degassing. Quantifying the flux of carbon in Iceland meltwater rivers would be useful based on the preliminary data presented herein, but is beyond the scope of this study.

$\text{CO}_2$ -rich water also forms by the mixing of magmatic  $\text{CO}_2$  with surface, non-thermal, or geothermal groundwater in Iceland (Arnorsson et al. 2010). Geothermal

waters in volcanic areas acquire solutes through the hydrothermal alteration processes of hydration, carbonation and sulfide formation (Ellis and Mahon 1978; Fournier 1981), and wallrock leaching (Sigvaldason 1981). Volcanic gases, especially H<sub>2</sub>S and CO<sub>2</sub>, are also usually dissolved during wallrock leaching (Sigvaldason 1981). An analysis of silicate versus carbonate weathering in Iceland revealed that 90% of the Ca in Icelandic rivers originates from the weathering of hydrothermal calcite as opposed to Ca-bearing silicate minerals (Jacobson et al. 2015). The order of preferential release of ions from the partially melted snow is H<sup>+</sup> > Mg<sup>2+</sup> > Cl<sup>-</sup> ≥ Na<sup>+</sup> > SO<sub>4</sub><sup>2-</sup> > K<sup>+</sup> > Ca<sup>2+</sup>. In general, the more soluble the element, the more it is diluted as runoff increases over time.

### 5.5.3. Other elements

Most of the Icelandic glacial meltwaters have low metal concentrations (Al, Ba, Cr, As, Mn, Ni, P, Se, Sr, V, and Zn), which are below or close to detectable limits in this study (Appendices 5, 6, and 7); however, Al, Fe, S, and Si are higher in some of the glacial runoff samples than the other samples. As for the major elements, the concentrations of Al and Fe at the river outlet of Kötlujökull, MKO1 (Mýrdalsjökull ice cap) (9.24 mg/L and 22.67 mg/L, respectively), are higher during August. The concentrations of the rest of the samples are very low and closer to the detectable limit, except for Kvíárjökull, VKV1 and VKV2 (Vatnajökull), where ranges vary for Al (1.26 to 5.13 mg/L) and Fe (2.42 to 8.33 mg/L). The others range from below detectable limits to 3.59 mg/L. The highest Si values are 20.19 mg/L (VKV1) and 23.07 mg/L (VKV2) during June, which are the lagoon and river outlets of Kvíárjökull (Vatnajökull).

The most common point between them is that they drain very close to active volcanic zones. Active volcanic systems and an interpolate volcanic belt are located close

to Kvíárjökull as well; thus, the high concentrations of these elements may be due to high reactivity of young rocks, magma degassing, and/or input from geothermal springs (Louvati et al. 2008). Chemical weathering rates are conversely correlated to the age of the rocks (Louvati and Allergre 1998). The rock formation types are variable in our study sites. The basement rock on which the icecaps are located differ in their ages, as Eyjafjallajökull and Mýrdalsjökull are formed on upper Pleistocene formation rocks (<0.7 My), while the sampling sites from Vatnajökull are formed in various geologic formations (Thordarson and Hoskuldsson 2002). Skeiðarárjökull formed on an older formation (3.3-0.7 My), but its outlet is on a younger formation (<10,000 years). The rest of the glaciers are formed on Upper Pleistocene rocks, like Eyjafjallajökull and Mýrdalsjökull (<0.7 My), with the exception of Jökulsárlón (<10,000 years). The basaltic rocks are younger near the active rift zones (Snæbjörnsdottir et al. 2014); thus, the differing ages of rocks, even within an icecap or glacier, could also influence the rate and composition of the weathering based on rock induration and remaining amounts of trace elements in the host bedrock at the time of erosion.

The youngest basaltic formations in Iceland are known to be the most feasible for carbon storage (Snæbjörnsdottir et al. 2014), which consist of lavas, hyaloclastic (glassy) formations, and associated sediments younger than 0.8 My covering one third of the landscape (Thordarson and Hoskuldsson 2002). These formations are made of highly porous and permeable basaltic lavas and hyaloclastite formations with abundant groundwater flow (Snæbjörnsdottir et al. 2014). Hydrothermal alteration and formation of secondary minerals takes place when the rocks are buried under younger formations and are then exposed to more heat and pressure. Most of the pore space in the older rocks is

filled, since the molar volume of secondary minerals is larger than the molar volume of primary minerals, and some secondary minerals contain water and CO<sub>2</sub> that could contribute to chemical weathering.

## 5.6 TDS Variability

A river's geochemistry can be classified based on total dissolved solid (TDS) concentrations, which, in turn, can be related to watershed bedrock types. The TDS values are highly variable with respect to sampling time and glacier. The classification for TDS (Stallard and Edmond 1983; Berner and Berner 2012) is as follows:

- 1) < 20 mg/L: Intensively weathered silicate-rich rocks
- 2) 20-40 mg/L: Silicate-rich igneous rocks and metamorphic rocks and shales
- 3) 40–250 mg/L: Marine sediments including carbonates, pyrite; minor evaporites
- 4) > 250 mg/L: Evaporitic rocks

The TDS values are color coded in Table 5.6, with the lightest color as group one and darkest as group four. The TDS values for meltwater draining from Eyjafjallajökull and Mýrdalsjökull indicate their source rock is marine sediments, including carbonates, pyrite, and minor evaporates during all sampling periods, except for the sites closer to the glacier, which are EGI1 and MSO1, respectively. Basaltic compositions are rich in MgO and CaO. Low potassium and high MgO basalts are encountered along the entire Icelandic rift system (Oskarsson et al. 1994), so it is likely these are causing the classification to mimic that of carbonate rock weathering. The TDS values of EGI1 and MSO1 indicate that they belong to intensively weathered silicate rocks. Vatnajökull has highly variable TDS values, as the classification changes temporally. Jökulsárlón, however, has a TDS > 250 mg/L, falling in the classification of evaporate rocks during all

sampling periods, which is likely due to the oceanic influence driving the values toward halite-like evaporate signatures. The rest of the glacier sites vary between groups three and four. Most of the samples from Vatnajökull belong to the Si-rich igneous and metamorphic rocks groups, while some indicating a dominance of Ca and Mg.

Table 5.6. Categorization of TDS with increasing values highlighted darker for sites

Ice cap	Glacier	Sample code	TDS June (mg/L)	TDS Aug (mg/L)	TDS Oct (mg/L)
Mýrdalsjökull	Solheimajokull	MSO1	1.975	0.866	9.507
		MSO2	68.1	48.497	47.118
		MSO3	62.24	44.664	40.759
	Kötlujökull	MKO1	63.9	104.298	38.738
		MKO2	76.96	111.64	46.068
		MKO3	79.76	83.703	75.611
Vatnajökull	Fjallsjökull	VFJ1	47.16	94.821	73.961
		VFJ2	49.1	15.229	13933
	Jökulsárlón	VJS1	22226.3	16010.344	9644.637
		VJS2	27,289.50	11,548.69	12,719.50
	Kvíárjökull	VKV1	56.14	27.814	29.407
		VKV2	56.32	27.771	29.241
	Falljökull	VFA1	2.77	3650	50.004
		VFA2	38.7	21.167	42.761
		VFA3	27.31	20.447	19.326
	Svínafellsjökull	VSV1	34.5	25.93	33.087
		VSV2	40.85	32.656	36.243
	Skeiðarárjökull	VSK1	80.14	49.303	48.301
	Eyjafjallajökull	Gígjökull	EGI1	6.8	1.324
EGI2			73.98	167.455	90.055
EGI3			170.13	247.886	187.91
Rivers		EYJ1	46.4	52.801	48.703
		EYJ2	56.15	76.344	60.635
Seljavallajökull		ESE1	125.93	271.557	157.212
Kaldaklifsjökull		EKA1	45.59	49.96	45.354

Source: Adapted by the author from Stallard and Edmond (1983) and Berner and Berner (2012).

## 5.7 Geochemical Composition of Jökulsárlón Lagoon

The results from Jökulsárlón proglacial lagoon (VJS1) and the site where the river meets the ocean (VJS2) are provided in Table 5.7. They stand out from the other sample points in this study, which was anticipated, and provide a comparative example of advanced glacial lagoon development. The pH values (8.12 to 9.03) are in the alkaline range, except for the October samples, which are slightly higher. Specific conductivity is high, ranging from the lowest, 14,307  $\mu\text{S}/\text{cm}$ , to the highest of 34,201  $\mu\text{S}/\text{cm}$ . The DO levels are highest during October for VJS1 (15.8 mg/L) and VJS2 (13.99 mg/L). The samples fall into category of Na-Cl dominance. Elevated concentrations of  $\text{NO}_3$  are found with the highest concentrations of 29.3 mg/L (VJS1) and 32.76 mg/L (VJS2) during June, probably due to the presence of birds in the area and the influence of seawater in the lagoon itself from mixing.

Table 5.7. Physical and chemical concentrations of Jökulsárlón.

Parameters	June		August		October	
	VJS1	VJS2	VJS1	VJS2	VJS1	VJS2
pH	8.26	8.12	8.16	8.26	9.03	8.57
Specific conductivity ( $\mu\text{S}/\text{cm}$ )	34201	41957	24629	17662	14307	17908
DO (mg/L)	11.02	10.99	12.19	14.1	15.8	13.99
TSS (mg/L)	0	6	0	7	40	26
Turbidity (NTU)	0	6	0	7	28	34
Ca (mg/L)	240.04	301.95	192.83	234.91	91.7	167.98
Mg (mg/L)	713.83	758.45	570.23	708.42	301.68	570.18
Na (mg/L)	5735.36	12012.16	5228.07	5862.83	2500	4457.16
K (mg/L)	327.43	398.91	154.58	175.36	80.65	137.39
$\text{HCO}_3$ (mg/L)	2049.6	2673.02	121.41	141.15	203.09	220.99
Cl (mg/L)	13257	17738	9434	11042	5379	8145
$\text{SO}_4$ (mg/L)	1680	2191	121.41	141.15	203.09	220.99
S (mg/L)	591.79	733.25	424.81	489.14	181.36	334.23
$\text{NO}_3$ (mg/L)	29.3	32.76	19.57	14.8	3.51	4.21

Source: Created by the author.

The concentrations are low for Ca, Mg, Na, K, HCO<sub>3</sub>, Cl, SO<sub>4</sub>, S, and NO<sub>3</sub> during October (Table 5.7), when the precipitation was highest (Figure 5.6), indicating the likely effect of dilution from the rain. Pulses, turnover, and seawater mixing could be the reason for more variability and melting in the area. The closeness of the lagoon to the ocean might also be the reason for higher concentrations of ions and high sensitivity to changes throughout the sampling period. It is important to study glaciers and lagoons closer to the ocean because they are sensitive to minor changes. Changes in their chemistry, like a decrease in coastal pH, can hamper the way organisms survive (NRC 2014). A small decrease in pH can make it difficult for them to manufacture their skeletons. Large tidewater glaciers in Alaska and the Arctic, and individual icecaps in Greenland and other parts of the Arctic, may be especially sensitive to an increase in sea levels and the direct impact of oceanic water (i.e., as result of wave erosion) (Zwally et al. 2002; Steffen et al. 2004). The Jökulsárlón sample sites are characterized by the highest concentrations of ions compared to the rest of samples from three icecaps with an exception of bicarbonate, which is higher in some of the samples from Eyjafjallajökull during August (EGI2, EGI3, and ESE1) and October (ESE1). Higher concentrations at Eyjafjallajökull might be due to its location close to active volcanic zones and above a tectonic plate boundary zone, and higher CO<sub>2</sub> inputs from volcanic activity (Dessert et al. 2002).

As glacier retreat has accelerated, leading to increases in lagoon size, some of the glacial lagoons closer to the ocean, like Kvíárjökull, Fjallsjökull, and Solheimajökull, might be susceptible to increased solutes in the future. This connection of fresh glacial and ocean water can lead to changes in lagoon hydrogeochemistry. More melting from a warmer ocean's influence on colder meltwater systems, as well as changes in ions like



sodium, can lower the melting temperature of ice and possibly cause an increase in glacier melting (Robin 1979). Moreover, Iceland's geographical position within the North Atlantic Ocean causes it to be highly sensitive to regional- and global-scale influences, such as changes in atmospheric temperature and fluctuations in the Gulf Stream, which directs warm ocean currents to the southern coast of the island (Chang et al. 2010) where the warmest ocean temperatures are also found.

In addition, the melting freshwater from glaciers alters the ocean, not only by directly contributing to global sea level rise, but by pushing down the heavier saltwater, thereby changing the thermohaline circulation (THC), which affects the temperature and salinity of the ocean and its currents. This has immediate effects on the region near the North Atlantic coast, but the impacts can ripple far beyond the immediate area and climate (EIS 2014). Studies have found that glaciers that have the warmest ocean temperatures near their fronts have retreated most significantly (Cook et al. 2016). The warm water melts the glacier fronts where they meet the ocean, which causes the glaciers to retreat, releasing water into the ocean, where it adds to sea level rise.

## **5.8 Spatial Variation with Respect to Geographic Location**

Differences in meltwater geochemistry were studied with respect to location of sampling sites (Table 5.4). The hydrogeochemistry of glacial meltwaters varies according to location of the sampling sites, which includes glaciers, proglacial lagoons, glacier river reaches, and mouths of glacial rivers (where the rivers meet the ocean). Figures 5.30 and 5.31 illustrate variations in specific conductivity, with and without Jökulsárlón, respectively.

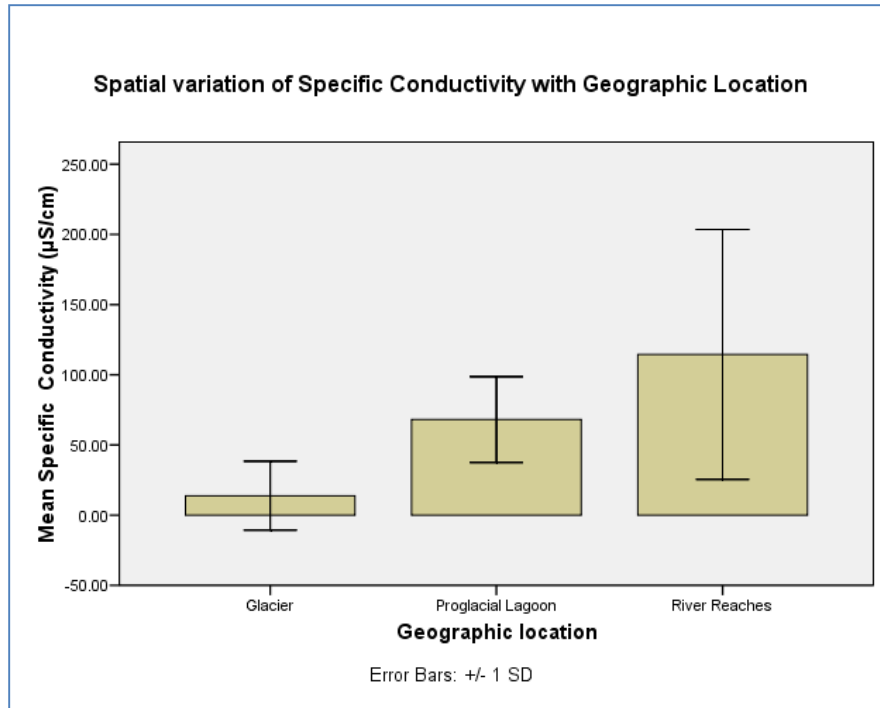


Figure 5.30. Spatial variation of specific conductivity with location excluding Jökulsárlón  
Source: Created by the author.

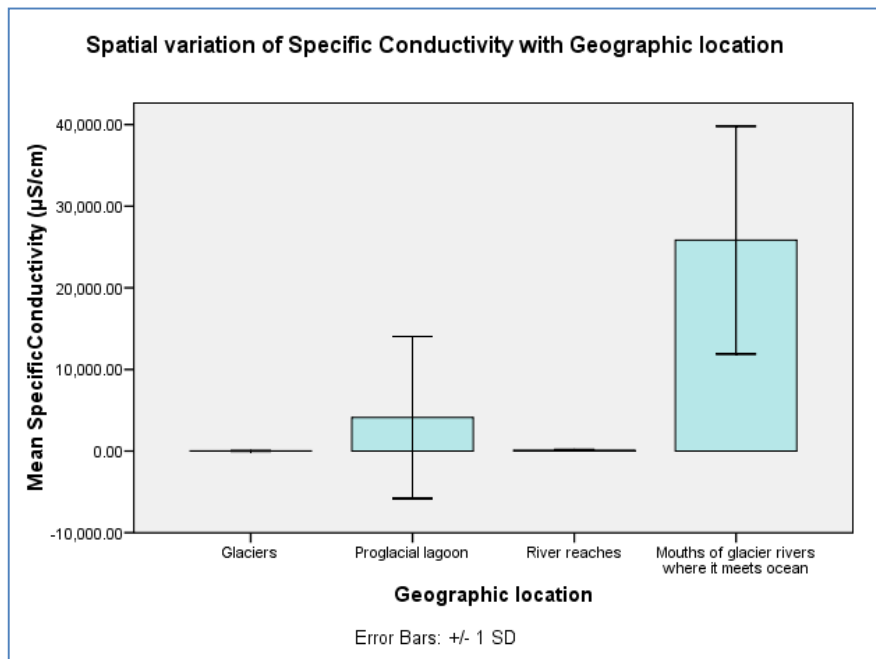


Figure 5.31. Spatial variation of specific conductivity with location including Jökulsárlón  
Source: Created by the author.

For most sites, the specific conductivity increases with distance downstream (Figure 5.30). It is the lowest at the glacier and higher closer to the mouth of the rivers. Higher concentrations of ions downstream might be due to an increase in weathering rates (Bhatt and McDowell 2007). The meltwaters from the glacial surface generally have low solute content, whereas waters are geochemically enriched after passing through the glacier (Hasnain et al. 1989), which could be the reason for higher solutes in downstream reaches of the meltwater rivers. Higher concentrations of ions at proglacial lagoons and river reaches might occur because of high rock-water interactions at these sites (Louvat et al. 2008).

Similar trends of an increase in specific conductivity downstream are not present when including the two Jökulsárlón sites in the dataset (Figure 5.31). The lagoon does not demonstrate geochemical characteristic like the rest of the glacial lagoons, but rather is higher in solutes similar to ocean water, most likely due to mixing with sea water. The Na and Cl ions are highest at the mouth of river where it meets the ocean, likely because they are the most common ions in seawater (Vasil'chuk 2009). It is important to note that the distinct difference seen in the Jökulsárlón sites may become a future trend as the glaciers continue to retreat and lagoons form and transgress toward the ocean in these coastal areas of Iceland. This could serve to enhance the melting rates and quicken the feedback process of glacier meltwater inputs to the oceans and sea level rise.

## Chapter 6

### Conclusions

The hydrogeochemical variations of Icelandic glacial meltwater were identified from volcanic influences, temporal change, and geographic location. This study presents the first temporal baseline of glacier meltwater hydrogeochemistry in Iceland for three icecaps and 11 of its glaciers. The physical and chemical parameters are highly variable between the sampling sites. A greater influence of volcanic activity and residuals from the 2010 eruption at Eyjafjallajökull might be the reason for the lower pH range and comparatively higher, and variable, specific conductivity, SO<sub>4</sub>, S, and F in the samples from the meltwater in 2016, demonstrating the long temporal impacts of ash and lava flows on glacier rivers. Active volcanic systems are located under all the sampled icecaps, and Eyjafjallajökull is located above a tectonic plate boundary zones (active volcanic zone). Recent eruptions over the past decade likely have influenced some of the sites nearest to them, but are only detectable at the Eyjafjallajökull river sites.

The lowest pH at Solheimajökull glacier, an outlet of Mýrdalsjökull (MSO2), could also be due to the result of limited rock-water interaction (Louvat et al. 2008) and deposition of volcanic dust (Xiao 2011) on the glacier. Heavy metals like As, Ba, Cr, As, Mn, Ni, P, Se, Sr, V, and Zn were below detectable limits for the sample sites, except Kötlujökull, MKO1 (Mýrdalsjökull icecap), and Kvíárjökull (Vatnajökull icecap), which had higher values for Al and Fe. Both of these sites drain close to active volcanic zones and Kvíárjökull is also located near an interpolated volcanic belt. The high concentrations of elements may be due to high reactivity of young rocks near active volcanic systems, magma degassing, or input from geothermal fluids (Louvat et al. 2008).

Precursor changes in geochemistry prior to volcanic eruption indicate possible early warnings in the data and support the use of hydrogeochemical parameters to forecast geothermal activity. An increase in parameters before a volcanic eruption that triggers a jökulhlaup could be used to design automatic warning systems if done at a high resolution (Lawler et al. 1996; Snorrason et al. 1997). The rivers draining from Eyjafjallajökull have higher values for ions and TDS, whereas Solheimajökull has the lowest pH. These values are similar to the chemical composition of water during jökulhlaups in the Skeidara River (Pálsson et al. 1999); therefore, the results from the characteristic of one jökulhlaup cannot be used in order to design and plan appropriate automatic warning systems, as similar values might be common with meltwater from a different glacier or icecap. Higher specific conductivity at Eyjafjallajökull also was noted before the 2010 eruption. This could be used to forecast volcanic activity, but temporal variation of the parameters should also be taken under consideration, since the highest value during one volcanic event could be a normal value in a time of higher melting or precipitation. Hourly specific conductivity, or a higher-resolution study, is recommended to be able to set a threshold to forecast these events. Baseline data for other glaciers should be generated to develop monitoring stations.

The concentration of solutes (Ca, Mg, K, Na, and  $\text{HCO}_3$ ) has increased since the study by Raiswell and Thomas (1984), compared to this 2016 study for Fjallsjökull, which could be due to an increased weathering rate due to temperature and  $\text{CO}_2$  increases under a changing climate, causing an increase in melting and more erosion beneath the glacier. Similar studies in hydrogeochemistry should be conducted to measure changes in the parameters and relate them with temperature and discharge over time to better

identify the possible causes for this multi-year change and what may occur in the future, if the same trend continues over time.

The temporal variation of DO is due to a variation in temperature, and the concentrations of TDS groupings, according to Stallard and Edmond (1983) and Berner and Berner (2012), show that the classification is highly variable. Highly spatial and seasonal variability of the TSS in Kötlujökull is useful in the possible planning of a hydropower station. The TSS concentrations are also highly variable in the Mýrdalsjökull and Vatnajökull sites and least variable in Eyjafjallajökull outputs. The variability for total suspended solids is important for hydrologic evaluation, since high concentrations negatively impact turbines and future hydropower production. Given Iceland's enormous potential for hydropower generation (up to 220 TWh/yr), careful spatial and temporal studies of the TSS should be undertaken before planning a hydropower project. Therefore, continued analysis of the TSS could be one of the future research projects considered in order to relate it to hydropower planning and generation.

The main weathering processes are important to understand, because they are the source of ions in the system and influence carbon sequestration and landscape denudation under a changing climate. In this study, it appears that some hydrogeochemical changes related to weathering were driven primarily by Na-HCO<sub>3</sub> and Ca-HCO<sub>3</sub> dissolution from carbonation reactions involving acid hydrolysis and pure dissolution, consuming protons from atmospheric CO<sub>2</sub>. There is a contribution from atmospheric precipitation to the observed dissolved ions of meltwater, except for the sample taken directly from Gígjökull (EG11), which indicates a relatively minor contribution from atmospheric precipitation to observed ion concentrations. Na is a major element in all igneous rock types (Stueber and

Goles 1967) and Ca may be derived from basaltic rocks (Snæbjörnsdóttir et al. 2014).  $\text{HCO}_3^-$  may be derived from two main sources, from the dissociation of atmospheric  $\text{CO}_2$  and the dissolution of carbonate minerals, such as calcite (Tranter et al. 1993). However, the high  $\text{HCO}_3^-$  concentrations found in all but two of the sites in this study suggest the need for a DIC and carbon isotope study on weathering and carbon source/sink flux, given that the likely source is from silicate rock weathering and may be higher than global averages estimated from other studies.

Higher concentrations of ions in Jökulsárlón were found due to mixing of ocean water with lagoon freshwater. There is a possibility of increased ion concentration in lagoons close to ocean in the future. As glacier retreat is accelerating and leading to increases in lagoon size in some locations closer to the ocean, including Kvíárjökull, Fjallsjökull, and Solheimajökull, these might be susceptible to increased solutes in the future. The connection of fresh glacial water and ocean water can lead to changes in the hydrogeochemistry of a lagoon and more melting from a warmer ocean on colder meltwater systems. With the addition of salt to the system as well, the melting temperature of ice at the glacier tongue and within the lagoons can be lowered and, thus, enhance the rate at which melting occurs.

This study of hydrogeochemical variation in Icelandic glaciers complements the database of physical and chemical compositions of understudied glaciers. The hydrogeochemical variations of Icelandic glacial meltwater throughout a diverse sample of glaciers and their respective icecaps are related to internal and external factors, including volcanic influences, temporal change, and location. Changes in hydrogeochemistry of the meltwater caused by volcanic activity may be used to forecast

eruptions and jökulhlaups; however, given the variability of Icelandic meltwater chemistry, high-resolution monitoring should be done in order to determine a precursor threshold for a volcanic event, as the values of one jökulhlaup could be within a normal range for a different glacier. Moreover, it is important to study temporal and spatial variability to plan projects, like hydropower plants, for which information on suspended sediments is of utmost significance. Parameters like these can change abruptly with different times and locations, including under the influence of precipitation and temperature spikes, as was witnessed on site at Falljökull during June and October.

In conclusion, the concentrations of ions varied with respect to geographic location, with specific conductivity increasing with distance downstream. The lowest values were from samples taken directly from the glacier and were higher at proglacial lagoons, then highest at downstream river reaches, which might be due to increased weathering rates downstream (Bhatt and McDowell 2007). Spatial variation did not exhibit a similar trend when Jökulsárlón was included, given higher concentrations of ions and its complex nature, due to mixing from the ocean at both Jökulsárlón sites. This information can be used as a foundation upon which future studies can be conducted to compare the changes occurring from enhanced melting under a changing climate over time, as well as for practical purposes, like infrastructure development, monitoring, and warning systems.



## References

- Aðalgeirsdóttir, G., Johannesson, T., Björnsson, H., Pálsson, F., Sigurdsson, O., 2006. Response of Hofsjökull and southern Vatnajökull, Iceland, to climate change. *Journal of Geophysical Research* 111(F3). Available online at: <http://onlinelibrary.wiley.com/doi/10.1029/2005JF000388/full>.
- Ageta, Y., Kadota, T., 1992. Predictions of changes of glaciers mass balance in the Nepal Himalaya and Tibetan Plateau: A case study of air temperature increase for three glaciers. *Annals of Glaciology* 16, 89-94.
- Ahmad, S., Hasnain, S.I., 2001. Snow and stream water chemistry of the Ganga headwaterbasin, Garhwal Himalaya, India. *Hydrological Sciences-Journal-Des Sciences Hydrologiques* 46(1), 103-111.
- Anders, A.M., Roe, G.H., Hallet, B., Montgomery, D.R., Finnegan, N.J., Putkonen, J., 2006. Spatial patterns of precipitation and topography in the Himalaya. In Willett, S.D., Hovius, N., Brandon, M.T., Fisher, D., (eds.) *Tectonics, Climate, and Landscape Evolution: Geological Society of America Special Paper* 398, 39-53
- Anderson, S.P., Drever, J.I., Humphrey, N.F., 1997. Chemical weathering in glacial environments. *Geology* 25(5), 399-402.
- APHA (American Public Health Association), 2014. *Standard Methods for the Examination of Water and Wastewater*, 22<sup>nd</sup> edn. Washington, D.C.: APHA.
- Arnorsson, S., Hurtig, N., Gysi, A.O., O'Day, P.A., 2010. Carbon dioxide waters in Iceland: A natural analogue to CO<sub>2</sub> sequestration in basaltic aquifers. In Birkle, P., Torres-Alvarado, I.S. (eds.) *13<sup>th</sup> International Symposium on Water-Rock Interaction*. Guanajuato, Mexico, 16-20 August. Boca Raton, FL: CRC Press, 836-841.
- Bagshaw, E.A., Tranter, M., Wadham, J.L., Fountain, A.G., Mowlem, M., 2011. High-resolution monitoring reveals dissolved oxygen dynamics in an Antarctic cryoconite hole. *Hydrological Processes* 25(8), 2868-2877.
- Bajracharya, S.R., Mool, P., Shrestha, B.R., 2006. *The Impact of Global Warming on the Glaciers of the Himalaya*. Paper presented at the International Symposium on Geo-disasters, Infrastructure Management and Protection of World Heritage Sites, Kathmandu, Nepal, 25-26 November. Available online at: <http://www.condesan.org/mtnforum/sites/default/files/publication/files/863.pdf>

- Barnett, T.P., Adam, J.C., Lettenmaier, D.P., 2005. Potential impacts of a warming climate on water availability in snow-dominated regions. *Nature* 438(17), 303-309.
- Barry, R., Seimon, A., 2000. Research for mountain area development: climatic fluctuations in the mountains of the Americas and their significance. *Ambio* 29 (7), 364-370.
- Berner, E.K., Berner, R.A., 2012. *Global Environment, Water, Air and Geochemical Cycle*. Princeton, NJ: Princeton University Press.
- Berner, R.A., Lasaga, A.C., Garrels, R.M., 1983. The carbonate-silicate geochemical cycle and its effect on atmospheric carbon dioxide over the past 100 million years. *American Journal of Science* 283(7), 641–83.
- Bhatia, M.P., Kujawinski, E.B., Das, S.B., Breier, C.F., Henderson, P.B., Charette, M.A., 2013. Greenland meltwater as a significant and potentially bioavailable source of iron to the ocean. *Nature Geoscience* 6, 274-278.
- Bhatt, M.P., McDowell, W.H., 2007. Evolution of chemistry along the Bagmati drainage network in Kathmandu valley. *Water, Air, and Soil Pollution* 185(1), 165–176.
- Bishwakarma, M.B., 2007. *Concept Paper for a Research on Optimum Sediment Handling in Run-Of-River Hydropower Plants*. Paper presented at the International Conference on Small Hydropower, Kandy, Sri Lanka, 22-24 October 2007, 1-9. Available online at:  
<http://www.ahec.org.in/links/International%20conference%20on%20SHP%20Kandy%20Srilanka%20All%20Details/Papers/Technical%20Aspects-A/A7.pdf>
- Björnsson, H., 1977. The cause of jökulhlaups in the Skafta´ river, Vatnajökull. *Jökull* 27, 71–78.
- Björnsson, H., 1978. The surface area of glaciers in Iceland. *Jökull* 28, 31.
- Björnsson, H. 1979. Glaciers in Iceland. *Jökull* 29, 74–80.
- Björnsson, H., Pálsson, F., 2008. Icelandic glaciers. *Jökull* 58, 365-386.
- Björnsson, H., Pálsson, F., Gudmundsson, S., Magnússon, E., Aðalgeirsdóttir, G., Jóhannesson, T., Berthier, E., Sigurdsson, O., Thorsteinsson, T., 2013. Contribution of Icelandic to sea level rise: Trends and variability since the Little Ice Age. *Geophysical Research Letters* 40(8), 1546–1550.
- Blum, J.D., Gazis, C.A., Jacobson, A.D., Chamberlain, C.P., 1998. Carbonate versus silicate weathering in the Raikhot watershed within the High Himalayan Crystalline Series. *Geology* 26(5) 411-414.

- Bradwell, T., Sigurdsson, O., Everest, J., 2013. Recent, very rapid retreat of a temperate glacier in SE Iceland. *Boreas* 42(4), 959–973.
- Brown, G.H., Tranter, M., Sharp, M., 1996. Subglacial chemical erosion – seasonal variations in solute provenance, Haut Glacier d’Arolla, Switzerland. *Annals of Glaciology* 22, 25–31.
- Brown, G.H., Tranter, M., Sharp, M.J., Gurnell, A.M., 1993. The impact of post mixing chemical reactions on the major ion chemistry of bulk meltwaters draining the Haut Glacier d’Arolla, Valais, Switzerland. *Hydrological Processes* 8, 465–480.
- Carswell, D.A., 1983. The volcanic rocks of the Solheimajokull area, South Iceland. *Jökull* 33, 61-71.
- Chang, C.H., Arrowsmith, C., Silvern, S.E., 2010. *Global Climate Change conceptual framework: Why does Earth have changing climates?* Working paper available online at: [http://cgge.aag.org/GlobalClimateChange1e/cfpart1/cfpart1\\_print.html](http://cgge.aag.org/GlobalClimateChange1e/cfpart1/cfpart1_print.html)
- Colbeck, S.C., 1981. A simulation of the enrichment of atmospheric pollutants in snow cover runoff. *Water Resources Research* 17(5), 1383-1388.
- Collins, D.N., 1979. Hydrochemistry of meltwaters draining from an Alpine Glacier. *Arctic and Alpine Research* 11(3), 307–324.
- Cook, A.J., Holland, P.R., Meredith, M.P., Luckman, A., Vaughan, D.G., 2016. Ocean forcing of glacier retreat in the Western Antarctic Peninsula. *Science* 353 (6296), 283-286. .
- Corell, R., Barry, T., Eamer, J., Hislop, L., Kullerud, L., Melillo, J., Nellesmann, C., Neretin, L., Reiersen, L., Samseth, J., 2013. *The view from the top. Searching for responses to a rapidly changing Arctic*. Washington, D.C.: United Nations Environment Programme Year Book, 19-35. Available online at: [http://staging.unep.org/yearbook/2013/pdf/View\\_from\\_the\\_top\\_new.pdf](http://staging.unep.org/yearbook/2013/pdf/View_from_the_top_new.pdf) (retrieved on November 10, 2016).
- Crochet, P., Jóhannesson, T., 2011. A data set of gridded daily temperature in Iceland, 1949-2010. *Jökull* 61, 1-17.
- CSI (Climate Science Investigations), 2015. *Impacts of climate change: Glaciers and Icesheets*. Boca Raton, FL: Florida Atlantic University. Available online at: <http://www.ces.fau.edu/nasa/impacts/melting-ice/ice-sheets-and-glaciers.php> (retrieved on October 6, 2015).
- Dessert, C., Dupre, B., Gaillardet, J., Francois, L.M., Allegre, C.J., 2002. Basalt weathering laws and the impact of basalt weathering on the global carbon cycle. *Chemical Geology* 202(3-4), 257-273.

- Dowdeswell, J.A., Hagen, J.O., Bjornsson, H., Glazovsky, A.F., Harrison, W.D., Holmlund, P., 1997. The mass balance of Circum-Arctic Glaciers and recent climate change. *Quaternary Research* 48(1), 1-14.
- Dupré, B., Dessert, C., Oliva, P., Goddéri, Y., Viers, J., François, L., Millot, R., Gaillardet, J., 2003. Rivers, chemical weathering and Earth's climate. *Comptes Rendus, Geoscience* 335(16), 1141-1160.
- Einarsson, M.A., 1984. Climate of Iceland. In Van Loon, H. (ed.) *World Survey of Climatology, Climate of the Oceans* 15, 673–697.
- Einarsson, M.A., 1994. *Geology of Iceland: Rocks and Landscape*. Reykjavik, Iceland: Mal Og Menning:
- Eiriksdottir, E.S., Gislason, S.R., Oelkers, E.H., 2015a. Direct evidence of the feedback between climate and nutrient, major, and trace element transport to the oceans. *Geochimica et Cosmochimica Acta* 166, 249-266.
- Eiriksdottir, E.S., Gislason, S.R., Oelkers, E.H., 2015b. Does temperature or runoff control the feedback between chemical denudation and climate? Insights from NE\_Iceland. *Geochimica et Cosmochimica Acta* 107, 65-81.
- Eiriksdottir, E.S., Oelkers, E.H., Hardardottir, J., Gislason, S.R., 2017. The impact of damming on riverine fluxes to the ocean: A case study from Eastern Iceland. *Water Research* 113, 124-138.
- Eiriksdottir, E.S., Sigurdsson, A., Gislason, S.R., Torssander, P., 2014. Chemical composition of precipitation and river water in southern Iceland: effects of Eyjafjallajökull volcanic eruptions and geothermal power plants. *Procedia Earth and Planetary* 10, 358-364.
- EIS (Extreme Ice Survey), 2014. *Why do glaciers matter?* Available online at: <http://extremeicesurvey.org/why-do-glaciers-matter/>. (Retrieved on February 16, 2017).
- Ellis, A.J., Mahon, W., 1978. *Chemistry and Geothermal Systems*. New York, NY: Academic Press.
- EPA (Environmental Protection Agency), 2012. *Water: Monitoring and Assessment*. Washington, D.C.: EPA. Available online at: <https://archive.epa.gov/water/archive/web/html/vms59.html> (retrieved on March 1, 2017).

- ESRI (Environmental Systems Research Institute), 2016. *World Imagery*. Redlands, CA: ESRI. Available online at: [http://goto.arcgisonline.com/maps/World\\_Imagery](http://goto.arcgisonline.com/maps/World_Imagery) (retrieved on April 22, 2016).
- Fenger, J. (ed.), 2007. *Impacts of Climate Change on Renewable Energy Sources: Their Role in the Nordic Energy System*. Copenhagen: Nordic Council of Ministers. A Comprehensive Report Resulting from a Nordic Energy Research Project. Available online at: <http://www.nordicenergy.org/wp-content/uploads/2012/01/impactsofclimatechange29mai08.pdf>.
- Fenn, C., Ashwell, I., 1987. Some observations on the characteristics of the drainage system of Kverkjökull, Central Iceland. *Jökull* 35, 79-82.
- Filizola, N., Guyot, J-L., Wittmann, H., Martinez, J-M., Oliveira, E. 2010. The Significance of Suspended Sediment Transport determination on the Amazonian Hydrological Scenario. In Manning, A.J. (ed.) *Sediment Transport in Aquatic Environments* Rijeka, Croatia: Intech Europe, 45-64.
- Fortner, S.K., Lyons, B.W., Fountain, A.G., Welch, K.A, Kehrwald, N.M., 2009. Trace element and major ion concentrations and dynamics in glacier snow and melt: Eliot Glacier, Oregon Cascade. *Hydrological Processes* 23, 2987-2996.
- Fortner, S.K., Tranter, M., Fountain, A.G., Lyons, B.W., Welch, K.A., 2005. The Geochemistry of Supraglacial Streams of Canada Glacier, Taylor Valley (Antarctica), and their Evolution into Proglacial Waters. *Aquatic Geochemistry*, 11(4), 391-412.
- Fournier, R.O., 1981. Application of water geochemistry to geothermal exploration and reservoir engineering. In Rybach, L., Muffler, L.J.P. (eds.) *Geothermal Systems: Principles and Case Histories*. New York, NY: John Wiley, 109–143.
- Galeczka, I., Eiriksdottir, E.S., Hardardottir, J., Oelkers, E.H., 2015. The effect of the 2002 glacial flood on dissolved and suspended chemical fluxes in the Skaftá river, Iceland. *Journal of Volcanology and Geothermal Research* 301, 253-276.
- Galloway, J.N., 1988. Atmospheric acidification: Projections for the future. *Ambio* 18(3), 161-166.
- Garrels, R.M., Mackenzie, F.T., 1971. *Evolution of Sedimentary Rocks*. New York, NY: W.W. Norton.
- Ghimire, N.P., Jha, P.K., Caravello, G., 2013. Physico-Chemical Parameters of High-Altitude Rivers in the Sagarmatha (Everest) National Park, Nepal. *Journal of Water Resource and Protection* 5, 761-767.
- Gibbs, R.J., 1970. Mechanisms Controlling World Water Chemistry. *Science, New Series* 170 (3962), 1088-1090.

- Gillaspy, R., 2017. *Glacial Erosion: Definition, Processes and Features*. Mountain View, CA: Study.com. Available online at: <http://study.com/academy/lesson/glacial-erosion-definition-processes-features.html> (retrieved on March 31, 2017).
- Gislason, S.R., 1990. The chemistry of precipitation on the Vatnajökull glacier, and chemical fractionation caused by the partial melting of snow. *Jökull* 40, 97-115.
- Gislason, S.R., Oelkers, E.H. 2003. Mechanism, rates, and consequences of basaltic glass dissolution: II. An experimental study of the dissolution rates of basaltic glass as a function of pH and temperature. *Geochimica Cosmochimica Acta* 67 (20), 3817–3832.
- Gislason, S.R., Arnorsson, S., Armannsson, H., 1996. Chemical weathering of basalt in Southwest Iceland: Effects of runoff, age of rocks and vegetative/glacial cover. *American Journal of Science* 296(8), 837-90.
- Gislason, S.R., Snorrason, Á., Kristmannsdóttir, H., Sveinbjörnsdóttir, Á., Torsander, P., Ólafsson, J., Castet, S., Dupré, B., 2002. Effects of volcanic eruptions on the CO<sub>2</sub> content of the atmosphere and the oceans: the 1996 eruption and flood within the Vatnajökull Glacier, Iceland. *Chemical Geology* 190, 181–205.
- Gislason, S.R., Oelkers, E.H., Eiriksdóttir, E.S., Kardjilov, M.I., Gisladóttir, G., Sigfusson, B., Snorrason, A., Elefsen, S., Hardardóttir, J., Torssander, P., Oskarsson, N., 2009. Direct evidence of the feedback between climate and weathering. *Earth and Planetary Science Letters* 277(1), 213-222.
- Goto-Azuma, K., Nakawo, M., Jiankang, H., Watanabe, O., Azuma, A., 1994. Melt-induced relocation of ions in glaciers and in a seasonal snowpack. *Snow and Ice Covers* 223, 287-297.
- Gurnell, A., Hannah, D., Lawler, D., 1996. Suspended sediment yield from glacier basins. In Walling, D.E., Webb, B.W. (eds.) *Erosion and Sediment Yield: Global and Regional Perspectives*, Proceedings of the Exeter Symposium, 15-19 July, Exeter, UK: International Association of Hydrological Sciences 236, 97-104.
- Hach (2013). *DR 900 User Manual*. Loveland, CO: Hach Company. Available online at: <http://www.hach.com/dr-900-multiparameter-handheld-colorimeter/product-downloads?id=15684103251>.
- Hannesdóttir, H., Zohrer, A., Davids, H., Sigurgeirsdóttir, S.I., Skirinnisdóttir, H., Arnason, P., 2013. *Vatnajökull National Park: Geology and Geodynamics*. Copenhagen, Denmark: Northern Environmental Education Development, 1-39. Available online at: [https://www2.uef.fi/documents/1347235/1368104/NEED+V\\_New+Geo+Review.pdf](https://www2.uef.fi/documents/1347235/1368104/NEED+V_New+Geo+Review.pdf).

- Hannesdóttir, H., Björnsson, H., Palsson, F., Aðalgeirsdóttir, G., Gudmundson, S., 2015. Changes in the southeast Vatnajökull ice cap, Iceland between 1890 and 2010. *The Cryosphere* 9, 565-585.
- Hardardóttir, J., Snorrason, A., 2003. Sediment monitoring of glacier rivers in Iceland: new data on bed load transport. *Erosion and Sediment Transport Mechanisms in Rivers* 283, 154-162.
- Hasnain, S.I., Subramanian, V., Dhanpal, K., 1989. Chemical characteristics and suspended sediment load of meltwaters from a Himalayan glacier in India. *Journal of Hydrology* 106(1-2), 99-108.
- IMO (Icelandic Meteorological Office), 2016. *Hydrological database of the Meteorological office*. Reykjavik, Iceland: IMO. Available online at: <http://en.vedur.is/> (retrieved on March 05, 2016).
- IPCC (Intergovernmental Panel on Climate Change), 2013. *Contribution of Working Group I to the Fifth Assessment Report of the Intergovernmental Panel on Climate Change*. New York, NY: Cambridge University Press.
- Jacobson, A.D., Andrews, M.G., Lehn, G.O., Holmden, C., 2015. Silicate versus Carbonate weathering in Iceland: New insights from Ca isotopes. *Earth and Planetary Science Letters* 416, 132-142.
- Jansson, P., Hock, R., Schneider, T., 2003. The concept of glacier storage: A review. *Journal of Hydrology* 282(1), 116-129.
- Jeandel, C., Oelkers, E.H., 2015. The influence of terrigenous particulate material dissolution on ocean chemistry and global element cycles. *Chemical Geology* 395, 50-66.
- Jóhannessen, M., Henriksen, A., 1978. Chemistry of snowmelt water: changes in concentration during melting. *Water Resource Research* 14, 615-619.
- Jóhannesson, T., 1997. The response of two Icelandic glaciers to climatic warming computed with a degree-day glacier mass-balance model coupled to a dynamic glacier model. *Journal of Glaciology* 43(144), 321-327.
- Jóhannesson, T., Sigurðsson, O., 1998. Interpretation of glacier variations in Iceland, 1930-1995. *Jökull* 45, 27-33.
- Jóhannesson, T., Björnsson, H., Palsson, F., Sigurdsson, O., Oorteinsson, P., 2011. LiDAR mapping of the Snaefellsjökull ice cap, western Iceland. *Jökull* 61, 19-32.

- Jóhannesson, T., Aðalgeirsdóttir, G., Björnsson, H., Crochet, P., Elíasson, E.B., Guðmundsson, S., Jónsdóttir, J.F., Ólafsson, H., Pálsson, F., Rögnvaldsson, O., Sigurðsson, O., Snorrason, A., Sveinsson, Ó.G.B., Thorsteinsson, T., 2007. *Effect of climate change on hydrology and hydro-resources in Iceland*. Reykavík, Iceland: National Energy Authority, Final report of the VO-project, OS-2007/011. Available online at: [http://www.raunvis.hi.is/~sg/CE\\_report.pdf](http://www.raunvis.hi.is/~sg/CE_report.pdf) (retrieved on April 05, 2016).
- Jónsson, J.F., 2014. Increasing conductivity in Skeiðará glacier river (Grímsfjall volcano). *Iceland Geology Blog: Volcano and Earthquake Activity*. Available online at: <http://www.jonfr.com/volcano/?p=4314> (retrieved on March 30, 2017).
- Kaser, G., Groshauer, M., Marzeion, B., 2010. Contribution potential of glaciers to water availability in different climate regimes. *Proceedings of the National Academy of Sciences* 107, 20223–20227.
- Krishna, A.P., 2011. Characteristics of snow and Glacier fed rivers in Mountainous regions with special reference to the Himalayan Basin. In Singh, V.J., Singh, P., Haritashya, U.K. (eds.) *Encyclopedia of Snow, Ice and Glaciers*. Amsterdam, Netherlands: Springer, 128-133.
- Krishnaswami, S., Singh, S.K., 2005. Chemical weathering in the river basins of the Himalaya, India. *Current Science* 89(5), 841-849.
- Kristmannsdóttir, H., Björnsson, A., Pálsson, S., Sveinbjörnsdóttir, À.E., 1999. The impact of the 1996 subglacial volcanic eruption in Vatnajökull on the River Jökulsá â Fjöllum, North Iceland. *Journal of Volcanology and Geothermal Research* 93, 359 - 372.
- Knudsen, N.T., Clement, J., Gasser, G., 2007. Suspended sediment transport in glacial meltwater during the initial quiescent phase after a major surge event at Kuannersuit Glacier, Greenland. *Danish Journal of Geography* 107(1), 1-7.
- Lami, A., Marchetto, A., Musazzi, S., Salerno, F., Tartari, G., Guilizzoni, P., 2010. Chemical and biological response of two small lakes. *Hydrobiologia* 648, 189–205.
- Larsen, G., 2000. Holocene eruptions within the Katla volcanic system, south Iceland: Characteristics and environmental impact. *Jökull* 49, 1–28.
- Lawler, D.M., Brown, R.M., 1992. A simple and inexpensive turbidity meter for the estimation of suspended sediment concentrations. *Hydrological Processes* 6, 159-168.



- Lawler, D.M., Bjornsson, H., Dolan, M., 1996. Impact of Subglacial Geothermal Activity on Meltwater Quality in the Jökulsá Á Sólheimasandi System, Southern Iceland. *Hydrological Processes* 10, 557-578.
- Lesnek, A.J., Martin, J.B., Deuerling, K., 2014. Hydrochemical Evidence for Differential Weathering in Proglacial and Deglaciaded Watersheds in Western Greenland. *Journal of Undergraduate Research* 15(3), 1-7.
- Liu, Z., Dreybrodt, W., Liu, H., 2011. Atmospheric CO<sub>2</sub> sink: Silicate weathering or carbonate weathering? *Applied Geochemistry* 26(2011), S292-S294.
- Livingstone, D.A., 1963. Chemical composition of Rivers and Lakes. In Fleischer, M. (ed.) *Data of Geochemistry*, 6<sup>th</sup> edn. Reston, VA: United States Geological Survey Professional Paper 440.
- Louvat, P., Allergre, C. J., 1998. Factors controlling present weathering rates: new contributions from basalt erosion studies. *Mineral Magazine A* 62, 907-908.
- Louvat, P., Gislason, R.S., Allegre, C.J., 2008. Chemical and Mechanical erosion rates in Iceland as deduced from river dissolved and solid material. *American Journal of Science* 308, 679-726.
- Mark, T., 2010. *A new eruption, a north-east wind and air transport faces more chaos*. London, U.K.: *The Guardian*. Available online at: <http://www.theguardian.com/world/2010/may/04/iceland-volcano-ireland> (retrieved on January 15, 2017).
- Maurer, M.A., Scott, R., 1992. *Copper River highway environmental impact studies: water quality of surface waters*. Fairbanks, AK: Department of Natural Resources, Division of Geological and Geophysical Surveys, Public data file 92-23. Available online at: <http://www.dggs.alaska.gov/pubs/id/1546> (retrieved on January 15, 2017).
- Meentemeyer, V., 1989. Geographical perspectives of space, time, and scale. *Landscape Ecology* 3(4), 163–173.
- Modenutti, B.E., Balseiro, E.G., Elser, J. J., Navarro, F.C., Laspoumaderes, C., Souza, M. S., Villanueva, V.D., 2013. Effect of volcanic eruption on nutrients, light, and phytoplankton in oligotrophic lakes. *Limnology and Oceanography* 58(4), 1165–1175.
- Moore, R.D., 2009. Glacier Change in Western North America: Influences on Hydrology, Geomorphic Hazards and Water Quality. *Hydrological Process* 23(1), 42-61.

- Mouri, G., Ros, F.C., Chalov, S., 2014. Characteristics of suspended sediment and river discharge during the beginning of snowmelt in volcanically active mountainous environments. *Geomorphology* 213, 266-276. .
- Murphy, S.F., 2007. *General Information on Dissolved Oxygen*. Denver, CO: USGS, Water Quality Monitoring. Available online at: <http://bcn.boulder.co.us/basin/data/NEW/info/DO.html> (retrieved on February 20, 2017).
- Nijampurkar, V.N., Satin, M.M., Rao, D.K., 1993. Chemical composition of snow and ice from ChhotaShigri glacier, Central Himalaya. *Journal of Hydrology* 151,19-34.
- NLSI (National Land Survey of Iceland), 2014. *Landmaelingar Islands*. Reykjavik, Iceland: NLSU. Available online at: <http://www.lmi.is/en/stafraen-gogn/>
- Nowak, A., Hodson, A., 2014. Changes in meltwater chemistry over a 20-year period following a thermal regime switch from polythermal to cold-based glaciation at Austre Brøggerbreen, Svalbard. *Polar Research* 33(1), 22779.
- NRC (National Research Council), 2014. *The Arctic in the Anthropocene: Emerging Research Questions*. Washington, D.C: National Academies Press.
- NSIDC (National Snow and Ice Data Center), 2015. *All about Glaciers: Glaciers and Climate Change*. Boulder, CO: NSIDC. Available online at: <https://nsidc.org/cryosphere/glaciers/questions/climate.html> (Retrieved October 4, 2015)
- Oelkers, E.H., Jones, M.T., Pearce, C.R., Jeandel, C., Eiriksdottir, E.S., Gislason, S.R., 2012. Riverine particulate material dissolution in seawater and its implications for the global cycles of the elements. *Comptes Rendus Geoscience* 344, 646–651.
- Orkustofnun, 2016. Hydropower. Reykjavik, Iceland: National Energy Authority. Available online at: <http://www.nea.is/hydro/>
- Oskarsson, N., Gronvold, K., Sigvaldason, G. E., 1994. Composition of Basalts above the Iceland mantle plume. *Mineralogical Magazine* 58, 676-677.
- Palacky, G.J., 1981. The airborne electromagnetic method as a tool of geological mapping. *Geophysical Prospecting* 29(1), 60-88.
- Pálsson, Z.S., Kristmannsdottir, H.S., Jonsson, P., 1999. *The first jökulhlaup from Grimsvötn in 1996* (in Icelandic). Reykjavik, Iceland: Orkustofmm Report OS-99115, 26.

- Pelto, M., 2010. *Gígjökull Retreat and Eruption Impact on this Glacier*. Washington, D.C.: AGU Blogosphere. Available online at: <http://blogs.agu.org/fromaglaciersperspective/2010/03/25/gigjokull-retreat-and-eruption-impact-on-this-glacier/> (retrieved on April 4, 2016).
- Phillips, E., Finlayson, A., Bradwell, T., Everest, J., Jones, L., 2014. Structural evolution triggers a dynamic reduction in active glacier length during rapid retreat: Evidence from Falljökull, SE Iceland. *Journal of Geophysical Research* 119(10), 2194-2208.
- Pilkey, O.H., Neal, W.J., Cooper, J.A.G., Kelly, J.T., 2011. *The World's beaches: A global guide to the science of the shoreline*. Berkeley, California: University of California Press.
- Piper, A.M., 1944. A graphical procedure in the geochemical interpretation of water analysis. *Transactions of the American Geophysical Union* 25, 914–923.
- Plass, G.N., 1959. Sustainability, Carbon Dioxide and Climate. *Scientific American* 201(1), 41-47. Available online at: <https://www.scientificamerican.com/article/carbon-dioxide-and-climate/> (retrieved on March 1, 2017).
- Polar Research, 2015. Arctic matters: *The global connection to changes in the Arctic*. Washington, D.C.: The National Academic Press, Polar Research. Available online at: <https://www.nap.edu/catalog/21717/arctic-matters-the-global-connection-to-changes-in-the-arctic> (retrieved on May 8, 2016).
- Raiswell, R., Thomas, A.G., 1984. Solute Acquisition in Glacial Melt Waters. I. Fjallsjökull (South-East Iceland): Bulk Melt Waters with Closed-System Characteristics. *Journal of Glaciology* 30(104), 35-43.
- Rasch, M., Elbering, B., Jakobsen, B.H., Hasholt, B., 2000. High-resolution measurements of water discharge, sediment, and solute transport in the River Zackenbergelven, Northeast Greenland. *Arctic, Antarctic and Alpine Research* 32, 336–345.
- Reynolds, B., Chapman, P.J., French, M.C., Jenkins, A., Wheeler, H.S., 1995. Major, minor and trace element chemistry of surface waters in the Everest region of Nepal. *Biochemistry of Seasonally Snow-Covered Catchments* 228, 405-412.
- Robin, G.de.Q., 1979. Formation, flow, and disintegration of iceshelves. *Journal of Glaciology* 24, 259–265.
- Rogora, M., Mosello, R., Arisci, S., 2003. The effect of climate warming on the hydrochemistry of alpine lakes. *Water, Air, and Soil Pollution* 148, 347–361.

- Rosenbauer, R.J., Thomas, B., Bischoff, J.L., Palandri, J., 2012. Carbon sequestration via reaction with basaltic rocks: Geochemical modeling and experimental results. *Geochimica et Cosmochimica Acta* 89, 116–133.
- Rummukainen, M., 2006. *The CE regional climate scenarios*. Proceedings of the European Conference of Impacts of Climate Change on Renewable Energy Sources. Reykjavík, Iceland: Orkustofnun, June 5–6.
- Schaner, N., Voisin, N., Nijssen, B., 2012. The contributions of glacier melt to streamflow. *Environmental Research Letters* 7, 29-34.
- Sigurðsson, O., 1998. Glacier variations in Iceland 1930-1995. *Jökull* 45, 3-25.
- Sigurðsson, O., 2005. Variations of termini of glaciers in Iceland in recent centuries and their connection with climate. In Caseldine, C., Russell, A., Harðardóttir, J., Knudsen, O. (eds.) *Iceland – Modern Processes and Past Environments* Amsterdam, Netherlands: Elsevier, 241–255.
- Sigurðsson, O., Jónsson, T., Jóhannesson, T., 2007. Relation between glacier-termini variations and summer temperatures in Iceland since 1930. *Annals of Glaciology*, 42, 395–401.
- Sigvaldason, G.E., 1981. Fluids in volcanic and geothermal systems. *Physics and Chemistry of the Earth* 13-14, 179-195.
- Singh, P., 1998. *Effect of global warming on the streamflow of a high-altitude Spiti River*. In Herman, A., Pokhrel, A.P., Lang, H., Molnar, L., Khanai, N.R., Chalise, S.R. (eds.) *Ecology of High Mountain Areas: Proceedings of the International Conference on Ecology of High Mountain Areas*, Kathmandu, Nepal, 24-28 March, 45-48.
- Singh, V.B., Ramanathan, A.L., Pottakkal, J.G., Sharma, P., Linda, A., Azam, M.F., Chatterjee, C., 2012. Chemical characterisation of meltwater draining from Gangotri Glacier, Garhwal Himalaya, India. *Journal of Earth System Science* 121(3), 625–636.
- Slatt, R.M., 1972. Geochemistry of Meltwater Streams from Nine Alaskan Glaciers. *The Geological Society of America* 83(4), 1125-1132.
- Snæbjörnsdóttir, S.O., Wiese, F., Fridriksson, T., Armansson, H., Einarsson, G.M., Gislason, S.R., 2014. CO<sub>2</sub> storage potential of basaltic rocks in Iceland and the oceanic ridges. *Energy Procedia* 63, 4585-4600.

- Snorrason, A., Jónsson, P., Pálsson, S., Árnason, S., Sigurðsson, O., Víkingsson, S., and Zóphóníasson, S., 1996. Hlaupið á Skeiðarársandi haustið 1996. Útbreiðsla, rennsli og aurburður. In Haraldsson, H. (ed.), *Vatnajökull. Gos og Hlaup* Reykjavík, Iceland: Icelandic Public Roads Administration, 79–137.
- Srinivasa, R.N., 1998. MHPT.BAS: a computer program for modified Hill–Piper diagram for classification of ground water. *Computers and Geosciences* 24(10), 991–1008.
- Stallard, R.F., Edmond, J.M., 1983. Geochemistry of the Amazon: 2. The influence of geology and weathering environment on the dissolved load. *Journal of Geophysical Research* 88, 9671–9688.
- Steffen, K., Cuillen, N., Huff, R., Stewart, C., Rignot, E., 2004. *Petermann Gletscher's floating tongue in northwestern Greenland: peculiar surface features, bottom melt channels, and mass balance assessment*. Proceedings of the 34th International Arctic Workshop, March 10–13, Institute of Arctic and Alpine Research, University of Colorado, Boulder, CO, 158–160.
- Steinþórsson, S., Óskarsson, N., 1983. Chemical monitoring of Jökulhaup water in Skeiðará and the geothermal system in Grimsvötn, Iceland. *Jökull* 33, 73–86.
- Stueber, A.M., Goles, G.G., 1967. Abundances of Na, Mn, Cr, Sc and Co in ultramafic rocks. *Geochimica et Cosmochimica Acta* 31(1), 75-93.
- Suzuki, K., 1982. Chemical changes of snow cover by melting. *Japanese Journal of Limnology* 43, 102-112.
- Tao, P., Yuanqing, H., Guofeng, Z., Huijuan, X., Weihong, C., Hewen, N., 2013. Hydrochemical characteristics of typical rivers in a temperate glacier basin, China. *Environmental Earth Sciences* 68(3), 615-621.
- Thomas, A.G., Raiswell, R., 1984. Solute acquisition in glacial meltwaters, Fjallsjökull (South-East Iceland): bulk melt waters with closed-system characteristics. *Journal of Glaciology* 30(104), 35-43.
- Thordarson, T., Hoskuldsson, A., 2002. *Iceland. Classic Geology in Europe 3*. Harpenden, UK: Terra Publishing..
- Thordarson, T., Larsen, G., 2007. Volcanism in Iceland in historical time: Volcano types, eruption styles and eruptive history. *Journal of Geodynamics* 43(1), 118-152.
- Thorsteinsson, T., Björnsson, H., 2011. *Climate Change and Energy Systems. Impacts, Risks and Adaptation in the Nordic and Baltic countries*. Copenhagen, Denmark: Nordic Council of Ministers. Available online at: [www.norden.org](http://www.norden.org) (retrieved on March 5, 2016).

- Thorsteinsson, T., Jóhannesson, T., Snorrason, A., 2013. Glaciers and ice caps: Vulnerable water resources in a warming climate. *Current Opinion in Environmental Sustainability* 5(6), 590-598.
- Tômasson, H., 1991. Glaciofluvial sediment transport and erosion. In Gjessing, Y., Hagen, J.O., Hassel, K.A., Sand, K., Wold, B. (eds.) *Arctic Hydrology: Present and Future Tasks*. Oslo, Norway: Norwegian National Committee for Hydrology, 27-36.
- Tranter, M., Brown, G.H., Sharp, M.J., Gurnell, A.M., 1993. A conceptual model of solute acquisition by Alpine glacial meltwaters. *Journal of Glaciology* 39, 573–581.
- Tuladhar, A., Kayastha, R., Gurung, S., Shrestha, A., 2015. Hydro-Chemical Characterization of Glacial Melt Waters Draining from Langtang Valley, Nepal. *Journal of Water Resource and Protection* 7, 605-613.
- UH (University of Houston), 2017. *Weathering*. Houston, TX: University of Houston. Available online at: <http://www.uh.edu/~geos6g/1330/weath.html> (retrieved on March 10, 2017).
- USGS (United States Geological Survey), 2011. *Volcano Hazards Program*. Reston, VA: USGA. Available online at: [https://volcanoes.usgs.gov/vsc/file\\_mgr/file153/FAQs.pdf](https://volcanoes.usgs.gov/vsc/file_mgr/file153/FAQs.pdf) (retrieved on January 25, 2017).
- USGS (United States Geological Survey), 2017. *The USGS Water Science School*. Reston, VA: USGS. Available online at: <https://water.usgs.gov/edu/dissolvedoxygen.html> (retrieved on February 25, 2017).
- Vasil'schik, Y.K., 2009. Chemical properties of Glacial and Ground Ice. In Khublaryan, M.G. (ed.) *Types and Properties of Waters, Vol. 2. Encyclopedia of Life Support Systems*. Geneva, Switzerland: UNESCO, 268-294. Available online at: <https://pdfs.semanticscholar.org/1f9e/9f53ac2d07c95bd757e5644df2825136cdb6.pdf> (Retrieved on February 10, 2017).
- Viviroli, D., Archer, D.R., Buytaert, W., 2011 Climate change and mountain water resources: Overview and recommendations for research, management and policy. *Hydrology and Earth System Sciences* 15, 471–504.
- Wadham, J.L., Hodson, A.J., Tranter, M., Dowdeswell, J.A., 1998. The hydrochemistry of meltwater draining a polythermal-based, high Arctic glacier, south Svalbard. I: The ablation season. *Hydrological Processes* 12, 1825–1849.

- Walker, J.C.G., Hays, P.B., Kasting, J.F., 1981. A negative feedback mechanism for the long-term stabilization of Earth's surface temperature. *Journal of Geophysical Research* 86, 9776–82.
- Walling, D.E., 1977. Assessing the accuracy of suspended sediment rating curves for a small basin. *Water Resources Research* 13(3), 531-538.
- Wallmann K., 2001. Controls on the Cretaceous and Cenozoic evolution of seawater composition, atmospheric CO<sub>2</sub> and climate. *Geochimica Chosmochimica Acta* 65, 3005–3025.
- Webb, E., Schuur, E., Natali, S., Oken, K., Bracho, R., Krapek, J., Risk, D., Nickerson, N., 2016. Increased wintertime CO<sub>2</sub> loss as a result of sustained tundra warming. *Journal of Geophysical Research Biogeosciences* 121(2), 249-265.
- Weier, J., 1999. *At the Edge: Monitoring Glaciers to watch Global Change*. Washington, D.C.: NASA (National Aeronautics and Space Administration). Available online at: <https://earthobservatory.nasa.gov/Features/Glaciers/> (Retrieved on May 8, 2016). f
- Welch, K.A., Lyons, W.B., Whisner, C., Gardner, C.B., Gooseff, M.N., Mcknight, D.M., 2010. Spatial variations in the geochemistry of glacial meltwater streams in the Taylor Valley, Antarctica. *Antarctica Science* 22(6), 662-672.
- White, A.F., Brantley, S.L., 2003. The effect of time on the weathering of silicate minerals: why do weathering rates differ in the laboratory and field? *Chemical Geology* 202(3-4), 479-506.
- Williams, M.W., Losleben, M., Caine, N., Greenland, D., 1996. Changes in climate and hydrochemical responses in a high-elevation catchment in the Rocky Mountains, USA. *Limnology and Oceanography* 41(5), 939-946.
- Wilson, L., Head, J.W. 2002. Heat transfer and melting in subglacial basaltic volcanic eruptions: implications for volcanic deposit morphology and meltwater volumes. *Geological Society, London, Special Publications* 202(1), 5-26.
- Xiao, C., 2011. Acidity of Glacier Ice. In Singh, V.J., Singh, P., Haritashya, U.K. (eds.) *Encyclopedia of Snow, Ice and Glaciers* Amsterdam, Netherlands: Springer 1388-4360, 3-4.
- YSI (Yellow Springs Instruments), 2014. *Pro DSS User Manual*. Yellow Springs, OH, YSI. Manual available online at: <https://www.yisi.com/File%20Library/Documents/Manuals/YSI-ProDSS-110714-Rev-B-626973-User-Manual.pdf626973-User-Manual.pdf>.

Zwally, H.J., Abdalati, W., Herring, T., Larson, K., Saba, J., Steffen, K., 2002. Surface melt-induced acceleration of Greenland ice-sheet flow. *Science* 297(5579), 218–222.



## APPENDICES

### APPENDIX 1: SAMPLING INFORMATION

S.N	Date (June)	Date (August)	Date (October)	Time (June)	Time (August)	Time (October)	Ice cap	Glacier	Sample code	GPS	Elevation (m.a.s.l)
1	6/7/2016	8/6/2016	10/12/2016	14:30	16:30	11:08	Mýrdalsjökull	Solheimajökull	MSO1	N 63.53487, W019.34981	114
2	6/7/2016	8/6/2016	10/12/2016	15:44	17:24	12:43	Mýrdalsjökull	Solheimajökull	MSO2	N 63.53460, W019.35603	92
3	6/7/2016	8/6/2016	10/12/2016	16:54	18:00	13:51	Mýrdalsjökull	Solheimajökull	MSO3	N 63.49889, W 019.40243	46
4	6/7/2016	8/6/2016	10/12/2016	19:29	14:10	15:54	Mýrdalsjökull	Kötujökull	MKO1	N 63.50663, W 018.85735	123
5	6/7/2016	8/6/2016	10/12/2016	20:29	12:37	n.a.	Mýrdalsjökull	Kötujökull	MKO2	N 63.43725, W 018.85395	35
6	6/7/2016	8/6/2016	10/12/2016	20:58	12:02	17:02	Mýrdalsjökull	Kötujökull	MKO3	N 63.44895, W018.67430	19
7	6/8/2016	8/7/2016	10/11/2016	13:42	14:03	13:06	Vatnajökull	Fjallsjökull	VFJ1	N 64.01232, W 016.39136	8
8	6/8/2016	8/7/2016	10/11/2016	14:15	14:27	13:41	Vatnajökull	Fjallsjökull	VFJ2	N 64.00407, W 016.3622	9
9	6/8/2016	8/7/2016	10/11/2016	15:18	13:13	13:35	Vatnajökull	Jökulsárlón	VJS1	N 64.05013, W 016.18051	1.2
10	6/8/2016	8/7/2016	10/11/2016	14:58	12:30	11:20	Vatnajökull	Jökulsárlón	VJS2	N 64.04285, W016.18074	0
11	6/8/2016	8/7/2016	10/11/2016	16:00	14:57	n.a.	Vatnajökull	Kviárjökull	VKV1	N 63.94141, W 016.44463	35
12	6/8/2016	8/7/2016	10/11/2016	16:42	15:21	14:33	Vatnajökull	Kviárjökull	VKV2	N 63.93710, W 016.43226	18
13	6/8/2016	8/7/2016	10/11/2016	18:23	16:18	15:42	Vatnajökull	Falljökull	VFA1	N 63.96833, W 016.80043	144
14	6/8/2016	8/7/2016	10/11/2016	18:49	16:52	14:04	Vatnajökull	Falljökull	VFA2	N 63.96605, W 016.80615	129
15	6/8/2016	8/7/2016	10/11/2016	19:31	17:21	n.a.	Vatnajökull	Falljökull	VFA3	N 63.95270, W 016.84809	71
16	6/8/2016	8/7/2016	10/11/2016	22:32	17:51	19:34	Vatnajökull	Svinafellsjökull	VSV1	N 64.00736, W 016.88180	98
17	6/8/2016	8/7/2016	10/11/2016	22:02	n.a.	17:10	Vatnajökull	Svinafellsjökull	VSV2	N 63.98384, w 016.87403	56
18	6/8/2016	8/7/2016	10/11/2016	23:24	19:37	20:55	Vatnajökull	Skeiðarárjökull	VSK1	N 63.93930, W 017.36369	55
19	6/9/2016	8/8/2016	10/10/2016	15:55	13:17	13:06	Eyjafjallajökull	Gígjökull	EG11	N 63.66838, W 019.62168	265
20	6/9/2016	8/8/2016	10/10/2016	16:10	13:36	13:35	Eyjafjallajökull	Gígjökull	EG12	N 63.66965, W 019.62240	246
21	6/9/2016	8/8/2016	10/10/2016	n.a.	15:11	14:35	Eyjafjallajökull	Gígjökull	EG13	N 63.68608, W 019.65036	157
22	6/9/2016	8/8/2016	10/10/2016	17:46	18:00	n.a.	Eyjafjallajökull	River	EJY1	N 63.68184, W 019.77543	101
23	6/9/2016	8/8/2016	10/10/2016	18:29	19:06	17:11	Eyjafjallajökull	River	EJY2	N 63.61637, W 020.01598	26
24	6/9/2016	8/8/2016	10/10/2016	19:07	11:05	17:42	Eyjafjallajökull	Seljavallajökull	ESE1	N 63.53095, W 019.61789	14
25	6/9/2016	8/8/2016	10/10/2016	19:21	10:48	17:58	Eyjafjallajökull	Kaldakirfjökull	EKA1	N 63.52776, W 019.60257	16

### APPENDIX 2: FIELD PARAMETERS (JUNE 2016)

S.N	Sample code	Temperature (°C)	pH	Specific conductivity (µS/cm)	Dissolved Oxygen (mg/L)	TDS (mg/L)	TSS (mg/L)	Turbidity (FAU)	Alkalinity (mg/L)	Nitrate (mg/L)	(out) T (°C)	Relative Humidity (%)	Wind speed (mph)
1	MSO1	2.9	6.67	3	14.18	1.975	24	22	11.655	0.02	17.6	54.6/14.4	1.7
2	MSO2	3.1	6.65	104.5	12.54	68.1	61	151	82.88	0.1	18	53/16.5	3.7
3	MSO3	3.6	7.14	95.8	13.39	62.24	189	71	75.11	0.13	13.9	51.1/13.2	11
4	MKO1	2.7	7.74	98.6	13.72	63.9	124	313	77.7	0.24	11.9	64.4/10.4	2.2
5	MKO2	4.3	7.70	118.4	12.59	76.96	106	236	84.175	0.25	11.6	70.8/11.9	14.9
6	MKO3	5.2	7.87	122.7	12.2	79.76	0	0	75.11	0.32	9.2	65.6/9.3	6.5
7	VFJ1	4.1	8.45	72.8	12.43	47.16	80	218	51.8	0.14	21.7	43.5/19.6	0
8	VFJ2	4.7	8.22	75.7	13.36	49.1	80	211	51.8	0.2	21.3	45.7/19.6	2
9	VJS1	9.9	8.26	34201	11.02	22226.3	0	9	191.66	29.3	16.2	57.1/15.1	4.1
10	VJS2	3.4	8.12	41957	10.99	27,289.50	6	8	142.45	32.76	16.2	50.4/14	2.5
11	VKV1	2.8	8.35	86.6	12.98	56.14	238	650	82.88	0.14	12.2	62.3/11.6	4.3
12	VKV2	3.3	8.03	86.6	13.52	56.32	266	672	87.542	0.17	27.2	46.1/18	1
13	VFA1	2.8	8.77	4.3	13.94	2.77	26	52	12.95	0.01	16.2	65.3/13.1	0.9
14	VFA2	0.8	8.93	58.1	17.18	38.7	280	715	41.44	0.28	9.8	72.7/9.3	2.3
15	VFA3	1.5	7.34	41.7	14.34	27.31	412	605	34.965	9.62	16.8	59/15.5	2.9
16	VSV1	1.1	8.74	53.1	12.85	34.5	242	318	49.21	0.68	8.7	75.7/8.3	0.6
17	VSV2	0.5	9.22	62.9	14.74	40.85	499	350	59.57	1.82	13.6	60.2/13.9	0.8
18	VSK1	1.3	7.13	123.3	13.22	80.14	208	226	108.78	0.2	10.5	72.2/15.3	3.8
19	EG11	3.9	7.27	10.2	13.62	6.8	53	21	9.065	0.02	5.4	83/7.5	1.6
20	EG12	1.6	7.37	110.8	13.91	73.98	197	317	59.57	0.16	10	83.8/10	0.5
21	EG13	6.5	8.09	261.7	12.37	170.13	20	52	165.76	0.28	16.9	70.9/16.6	12.8
22	EJY1	7.7	7.71	71.2	12.06	46.4	45	104	51.8	0.12	15.9	61.1/15.1	6
23	EJY2	10.9	7.81	86.4	11.19	56.15	40	97	59.57	0.14	14.1	73.1/14.2	13.4
24	ESE1	6.6	8.25	193.7	12.57	125.93	0	25	181.3	0.18	16.2	65.3/15.6	1
25	EKA1	6.8	7.62	70.2	12.44	45.59	11	47	54.39	0.15	16.5	62.7/17.5	2.9

APPENDIX 3: FIELD PARAMETERS (AUGUST 2016)

S.N	Sample code	Temperature (°C)	pH	Specific conductivity (µS/cm)	Dissolved Oxygen (mg/L)	TDS (mg/L)	TSS (mg/L)	Turbidity (FAU)	Alkalinity (mg/L)	Nitrate (mg/L)	(out) T (°C)	Relative Humidity (%)	Wind speed (mph)
1	MSO1	0.5	7.41	1.3	15.73	0.866	25	61	5.50375	0	11.8	57.9/11	5.7
2	MSO2	1.5	6.62	74.6	14.64	48.497	209	89	60.865	0.02	12.1	57.8/12.4	8.4
3	MSO3	2.9	6.91	68.7	14.91	44.664	200	125	56.98	0.07	16.2	56.6/14.4	4.3
4	MKO1	2.3	6.98	159.9	14.69	104.298	741	340	142.45	0.08	13.9	63.7/13.8	9.7
5	MKO2	4.6	7.15	171.7	14.4	111.64	1017	401	150.22	0.08	17.6	56.1/15.16	10
6	MKO3	7.6	7.62	128.8	12.88	83.703	2	5	80.29	0.07	18.9	53.2/18	7
7	VFJ1	3.2	9.04	149.2	14.04	94.821	178	78	36.26	0.69	14.8	42.7/14.3	5.3
8	VFJ2	10.3	7.64	23.4	12.71	15.229	34	24	18.13	0.02	18.9	38.8/17.6	10
9	VJS1	4	8.16	24629	12.19	16010.34	0	8	101.01	19.57	17	39.6/17.7	2.3
10	VJS2	2.5	8.26	17662	14.1	11,548.69	7	0	117.845	14.8	17.1	39.6/17.7	4.5
11	VKV1	2.6	9.08	42.8	16.84	27.814	709	256	42.735	0.31	17.5	36.7/16.1	7.9
12	VKV2	2.6	8.97	42.7	15.74	27.771	694	249	41.44	0.68	18.3	37/16.3	5.1
13	VFA1	0.9	8.50	5.6	15.79	3650	166	91	10.36	0.04	17.2	32.9/15.7	1.1
14	VFA2	2.2	7.71	32.7	15.36	21.167	845	190	28.49	0.14	17.2	32.9/15.7	9.6
15	VFA3	2.6	7.28	31.5	15.18	20.447	257	109	28.49	0.11	18.6	28/18.3	1.4
16	VSV1	0.9	7.65	39.9	14.95	25.93	285	126	36.26	0.26	20.3	24/17.3	2
17	VSV2	1	9.17	50.2	17.11	32.656	411	164	46.62	1.74	19.5	31.8/18.4	4.9
18	VSK1	1.3	7.41	75.8	15.38	49.303	533	190	85.47	0.14	12.2	48.7/11.7	23.3
19	EGI1	2.4	8.25	2.1	15.75	1.324	67	30	5.18	0.03	11.3	93.6/11.3	4
20	EGI2	2.4	7.26	257.8	15.17	167.455	215	78	142.45	0.15	13.1	57.56/14.4	1.2
21	EGI3	6.4	8.12	381.4	13.74	247.886	89	32	204.61	0.41	17.9	50.4/16.9	2.1
22	EJY1	8.6	7.81	81.6	13.01	52.801	72	33	50.505	0.13	14.9	57.5/14.6	7.7
23	EJY2	10.9	7.90	117.5	12.31	76.344	207	75	90.65	0.1	16.1	58.6/14.7	5.3
24	ESE1	8	8.35	418	13.66	271.557	21	12	401.45	0.51	16.9	62.7/17.2	11.3
25	EKA1	6.6	7.35	76.9	13.99	49.96	73	29	49.21	0.29	16.9	62.7/17.2	11.3

APPENDIX 4: FIELD PARAMETERS (OCTOBER 2016)

S.N	Sample code	Temperature (°C)	pH	Specific conductivity (µS/cm)	Dissolved Oxygen (mg/L)	TDS (mg/L)	TSS (mg/L)	Turbidity (FAU)	Alkalinity (mg/L)	Nitrate (mg/L)	(out) T (°C)	Relative Humidity (%)	Wind speed (mph)
1	MSO1	2.2	7.64	14.6	14.62	9.507	100	94	5.18	0.46	8.8	100	2.7
2	MSO2	1.9	6.69	72.8	14.99	47.118	692	284	69.93	1.21	8.8	100	3.4
3	MSO3	2.3	7.38	62.7	14.67	40.759	1044	369	68.635	1.45	9.3	100	14.8
4	MKO1	1.1	7.32	59.6	14.47	38.738	2440	906	68.635	0.94	9.9	100	26
5	MKO2	4.1	7.34	70.9	13.75	46.068	2070	753	75.11	1.31	9.3	100	11.5
6	MKO3	6.1	7.64	116.4	12.55	75.611	521	224	75.11	2.64	10.2	100	9.6
7	VFJ1	2.6	9.79	114.7	14.41	73.961	152	86	41.44	1.39	6.7	100	0.1
8	VEJ2	4	8.52	21.4	14.14	13933	142	55	15.54	0.1	6.7	100	0.9
9	VJS1	1.3	9.03	14307	15.8	9644.637	40	28	183.89	3.51	9.2	80.1/8.5	1.4
10	VJS2	1.8	8.57	17908	13.99	12,719.50	26	34	187.775	4.21	9.2	80.1/8.5	1.3
11	VKV1	0.6	9.43	45.4	18.5	29.407	1050	403	45.325	6.82	8.6	100	2.6
12	VKV2	0.8	9.57	45	16.04	29.241	1110	381	46.62	4.71	9.1	100	2.1
13	VFA1	1.6	9.56	78.4	15.37	50.004	150	69	10.36	1.33	11.2	100	0.7
14	VFA2	2.6	9.40	70.1	13.96	42.761	270	121	30.303	2.67	11.2	100	0.9
15	VFA3	0.7	8.73	29.7	15.44	19.326	663	258	25.9	0.72	16.5	89.7	0.9
16	VSV1	1.5	9.27	51.4	14.63	33.087	285	13.5	32.375	3.54	7.9	98.8	5.8
17	VSV2	0.3	9.42	55.7	16.93	36.243	1210	411	64.75	0.68	9.1	100	0.5
18	VSK1	1.2	7.89	74.5	15.07	48.301	862	325	81.585	0.23	10.4	95	6.7
19	EGH1	0.7	8.33	5.1	15.23	3.3	38	26	7.77	0.01	7.9	74.7	0.9
20	EGH2	1.9	7.52	143.9	14.7	90.055	145	60	94.535	0.06	7.9	74.9.2	0.9
21	EGH3	4.3	7.93	289.6	13.27	187.91	93	33	160.58	0.17	11.2	69.2/10.6	3.4
22	EJY1	4.7	7.76	74.8	13.64	48.703	156	61	49.21	0.05	16	64.5/15.2	1.9
23	EJY2	6.5	8.25	93.3	13.1	60.635	230	81	67.34	0.16	10.4	75.2/9.9	3.7
24	ESE1	5.5	8.25	241.9	13.46	157.212	78	23	217.56	0.09	12.4	68/13.6	2
25	EKA1	4.8	7.54	69.8	13.75	45.354	141	61	46.62	0.04	12.5	68/13.6	2.1



APPENDIX 7: METALS (OCTOBER 2016) mg/L

S.N	Sample code	Al	As	Ba	Ca	Cr	Cu	Fe	K	Mg	Mn	Na	Ni	P	Pb	S	Se	Si	Sr	V	Zn
1	M5O1	0.105	0.026	<0.002	0.438	<0.001	<0.003	0.152	0.117	0.252	0.006	1.721	<0.001	0.021	<0.006	0.302	<0.014	0.239	<0.001	<0.001	0.005
2	M5O2	1.087	<0.018	0.003	8.277	<0.001	0.003	2.256	0.747	2.326	0.061	5.959	<0.001	0.141	<0.006	0.743	<0.014	4.019	0.030	0.013	0.006
3	M5O3	1.357	0.025	0.005	7.367	0.002	0.004	2.677	0.760	2.384	0.061	5.378	<0.001	0.200	<0.006	0.630	<0.014	4.239	0.030	0.011	0.008
4	MKO1	2.398	<0.018	0.007	8.288	0.004	0.003	5.593	0.918	2.395	0.167	5.190	<0.001	0.225	<0.006	0.847	0.010	3.045	0.034	0.015	0.012
5	MKO2	1.945	<0.018	0.006	9.074	0.002	<0.003	4.466	0.919	2.349	0.126	6.300	<0.001	0.215	<0.006	1.472	<0.014	5.608	0.035	0.012	0.010
6	MKO3	0.355	<0.018	<0.002	9.957	<0.001	<0.003	0.750	1.229	2.844	0.017	10.762	<0.001	0.158	0.021	3.447	<0.014	9.992	0.028	0.018	0.002
7	VFJ1	0.378	<0.018	<0.002	6.781	<0.001	<0.003	0.513	0.402	1.217	0.014	6.295	<0.001	0.038	<0.006	1.731	<0.014	1.433	0.015	0.002	<0.004
8	VFJ2	0.581	<0.018	0.002	1.332	<0.001	<0.003	0.480	0.467	0.664	0.012	3.355	<0.001	0.072	<0.006	0.373	<0.014	3.806	0.003	0.003	<0.004
9	VJS1	0.036	22.453	0.099	91.704	6.843	<0.003	<0.003	80.648	301.675	0.074	2500.004	<0.001	10.474	<0.006	181.359	<0.014	0.000	0.290	<0.001	0.397
10	VJS2	0.236	2.235	0.103	167.981	6.301	<0.003	<0.003	137.389	570.181	<0.002	4457.161	<0.001	11.314	<0.006	334.231	<0.014	9.994	1.463	<0.001	<0.004
11	VKV1	3.061	<0.018	0.011	6.804	0.014	0.011	6.359	0.682	3.262	0.108	7.292	<0.001	0.307	<0.006	0.738	<0.014	6.366	0.014	0.014	0.014
12	VKV2	1.404	<0.018	0.005	5.368	0.011	0.003	3.256	0.480	1.828	0.052	6.013	<0.001	0.144	<0.006	0.549	<0.014	5.356	0.008	0.010	0.006
13	VFA1	0.209	<0.018	<0.002	1.191	<0.001	<0.003	0.316	0.157	0.446	0.007	1.211	<0.001	0.046	<0.006	0.134	<0.014	0.809	0.001	0.001	<0.004
14	VFA2	0.856	<0.018	0.004	3.372	<0.001	0.003	1.226	0.617	1.208	0.037	3.940	<0.001	0.139	0.024	0.790	<0.014	3.462	0.008	0.006	0.004
15	VFA3	1.396	0.026	0.008	2.975	<0.001	0.004	1.924	0.753	1.202	0.074	3.916	<0.001	0.241	<0.006	0.461	0.017	4.440	0.009	0.005	0.007
16	VSV1	0.681	<0.018	<0.002	4.531	<0.001	0.004	1.189	0.236	0.748	0.025	2.231	<0.001	0.060	0.049	0.694	<0.014	2.276	0.006	0.005	<0.004
17	VSV2	0.889	<0.018	0.002	7.049	<0.001	0.003	1.538	0.460	1.322	0.036	4.298	<0.001	0.112	0.012	0.947	<0.014	3.574	0.014	0.006	0.006
18	VSK1	1.761	<0.018	<0.002	9.534	0.003	0.007	2.953	0.379	2.474	0.064	6.513	<0.001	0.057	0.015	1.060	0.021	6.287	0.007	0.013	0.006
19	EGH1	0.123	<0.018	<0.002	0.250	<0.001	<0.003	0.133	0.063	0.096	0.012	0.331	<0.001	0.025	<0.006	0.129	0.022	0.337	<0.001	<0.001	<0.004
20	EGH2	0.485	<0.018	<0.002	8.888	<0.001	<0.003	0.534	2.781	4.754	0.025	17.133	<0.001	0.094	<0.006	3.179	<0.014	11.170	0.040	0.006	<0.004
21	EGH3	0.305	<0.018	0.003	19.731	0.066	<0.003	0.406	3.157	9.799	0.020	36.580	<0.001	0.000	<0.006	6.637	<0.014	13.359	0.050	0.009	0.013
22	EJY1	0.414	<0.018	<0.002	4.800	<0.001	<0.003	0.799	0.955	2.145	0.022	8.115	<0.001	0.075	0.013	1.698	0.015	7.512	0.015	0.007	<0.004
23	EYJ2	0.553	<0.018	<0.002	7.264	<0.001	<0.003	1.144	1.027	2.920	0.025	8.874	<0.001	0.074	0.019	2.621	0.032	8.538	0.024	0.008	<0.004
24	ESE1	0.095	<0.018	0.001	23.121	<0.001	<0.003	0.120	2.314	11.509	0.008	12.203	<0.001	0.046	0.033	1.966	<0.014	8.303	0.088	0.004	0.002
25	EKA1	0.455	<0.018	0.002	6.820	0.008	<0.003	0.846	0.701	1.761	0.030	6.920	<0.001	0.102	<0.006	1.917	<0.014	5.725	0.025	0.005	<0.004

APPENDIX 8: ANIONS (JUNE 2016) mg/L

S.N	Sample code	F	Cl	SO4	NO3	HCO3
1	MSO1	n.a.	n.a.	n.a.	0.02	14.219
2	MSO2	0.15	6.627	2.62	0.1	101.114
3	MSO3	0.145	6.377	2.238	0.13	91.634
4	MKO1	0.294	5.824	4.763	0.24	94.794
5	MKO2	0.308	5.946	9.412	0.25	102.694
6	MKO3	0.509	8.087	9.149	0.32	91.634
7	VFJ1	0.101	4.011	5.676	0.14	63.196
8	VFJ2	0.122	4.157	5.559	0.2	63.196
9	VJS1	n.a.	13257	1680	29.3	2049.600
10	VJS2	n.a.	17738	2191	32.76	2673.020
11	VKV1	0.477	11.364	2.691	0.14	3.209
12	VKV2	0.48	8.492	2.313	0.17	3.245
13	VFA1	n.a.	0.85	n.a.	0.01	15.799
14	VFA2	0.182	6.12	1.805	0.28	50.557
15	VFA3	0.186	5.293	1.623	9.62	42.657
16	VSV1	0.143	2.85	2.373	0.68	60.036
17	VSV2	0.163	5.585	3.587	1.82	72.675
18	VSK1	0.142	3.672	5.033	0.2	132.712
19	EGI1	n.a.	0.095	n.a.	0.02	11.059
20	EGI2	0.323	6.929	3.725	0.16	72.675
21	EGI3	0.63	29.582	12.82	0.28	202.227
22	EJY1	0.254	5.378	4.137	0.12	63.196
23	EYJ2	0.303	5.854	5.533	0.14	72.675
24	ESE1	0.171	7.252	3.349	0.18	221.186
25	EKA1	0.179	5.55	5.054	0.15	66.356

APPENDIX 9: ANIONS (AUGUST 2016) mg/L

S.N	Sample code	F	Cl	SO4	NO3	HCO3
1	MSO1	n.a.	n.a.	n.a.	0.00	6.678
2	MSO2	0.13	3.458	3.417	0.02	74.175
3	MSO3	0.099	3.09	1.976	0.07	69.412
4	MKO1	0.328	4.395	6.593	0.08	173.513
5	MKO2	0.359	4.383	7.604	0.08	182.897
6	MKO3	0.465	7.881	9.09	0.07	97.482
7	VFJ1	0.052	7.982	4.115	0.69	39.471
8	VFJ2	0.096	2.481	0.991	0.02	21.987
9	VJS1	n.a.	9434	1264	19.57	121.414
10	VJS2	n.a.	11042	1406	14.8	141.151
11	VKV1	0.191	3.897	1.264	0.31	46.154
12	VKV2	0.192	4.766	1.443	0.68	45.926
13	VFA1	n.a.	n.a.	n.a.	0.04	12.079
14	VFA2	0.128	3.503	1.651	0.14	34.537
15	VFA3	0.123	2.92	1.164	0.11	34.661
16	VSV1	0.071	1.896	1.741	0.26	43.996
17	VSV2	0.104	2.829	1.95	1.74	49.109
18	VSK1	0.116	1.774	2.991	0.14	103.938
19	EGI1	0.102	n.a.	n.a.	0.03	6.105
20	EGI2	0.519	29.07	12.798	0.15	173.367
21	EGI3	0.602	50.897	19.542	0.41	246.328
22	EJY1	0.261	4.606	3.823	0.13	61.165
23	EYJ2	0.309	4.935	6.058	0.1	109.653
24	ESE1	0.165	12.906	5.663	0.51	479.227
25	EKA1	0.163	4.449	5.93	0.29	59.857

APPENDIX 10: ANIONS (OCTOBER 2016) mg/L

S.N	Sample code	F	Cl	SO4	NO3	HCO3
1	MSO1	n.a.	2.349	0.025	0.46	6.263
2	MSO2	0.126	2.736	0.851	1.21	85.216
3	MSO3	0.122	2.471	0.681	1.45	83.477
4	MKO1	0.197	2.082	1.437	0.94	83.503
5	MKO2	0.188	2.864	2.947	1.31	91.373
6	MKO3	0.455	7.583	7.938	2.64	91.173
7	VFJ1	n.a.	2.401	2.313	1.39	29.606
8	VFJ2	0.072	2.674	0.089	0.1	18.179
9	VJS1	n.a.	5379	119	3.51	203.090
10	VJS2	n.a.	8145	584	4.21	220.991
11	VKV1	0.24	3.843	0.649	6.82	42.793
12	VKV2	0.278	3.08	0.662	4.71	40.448
13	VFA1	n.a.	0.477	n.a.	1.33	7.767
14	VFA2	0.128	2.729	1.283	2.67	28.650
15	VFA3	0.124	2.541	0.49	0.72	29.748
16	VSV1	0.096	1.766	1.028	3.54	32.626
17	VSV2	0.142	2.288	1.668	0.68	62.008
18	VSK1	0.117	1.884	1.703	0.23	98.701
19	EGI1	0.079	0.519	n.a.	0.01	9.159
20	EGI2	0.522	14.488	7.387	0.06	114.879
21	EGI3	0.829	33.733	17.241	0.17	194.174
22	EJY1	0.236	4.767	3.635	0.05	59.639
23	EYJ2	0.273	4.762	5.491	0.16	80.644
24	ESE1	0.138	8.987	3.333	0.09	260.782
25	EKA1	0.129	4.378	3.695	0.04	56.633

APPENDIX 11: ELEMENTAL RATIO AND CHARGE BALANCE (JUNE 2016)

S.N	Sample code	Ca/Si (June)	K/Na (June)	Na/Cl (June)	K/Cl (June)	C ratio (June)	Charge Balance
1	MSO1	2.151	1.622	n.a.	n.a.	1.000	70.715
2	MSO2	1.366	0.116	1.517	0.176	0.975	14.666
3	MSO3	1.216	0.128	1.470	0.189	0.976	13.818
4	MKO1	1.520	0.149	1.480	0.221	0.952	17.209
5	MKO2	1.611	0.107	1.607	0.172	0.916	18.888
6	MKO3	1.120	0.111	1.375	0.152	0.909	17.513
7	VFJ1	3.798	0.118	1.085	0.128	0.915	17.048
8	VFJ2	2.555	0.120	1.066	0.128	0.918	11.713
9	VJS1	262.066	0.057	0.433	0.025	1.000	4.505
10	VJS2	941.809	0.033	0.677	0.022	1.000	11.209
11	VKV1	0.421	0.101	4.203	0.424	1.000	23.225
12	VKV2	0.351	0.177	2.434	0.430	1.000	6.964
13	VFA1	0.644	0.214	1.443	0.309	1.000	30.846
14	VFA2	0.536	0.219	1.091	0.239	0.962	3.957
15	VFA3	0.526	0.199	1.145	0.228	0.963	11.993
16	VSV1	1.948	0.083	1.627	0.135	0.960	18.959
17	VSV2	2.167	0.117	0.894	0.105	0.945	30.913
18	VSK1	1.751	0.061	2.770	0.170	0.963	17.409
19	EGI1	0.935	0.353	7.005	2.473	1.000	35.538
20	EGI2	0.764	0.181	1.282	0.231	0.951	19.971
21	EGI3	1.373	0.172	0.867	0.149	0.940	26.026
22	EJY1	0.809	0.136	1.385	0.188	0.938	20.951
23	EYJ2	0.834	0.138	1.411	0.195	0.929	20.065
24	ESE1	3.140	0.197	1.341	0.264	0.985	30.771
25	EKA1	1.129	0.110	1.398	0.154	0.929	27.263



APPENDIX 12: ELEMENTAL RATIO AND CHARGE BALANCE (AUGUST 2016)

S.N	Sample code	Ca/Si (August)	K/Na (August)	Na/Cl (August)	K/Cl (August)	C ratio (August)	Charge Balance
1	MSO1	1.417	0.612	n.a.	n.a.	1.000	0.000
2	MSO2	1.594	0.119	2.007	0.240	0.956	25.078
3	MSO3	1.296	0.115	2.021	0.232	0.972	23.829
4	MKO1	1.130	0.169	2.689	0.454	0.963	47.174
5	MKO2	1.659	0.120	2.460	0.294	0.960	30.642
6	MKO3	1.047	0.114	1.366	0.156	0.915	17.045
7	VFJ1	4.193	0.084	0.365	0.031	0.906	3.400
8	VFJ2	0.323	0.147	1.250	0.183	0.957	19.150
9	VJS1	78.765	0.030	0.554	0.016	0.088	18.697
10	VJS2	32.858	0.030	0.531	0.016	0.091	17.408
11	VKV1	0.883	0.107	1.669	0.179	0.973	18.368
12	VKV2	0.754	0.093	1.131	0.105	0.970	10.853
13	VFA1	0.802	0.136	n.a.	n.a.	1.000	0.000
14	VFA2	0.769	0.140	1.341	0.188	0.954	19.659
15	VFA3	0.458	0.143	1.562	0.224	0.968	23.125
16	VSV1	1.856	0.097	1.630	0.159	0.962	16.484
17	VSV2	2.019	0.111	1.343	0.149	0.962	15.503
18	VSK1	1.237	0.066	3.898	0.259	0.972	26.662
19	EGI1	0.715	0.142	n.a.	n.a.	1.000	0.000
20	EGI2	1.057	0.171	0.818	0.140	0.931	15.016
21	EGI3	1.391	0.163	0.691	0.113	0.926	12.177
22	EJY1	0.515	0.121	2.061	0.250	0.941	26.527
23	EYJ2	0.914	0.116	2.298	0.267	0.948	28.208
24	ESE1	3.749	0.208	1.024	0.212	0.988	21.496
25	EKA1	0.947	0.095	2.035	0.194	0.910	21.304

APPENDIX 13: ELEMENTAL RATIO AND CHARGE BALANCE (OCTOBER 2016)

S.N	Sample code	Ca/Si (October)	K/Na (October)	Na/Cl (October)	K/Cl (October)	C ratio (October)	Charge Balance
1	MSO1	1.829	0.068	0.733	0.050	0.996	-4.634
2	MSO2	2.059	0.125	2.178	0.273	0.990	17.338
3	MSO3	1.738	0.141	2.176	0.308	0.992	17.646
4	MKO1	1.636	0.177	2.493	0.441	0.983	-5.734
5	MKO2	1.618	0.146	2.200	0.321	0.969	11.708
6	MKO3	0.997	0.114	1.419	0.162	0.920	19.432
7	VFJ1	4.733	0.064	2.622	0.167	0.928	7.795
8	VFJ2	0.350	0.139	1.255	0.175	0.995	2.534
9	VJS1	-31.248	0.032	0.465	0.015	0.631	-3.469
10	VJS2	16.808	0.031	0.547	0.017	0.275	3.535
11	VKV1	1.069	0.094	1.897	0.178	0.985	-1.688
12	VKV2	1.002	0.080	1.952	0.156	0.984	14.114
13	VFA1	1.472	0.130	2.538	0.330	1.000	18.076
14	VFA2	0.974	0.156	1.444	0.226	0.957	16.935
15	VFA3	0.670	0.193	1.541	0.297	0.984	-2.760
16	VSV1	1.991	0.106	1.263	0.133	0.969	28.273
17	VSV2	1.972	0.107	1.878	0.201	0.974	25.256
18	VSK1	1.516	0.058	3.457	0.201	0.983	13.968
19	EGI1	0.744	0.191	0.639	0.122	1.000	48.061
20	EGI2	0.796	0.162	1.183	0.192	0.940	15.172
21	EGI3	1.477	0.086	1.084	0.094	0.918	10.236
22	EJY1	0.639	0.118	1.702	0.200	0.943	13.248
23	EYJ2	0.851	0.116	1.863	0.216	0.936	14.648
24	ESE1	2.785	0.190	1.358	0.257	0.987	25.637
25	EKA1	1.191	0.101	1.581	0.160	0.939	9.083

APPENDIX 14: MEAN CORRELATIONS

Parameters	pH	Specific Conductivity (µS/cm)	DO (mg/L)	TSS (mg/L)	Turbidity (mg/L)	HCO3 (mg/L)	WaterTemp (°C)	AirTemp (°C)	TDS (mg/L)	Ca (mg/L)	Fe (mg/L)	K (mg/L)	Mg (mg/L)	Na (mg/L)	S (mg/L)	Se (mg/L)	Si (mg/L)	F (mg/L)	Cl (mg/L)	SO4 (mg/L)	NO3 (mg/L)	
pH	1																					
Specific Conductivity (µS/cm)	0.096	1																				
DO (mg/L)	0.321	-0.327	1																			
TSS (mg/L)	0.006	-0.192	0.402	1																		
Turbidity (mg/L)	-0.001	-0.230	0.283	0.739	1																	
HCO3 (mg/L)	0.008	0.829	-0.384	-0.130	-0.174	1																
WaterTemp (°C)	-0.194	0.101	-0.709	-0.331	-0.364	0.221	1															
AirTemp (°C)	-0.137	0.084	-0.213	-0.213	-0.068	0.107	0.318	1														
TDS (mg/L)	0.123	0.945	-0.298	-0.203	-0.249	0.772	0.090	0.023	1													
Ca (mg/L)	0.083	0.972	-0.324	-0.192	-0.233	0.761	0.101	0.103	0.914	1												
Fe (mg/L)	-0.129	-0.207	0.171	0.418	0.554	-0.053	-0.205	0.078	-0.196	-0.135	1											
K (mg/L)	0.080	0.987	-0.341	-0.183	-0.217	0.883	0.120	0.098	0.932	0.963	-0.195	1										
Mg (mg/L)	0.105	0.961	-0.285	-0.201	-0.241	0.695	0.074	0.080	0.910	0.990	-0.196	0.944	1									
Na (mg/L)	0.085	0.972	-0.310	-0.184	-0.221	0.808	0.050	0.090	0.918	0.969	-0.200	0.971	0.948	1								
S (mg/L)	0.087	0.986	-0.338	-0.208	-0.250	0.791	0.095	0.126	0.931	0.992	-0.212	0.983	0.985	0.979	1							
Se (mg/L)	-0.132	-0.107	-0.155	0.062	0.064	-0.002	0.144	0.222	-0.119	-0.127	0.415	-0.085	-0.195	-0.103	-0.088	1						
Si (mg/L)	-0.225	-0.198	-0.173	0.051	0.305	-0.111	0.211	0.205	-0.214	-0.106	0.515	-0.178	-0.146	-0.172	-0.194	-0.012	1					
F (mg/L)	-0.089	0.504	-0.294	-0.137	0.099	0.230	0.225	0.081	-0.107	0.357	0.162	0.770	0.430	0.867	0.855	-0.295	0.830	1				
Cl (mg/L)	0.093	0.989	-0.305	-0.205	-0.246	0.793	0.069	0.093	0.938	0.991	-0.212	0.984	0.983	0.985	0.998	-0.131	-0.208	0.650	1			
SO4 (mg/L)	0.071	0.965	-0.344	-0.204	-0.248	0.811	0.098	0.130	0.911	0.972	-0.195	0.976	0.950	0.968	0.986	0.080	-0.216	0.680	0.978	1		
NO3 (mg/L)	0.132	0.929	-0.279	-0.089	-0.115	0.828	0.075	0.088	0.868	0.897	0.061	0.939	0.872	0.903	0.925	0.140	-0.207	-0.085	0.918	0.947	1	

APPENDIX 15: BULK MELTWATERS FROM FJALLSJÖKULL (MG/L)

Type	Ca	Mg	K	Na	HCO3	SO2
Bulk meltwater	0.104	0.0156	0.0028	0.0309	0.22	0.0128
	0.122	0.0263	0.0054	0.077	0.28	0.0234
	0.115	0.0247	0.0049	0.0757	0.25	0.0124
	0.126	0.0259	0.0051	0.0683	0.255	0.0212
	0.12	0.0255	0.0051	0.0726	0.29	0.0239
	0.137	0.0284	0.0056	0.0705	0.3	0.0291
	0.121	0.0218	0.0072	0.0774	0.27	0.0218
	0.111	0.016	0.0033	0.0896	0.19	0.0202
	0.129	0.0276	0.0066	0.087	0.29	0.0135
	0.123	0.0177	0.0033	0.0313	0.26	0.0187
	0.12	0.028	0.0056	0.0957	0.24	0.0176
	0.129	0.0284	0.0063	0.1031	0.25	0.0239
	0.135	0.0292	0.0061	0.1044	0.32	0.0332
	0.133	0.0292	0.006	0.1135	0.3	0.026
	0.105	0.03	0.0069	0.1209	0.26	0.028
	0.137	0.028	0.0061	0.0761	0.255	0.0249
	0.118	0.0304	0.0069	0.1109	0.21	0.027
	0.106	0.028	0.0064	0.1018	0.23	0.0265
Supra-glacial	0.061	0.0045	0.0018	0.0022	0.18	0.0067
	0.101	0.0037	0.0018	0.0065	0.29	0.0101
Average	0.11765	0.023445	0.00516	0.07577	0.257	0.021045
SD	0.0173	0.0080	0.0017	0.0340	0.0375	0.0070

APPENDIX 16: MAPS SHOWING MAJOR IONS

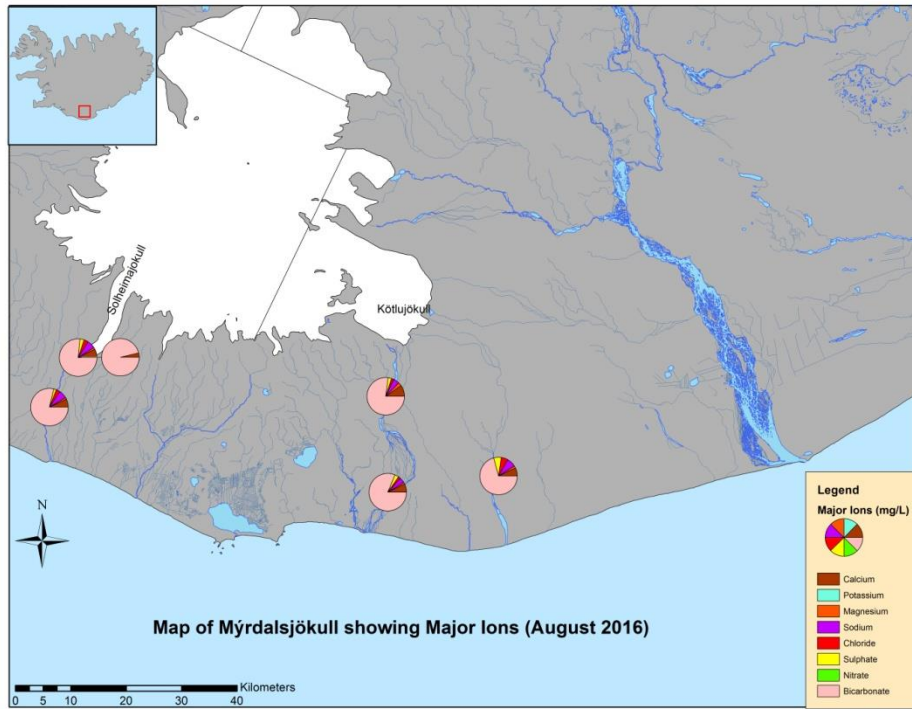


Figure A1. Map of Mýrdalsjökull showing Major Ions (August 2016).  
Source: Created by the author with an NLSI (2014) base map.

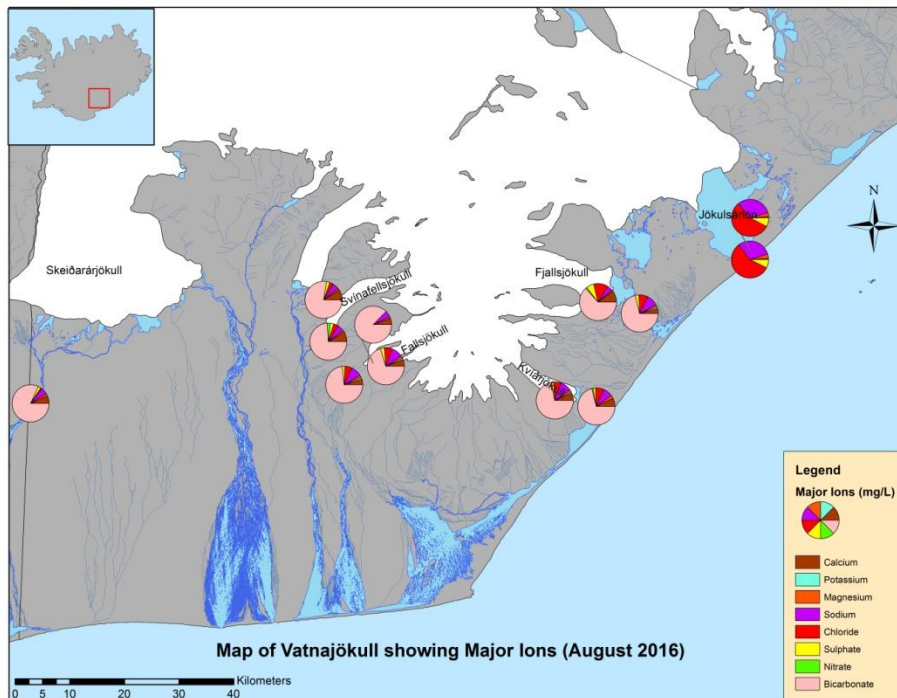


Figure A2. Map of Vatnajökull showing major Ions (August 2016).  
Source: Created by the author with an NLSI (2014) base map.

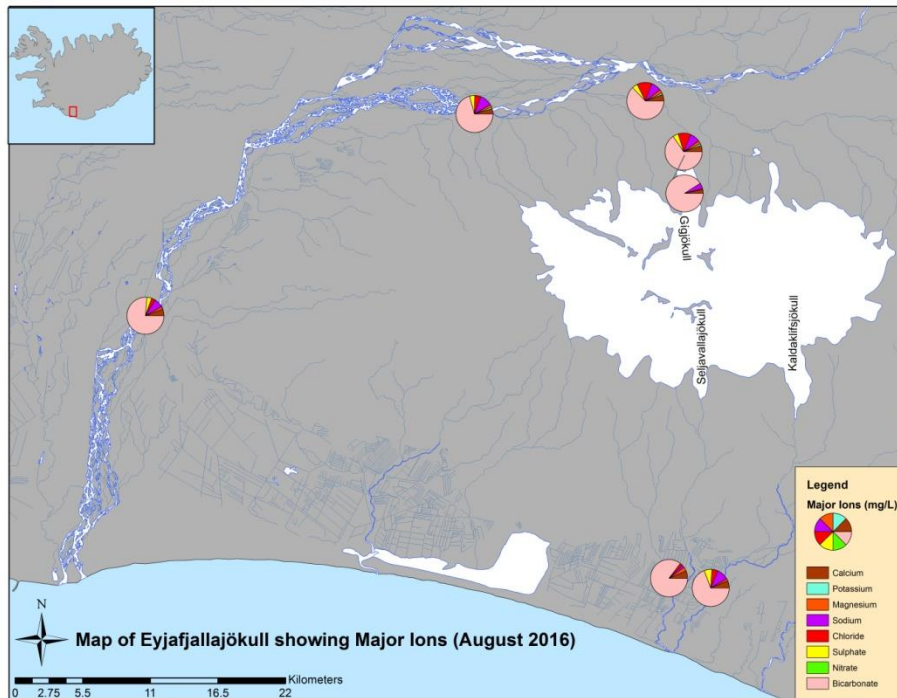


Figure A3. Map of Eyjafjallajökull showing major ions (August 2016).  
Source: Created by the author with an NLSI (2014) base map.

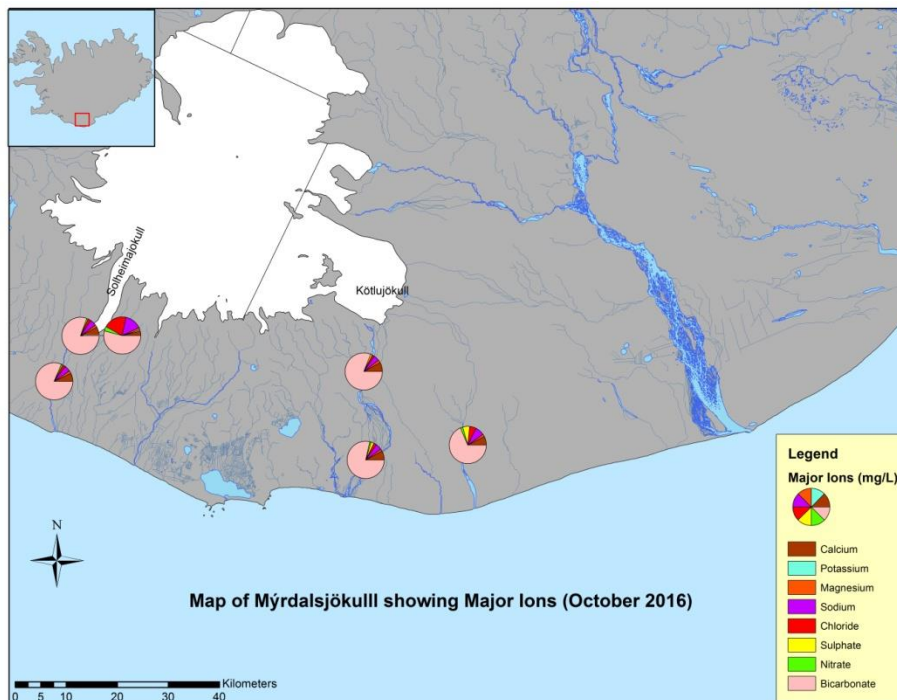


Figure A4. Map of Mýrdalsjökull showing Major Ions (October 2016).  
Source: Created by the author with an NLSI (2014) base map.

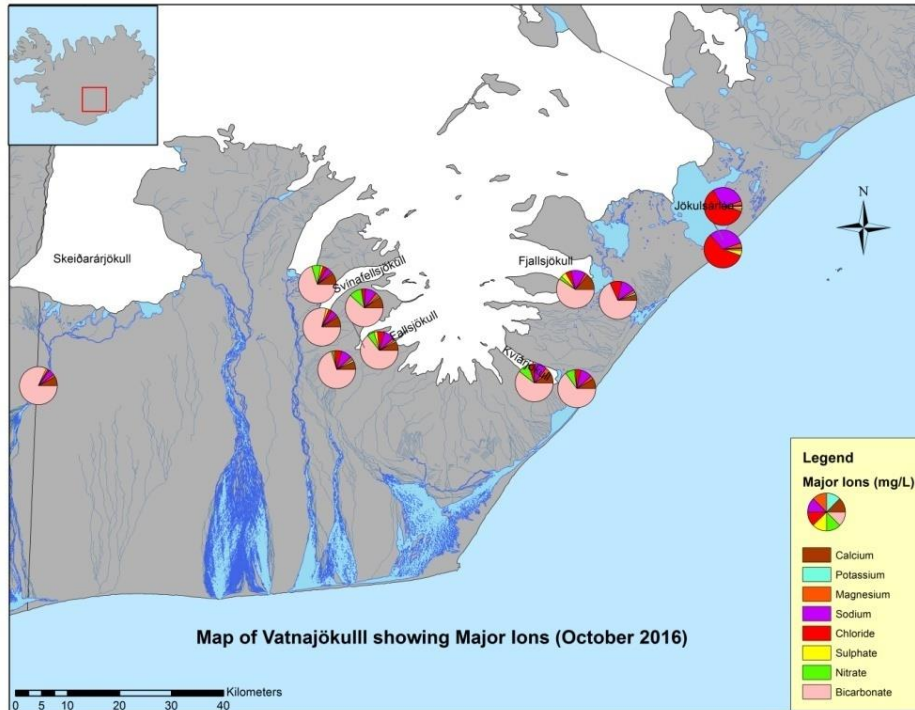


Figure A5. Map of Vatnajökull showing Major Ions (October 2016).  
Source: Created by the author with an NLSI (2014) base map.

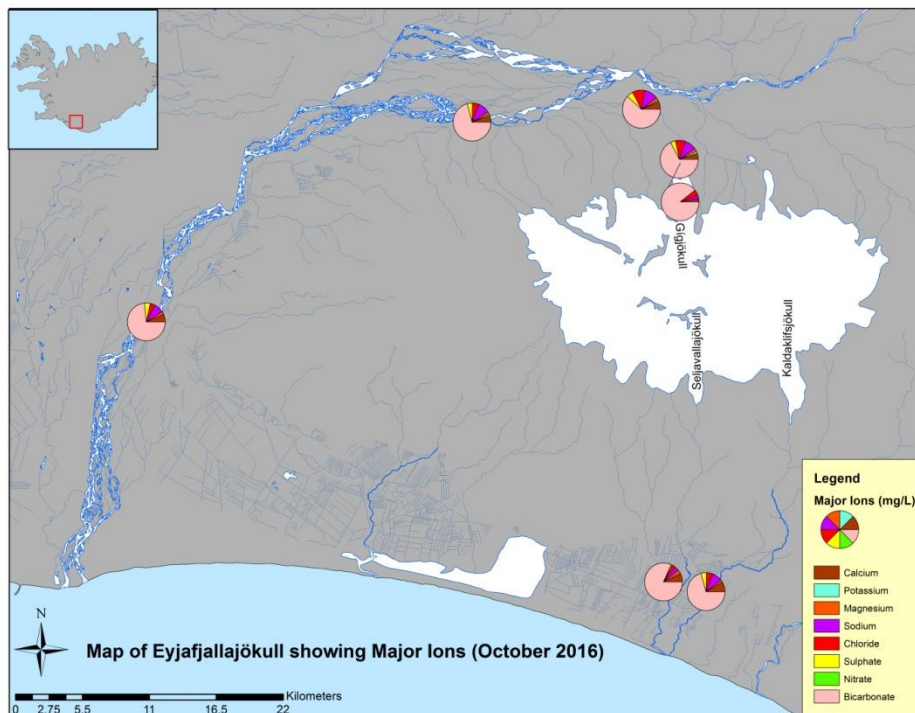


Figure A6. Map of Eyjafjallajökull showing major ions (October 2016).  
Source: Created by the author with an NLSI (2014) base map.

## APPENDIX 17: PIPER PLOTS

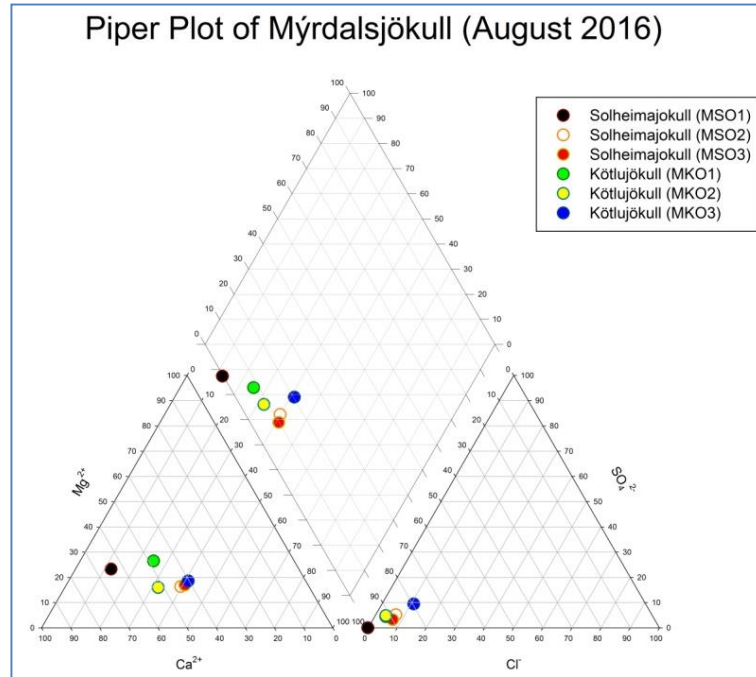


Figure A7. Piper plot of Mýrdalsjökull (August 2016).  
Source: Created by the author.

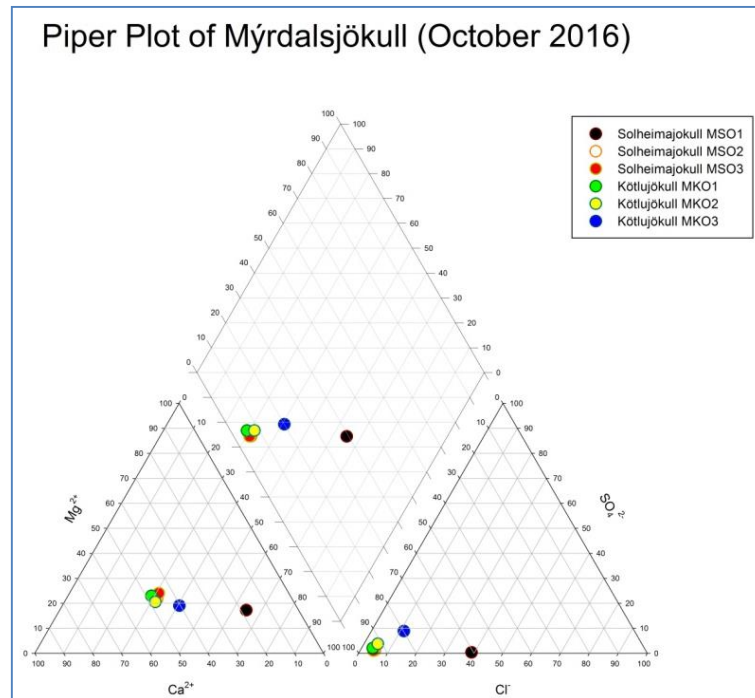


Figure A8. Piper plot of Mýrdalsjökull (October 2016).  
Source: Created by the author.

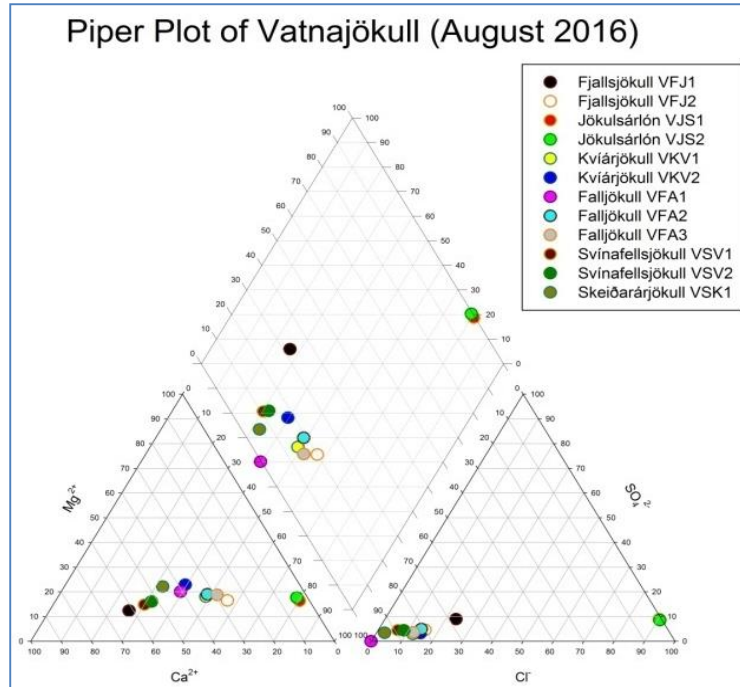


Figure A9. Piper plot of Vatnajökull (August 2016).  
Source: Created by the author.

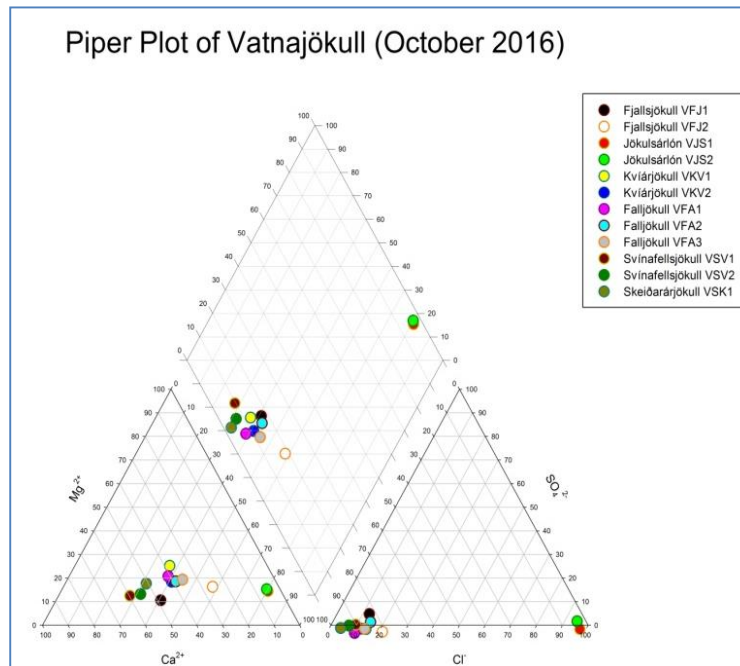


Figure A10. Piper plot of Vatnajökull (October 2016).  
Source: Created by the author.



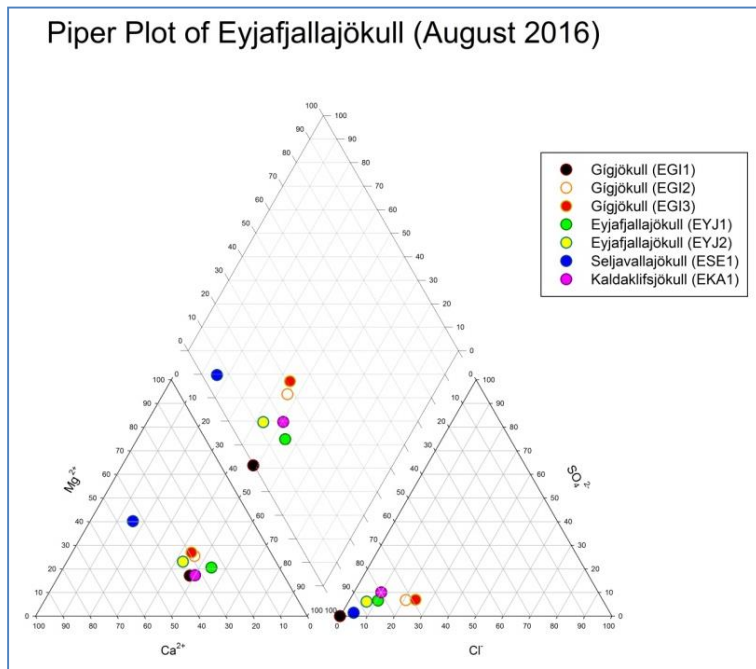


Figure A11. Piper plot of Eyjafjallajökull (August 2016).  
Source: Created by the author.

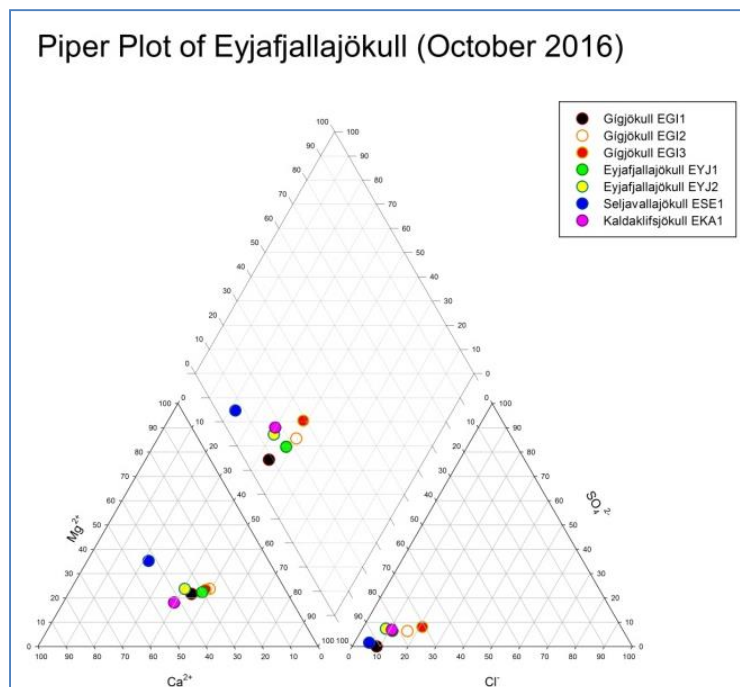


Figure A12. Piper plot of Eyjafjallajökull (October 2016).  
Source: Created by the author.